

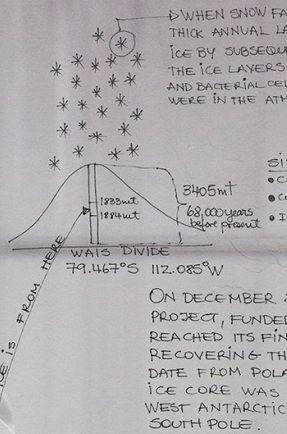
# Earth Systems Processes

This piece of ice is part of a project that presents the first long-term highly resolved bacterial cell concentration record obtained from a polar ice core. This record, retrieved from the West Antarctic Ice Sheet (WAIS) Divide (WD), spans from the Last Glacial Maximum (LGM: 26,000-20,000 years before present) to the early

Holocene (EH: 11,600-9,600 years before present). The bacterial cell concentration record shows distinct fluctuations in cell concentration coincident with major climatic states. The time series also reveals a 1,500 year periodicity with greater amplitude during the Last Deglaciation (20,000-11,600 years before present) and higher bacterial cell concentration and lower variability occurred during the LGM and the EH that during the Last Deglaciation.

Collectively, statistical models, together with visual observations indicate that the temporal variability in concentration of airborne bacterial cells mainly reflects changes in marine/sea-ice regional environments of the WAIS Divide. Our data show that airborne Antarctic bacterial concentrations from WD ice core are sensitive to large-scale changes in mean climate states and millennial scale variations.

ANTARCTIC AIRBORNE BACTERIA FROM WD ICE CORE MIRROR CLIMATE



HERE: 63cm of ice that represents approx 6years

PIECE OF ICE FROM THE WEST ANTARCTIC ICE SHEET (WAIS) DIVIDE ICE CORE

ICE CORES ARE RECORDERS OF CLIMATE VARIABILITY.

ICE CORES ARE UNIQUE BECAUSE WE CAN OBTAIN DIRECT MEASUREMENTS OF PAST ATMOSPHERIC COMPOSITION.

THE INFORMATION ARCHIVED IN ICE CORES IS DERIVED FROM DIFFERENT COMPONENTS SUCH AS CHEMICAL SPECIES, INSOLUBLE PARTICLES, ISOTOPES FOR THE WATER MOLECULE, AND GASES FOR AIR BUBBLES.

ICE CORES ARE USED TO STUDY THE PAST CLIMATE BECAUSE THEY ARCHIVED DIFFERENT INFORMATION ABOUT THE PAST.

THAT ARCHIVED INFORMATION IS USED TO RECONSTRUCT THE PAST, PAST CLIMATE AND PAST ENVIRONMENTAL CONDITIONS.

- WE CAN OBTAIN PROXIES OF:
- PAST TEMPERATURES
  - PAST AEOLIAN ACTIVITY
  - PAST ATMOSPHERIC CIRCULATION
  - PAST POLLUTION
  - PAST ATMOSPHERIC CONCENTRATION OF GREENHOUSE GASES [CO<sub>2</sub>, CH<sub>4</sub>, N<sub>2</sub>O]
  - PAST DUST CONCENTRATION
  - PAST SEA ICE EXTENT
  - AMON OTHERS

BACTERIAL CELL SIZE IS AROUND 1 MICROMETER (1 MICROMETER = 0.0001cm) SAMPLES ARE PROCESSED IN CLEAN-COLD ROOMS TO PREVENT CONTAMINATION

TOP DEPTH: 1833 MT THAT CORRESPOND TO 10,824-105 years before present

BOTTLES THAT TO 10 before present



# Chapter 3. Earth Systems Processes

## Authors and Contributors

### Federal Coordinating Lead Author

**Adam Terando**, US Geological Survey

### Chapter Lead Author

**L. Ruby Leung**, Pacific Northwest National Laboratory

### Agency Chapter Lead Authors

**Renu Joseph**, US Department of Energy

**George Tselioudis**, NASA Goddard Institute for Space Studies

### Chapter Authors

**Lori M. Bruhwiler**, NOAA Global Monitoring Laboratory

**Benjamin Cook**, NASA Goddard Institute for Space Studies

**Clara Deser**, National Center for Atmospheric Research

**Alex Hall**, University of California, Los Angeles

**Benjamin D. Hamlington**, NASA Jet Propulsion Laboratory

**Andrew Hoell**, NOAA Physical Sciences Laboratory

**Forrest M. Hoffman**, Oak Ridge National Laboratory

**Stephen Klein**, Lawrence Livermore National Laboratory

**Vaishali Naik**, NOAA Geophysical Fluid Dynamics Laboratory

**Angeline G. Pendergrass**, Cornell University

**Claudia Tebaldi**, Pacific Northwest National Laboratory

**Paul A. Ullrich**, University of California, Davis

**Michael F. Wehner**, Lawrence Berkeley National Laboratory

### Technical Contributors

**Flavio Lehner**, Cornell University

**Adam S. Phillips**, National Center for Atmospheric Research

### Review Editor

**Gavin Schmidt**, National Aeronautics and Space Administration

### Cover Art

**Ian van Coller**

### Recommended Citation

Leung, L.R., A. Terando, R. Joseph, G. Tselioudis, L.M. Bruhwiler, B. Cook, C. Deser, A. Hall, B.D. Hamlington, A. Hoell, F.M. Hoffman, S. Klein, V. Naik, A.G. Pendergrass, C. Tebaldi, P.A. Ullrich, and M.F. Wehner, 2023: Ch. 3. Earth systems processes. In: *Fifth National Climate Assessment*. Crimmins, A.R., C.W. Avery, D.R. Easterling, K.E. Kunkel, B.C. Stewart, and T.K. Maycock, Eds. U.S. Global Change Research Program, Washington, DC, USA. <https://doi.org/10.7930/NCA5.2023.CH3>

# Table of Contents

<b>Introduction .....</b>	<b>5</b>
 Key Message 3.1	
<b>Human Activities Have Caused the Observed Global Warming .....</b>	<b>5</b>
Anthropogenic Drivers.....	6
Natural Drivers .....	8
Global Surface Temperature Response to Climate Drivers .....	8
 Key Message 3.2	
<b>The Estimated Range of Climate Sensitivity Has Narrowed by 50% .....</b>	<b>10</b>
 Key Message 3.3	
<b>New Data and Analysis Methods Have Advanced Climate Science .....</b>	<b>13</b>
Advances in Earth System Observations.....	13
New Scenarios and Climate Projections .....	14
Large Ensemble Simulations.....	16
Emergent Constraints on Future Projections.....	17
Extreme Event Attribution .....	18
 Key Message 3.4	
<b>Humans Are Changing Earth System Processes .....</b>	<b>18</b>
Natural Variability .....	18
Atmospheric Circulation Changes.....	20
Water Cycle Changes .....	21
Changes in the Carbon and Biogeochemical Cycles .....	23
Changes in the Ocean .....	25
Changes in the Cryosphere .....	26
Sea Level Rise.....	27
Regional-Scale Changes .....	28
 Key Message 3.5	
<b>Humans Are Changing Weather and Climate Extremes .....</b>	<b>30</b>
Extreme Heat and Cold .....	30
Extreme Precipitation and Flooding .....	30
Drought.....	30
Wildfire .....	32
Compound Events .....	32

<b>Traceable Accounts</b> .....	<b>34</b>
Process Description .....	34
Key Message 3.1 .....	34
Key Message 3.2 .....	36
Key Message 3.3 .....	37
Key Message 3.4 .....	41
Key Message 3.5 .....	46
<b>References</b> .....	<b>48</b>

## Introduction

The Earth system consists of the atmosphere, land, oceans, and cryosphere, which interact and cycle energy, water, and essential elements of life such as carbon, nitrogen, and phosphorus. Powered by the sun, these interactions and cycles determine Earth's climate, which naturally varies at a broad range of timescales from days to millennia through diverse Earth system processes.

Since industrialization, human activities have dramatically altered atmospheric composition and land cover, with consequential impacts on climate. Human-caused emissions of greenhouse gases have warmed the planet by trapping more outgoing energy, leading to a change in the net energy balance at the top of the atmosphere. The net increase in energy input warms the surface and the air and increases moisture in the lower atmosphere, resulting in significant changes in Earth system processes, including changes in atmospheric and oceanic circulations, clouds, and precipitation and melting of sea ice, glaciers, and ice sheets. The increase in energy input also provides fuel for increasing the frequency and intensity of extreme weather events such as heatwaves and convective storms.

In recent years, advances have been made in understanding the changes that have already occurred, attributing changes to human influence, and projecting future changes. These advances are facilitated by new and diverse observations, improved models and experiments, and the combination of observations and models to support multiple lines of evidence and inquiry. Building on previous scientific assessments, these advances have enabled scientists to unequivocally attribute the observed global warming to human activities and to narrow by 50% the range of estimated global warming that would be caused by a doubling of atmospheric carbon dioxide concentration. Complementary to Chapter 2, which focuses on past and future climate trends, particularly in the US, this chapter discusses more generally how Earth system processes respond to the drivers of climate change. It begins by introducing the natural and human (anthropogenic) drivers of climate change (KM 3.1). Next, it addresses our understanding of the climate response to those drivers, including the sensitivity of the climate to changing greenhouse gas concentrations and the feedback processes that can amplify or partially counteract the influences of human activities (KM 3.2). Recent advances in observations, modeling, and attribution of climate change are then discussed (KM 3.3). Lastly, changes in Earth system processes that underpin the many facets of global and regional climate change (KM 3.4) and changes in extreme events (KM 3.5) are discussed.

### Key Message 3.1

#### Human Activities Have Caused the Observed Global Warming

Human activities—primarily emissions of greenhouse gases from fossil fuel use—have unequivocally caused the global warming observed over the industrial era. Changes in natural climate drivers had globally small and regionally variable long-term effects over that period.

Shifts in climate at the global scale occur primarily in response to processes that change the balance between incoming solar energy and the outgoing energy radiated from Earth at the top of the atmosphere (TOA). The drivers of change are both natural and human-caused and may be transient or long-lived. Changes in TOA net radiation balance resulting from a perturbation in climate drivers can be quantified in terms of the effective radiative forcing (ERF), measured in units of watts per square meter ( $W/m^2$ ). The main natural drivers of climate change—variations in solar radiation and volcanic aerosols—have negligible contributions to long-term climate forcing.<sup>1,2</sup> Warming from fossil fuel emissions of carbon dioxide ( $CO_2$ ) is expected to last centuries to millennia, because of the slow rate of the natural processes that remove  $CO_2$

from the atmosphere. Changes in climate may be further amplified or diminished through feedbacks in the climate system. Feedbacks are processes changed by the warming that then modify the TOA radiation balance and the overall level of warming. In the surface–albedo feedback, for example, warming melts ice cover over the land and ocean, exposing darker surfaces beneath that absorb more energy rather than reflecting it, contributing to further warming. See Chapter 2 of the Climate Science Special Report<sup>3</sup> for further details on emissions sources, radiative forcing, and ERF.

### Anthropogenic Drivers

#### Well-Mixed Greenhouse Gases

Since the release of the Fourth National Climate Assessment (NCA4) in 2018, global atmospheric abundances of the main well-mixed greenhouse gases (WMGHGs), including CO<sub>2</sub>, methane (CH<sub>4</sub>), and nitrous oxide (N<sub>2</sub>O), have continued to increase (KM 2.1). Atmospheric abundances of halogenated gases have also changed, some increasing and some decreasing due to ozone-depletion policies. Preindustrial to present-day (1750–2019) increases in WMGHG concentrations contributed the bulk of the total human-caused forcing, with increases in CO<sub>2</sub> contributing an ERF of  $2.16 \pm 0.26$  W/m<sup>2</sup>, followed by  $0.54 \pm 0.11$  W/m<sup>2</sup> from CH<sub>4</sub>,  $0.41 \pm 0.08$  W/m<sup>2</sup> from halogenated compounds, and  $0.21 \pm 0.03$  W/m<sup>2</sup> from N<sub>2</sub>O.<sup>2</sup> The ERF due to changes in CH<sub>4</sub> abundance is lower than that due to changes in emissions because of offsetting effects of other chemical constituents as discussed below.

The growth in global atmospheric CO<sub>2</sub> levels since 1750 was primarily driven by direct emissions from human activities such as fossil fuel combustion, cement manufacturing, and land-use change. About 41%  $\pm$  11% of the  $700 \pm 75$  PgC of CO<sub>2</sub> (1PgC = 1 billion metric tons of carbon [GtC]) emissions between 1750 and 2019 remain in the atmosphere today, with the rest absorbed by oceans and the land biosphere.<sup>4</sup>

Methane is considered both a WMGHG and a short-lived climate forcer due to its chemical reactivity and an approximate 10-year atmospheric lifetime. Methane is produced by both natural processes and human activities. Observational evidence points to microbial sources (agriculture, waste, and natural wetlands) as the predominant cause of the observed increase in global growth in atmospheric CH<sub>4</sub> since 2006,<sup>5,6</sup> with a smaller contribution from fossil fuel production.

In addition to its direct effect on radiative forcing, CH<sub>4</sub> also has an indirect influence through its chemical effects on other climate drivers, including CO<sub>2</sub>, ozone, stratospheric water vapor, aerosols, and halogenated gases.<sup>7</sup> This leads to an increased effect of CH<sub>4</sub> on the amount of energy trapped in the Earth system. Over 20 and 100 years, a given mass of CH<sub>4</sub> emissions is about 80 and 30 times, respectively, more efficient at trapping energy in the climate system than the same emitted mass of CO<sub>2</sub>.<sup>2</sup> This comparison of energy trapped due to a given mass of emitted gas compared to the same emitted mass of CO<sub>2</sub> is known as the global warming potential (GWP), and it is always specified for a given time horizon due to the varying chemical lifetimes of non-CO<sub>2</sub> greenhouse gases. For CH<sub>4</sub>, the 100-year GWP is about 30 (relative to a GWP for CO<sub>2</sub> being, by definition, equal to 1 over the same 100-year period).

The increase in atmospheric N<sub>2</sub>O levels since 1750 is small compared to that of CO<sub>2</sub> and CH<sub>4</sub>, although rates have increased in recent years due to increased nitrogen fertilizer use in agriculture.<sup>8</sup> Nitrous oxide has an atmospheric lifetime of about 116 years and is nearly 300 times more efficient at trapping energy than CO<sub>2</sub> over a 100-year period.<sup>9</sup>

Many halogenated compounds, which are primarily manufactured gases, also contribute to climate change. These include chlorofluorocarbons (CFCs), perfluorocarbons (PFCs), and sulfur hexafluoride (SF<sub>6</sub>), with lifetimes of decades to millennia, and hydrogen-containing halogenated compounds like hydrochlorofluorocarbons (HCFCs) and hydrofluorocarbons (HFCs), with lifetimes of months to decades. The atmospheric abundances of most CFCs have continued to decline in response to regulations under the Montreal

Protocol on Substances that Deplete the Ozone Layer and its amendments.<sup>10</sup> Atmospheric levels of HFCs are increasing, while the rates of atmospheric growth of major HCFCs have slowed down in recent years.

### Non-methane Short-Lived Climate Forcers

Short-lived climate forcers (SLCFs) are chemically reactive in the troposphere (lower atmosphere), with atmospheric lifetimes typically shorter than two decades, and include ozone, aerosols, and methane. Most SLCFs are also air pollutants or precursors for air pollution (see KM 14.5). An assessment of the ERF effects for two primary non-methane SLCFs are given below.

**Ozone:** Ozone is a greenhouse gas that occurs naturally throughout the atmosphere and is a harmful air pollutant near the surface (KM 14.1). It is formed in the atmosphere through chemical reactions involving sunlight: in the stratosphere, ozone production occurs via chemical reactions involving the breakdown of oxygen molecules by sunlight, while in the troposphere, it is produced by chemical reactions involving emissions of methane, nitrogen oxides (nitric oxide and nitrogen dioxide), carbon monoxide, and non-methane volatile organic compounds in the presence of sunlight. Increases in human-caused emissions of these precursors since preindustrial times are responsible for increases in tropospheric ozone.<sup>7,11</sup> In the stratosphere, increases in human-caused halogenated ozone-depleting substances (ODSs) have contributed to declining ozone abundances. Over the period 2000–2017, stratospheric ozone concentrations have increased slightly in response to declining ODSs because of the Montreal Protocol and its amendments.<sup>10</sup> The combined changes in tropospheric and stratospheric ozone from the preindustrial era to the present have had an overall warming effect of  $0.47 \pm 0.23 \text{ W/m}^2$ , with a smaller contribution from stratospheric ozone changes.<sup>2</sup>

**Aerosols:** Aerosols are small particles that are emitted directly from human activities and natural processes and are also formed in the atmosphere via reactions involving gaseous precursor emissions. Ice core records indicate that aerosol concentrations increased from the preindustrial era until the 1970s and 1980s, driven by northern midlatitude emissions, and declined thereafter.<sup>10</sup> This decline is attributed to reductions in emissions from Europe and North America due to air quality regulations. Satellite data and ground-based records over the modern period confirm the decline in aerosol concentrations over the northern midlatitude and Southern Hemisphere continents but show increases over South Asia and East Africa.<sup>10,12</sup> Globally, aerosol concentrations have been declining since 2000, driven by reductions in some regions. Aerosols from human activities are also air pollutants (KMs 14.1, 2.1) and influence Earth's radiation balance directly by scattering or absorbing solar radiation, through interactions between aerosols and clouds, and by changing the surface reflectivity when light-absorbing aerosols are deposited on snow and ice. Changes in aerosols over the period 1750–2014 have had an overall cooling effect of  $-1.3 \pm 0.7 \text{ W/m}^2$ .<sup>2</sup> Since NCA4, the uncertainty in total aerosol ERF has been reduced, and it is now *virtually certain* that the total aerosol ERF is negative, as discussed in the Technical Summary of the Working Group I contribution to the Intergovernmental Panel on Climate Change Sixth Assessment Report.<sup>13</sup>

### Land-Use Effects on Surface Albedo

Anthropogenic water storage, agricultural practices, and forest cover changes modify the land surface and alter the surface energy balance. Increased water storage on land reduces surface reflectivity and has a localized cooling effect due to evaporation. Irrigation of crops has a similar localized cooling effect through both increased evaporation and plant transpiration.<sup>14</sup> Forests can induce warming because they absorb surface energy or induce cooling because of transpiration.<sup>15</sup> Deforestation can cause cooling by brightening the surface and increasing ground evaporation, but it may also cause warming by reducing ground shading and plant transpiration.<sup>16</sup> Overall, global changes in land use have contributed a net negative ERF (cooling effect) of  $-0.20 \pm 0.10 \text{ W/m}^2$ .

## **Natural Drivers**

### **Solar Irradiance**

Climate forcing from changes in solar irradiance are small relative to changes in anthropogenic greenhouse gases over the industrial era. Changes in solar irradiance over the period 1750–2019 have contributed an ERF of  $0.01 \pm 0.07 \text{ W m}^{-2}$ .<sup>2</sup>

### **Volcanic Aerosols**

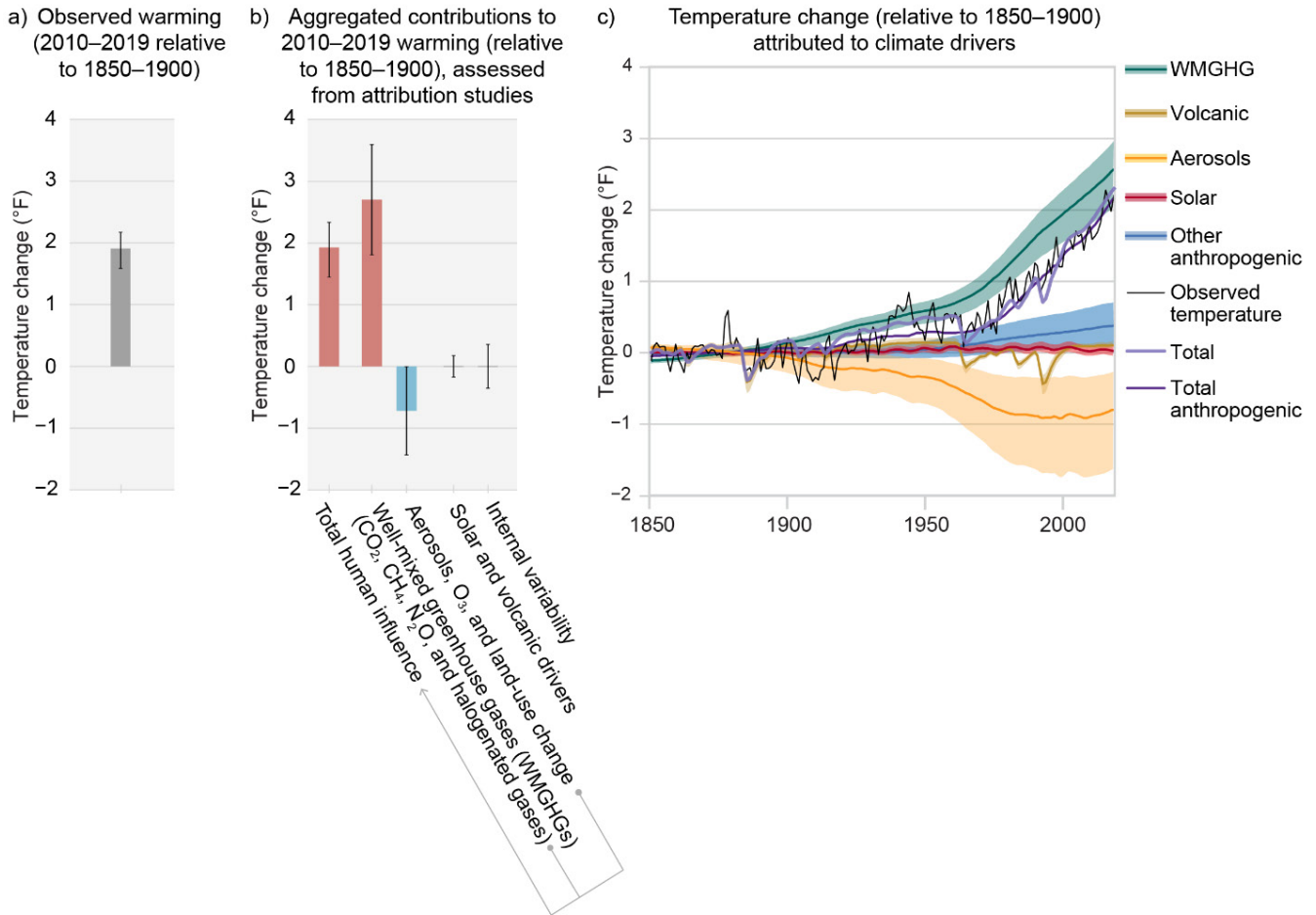
Sulfate aerosols formed in the stratosphere from injections of sulfur dioxide ( $\text{SO}_2$ ) from explosive, episodic volcanic eruptions and more frequent smaller eruptions reduce incoming solar radiation and lead to a cooling effect. Volcanic aerosols can also trigger changes in upper-tropospheric clouds, leading to warming,<sup>17,18</sup> although the magnitude of this effect is highly uncertain.<sup>19</sup> Quantitative assessment of the net ERF over the industrial era for volcanic aerosols shows negligible effects on the long-term temperature trends.

## **Global Surface Temperature Response to Climate Drivers**

A notable recent advance is the quantification of the contributions to global surface air temperature change over the preindustrial to present-day period due to forcings from changes in different climate drivers.<sup>2</sup> Panels a and b in Figure 3.1 show that observed warming in 2010–2019 (compared to 1850–1900) is dominated by contributions from WMGHGs and ozone. This warming has been partially counteracted by the cooling effect from aerosols and land-use change. Because of declining aerosols, the global aerosol cooling effect has weakened since about 1980, and the rate of global warming has increased, mainly due to increasing greenhouse gases (Figure 3.1c). The aerosol cooling effect has a strong regional dependence,<sup>7</sup> contributing to differences in regional climate change (KM 3.4). Natural drivers over the historical period have contributed a small, highly variable cooling effect. Uncertainties in the ERF values, especially of aerosols, contribute to uncertainty in the attribution of observed warming.



### Observed Global Warming and Attribution to Climate Drivers



**The warming observed over the industrial era was driven by emissions from human activities, with greenhouse gas warming partly masked by aerosol cooling.**

**Figure 3.1.** The figure shows (a) observed change in global average surface temperature in 2010–2019 relative to 1850–1900; (b) temperature change over the same period (also relative to 1850–1900) attributed to total human influence, including changes in well-mixed greenhouse gas concentrations (including carbon dioxide [CO<sub>2</sub>], methane [CH<sub>4</sub>], nitrous oxide [N<sub>2</sub>O], and halogenated gases); combined changes in aerosols, ozone (O<sub>3</sub>), and land use (land-use reflectance); and solar and volcanic drivers and natural climate variability; and (c) time evolution of observed temperature (2010–2019, relative to 1850–1900; black line) attributed to different climate drivers from 1850 to 2019, as well as total human influence (“Total anthropogenic”; purple line) and combined natural and human influence (“Total”; lavender line). Whiskers in (a) and (b) show the *very likely* range, while shaded uncertainty bands in (c) show *very likely* (5%–95%) ranges. Note that in (b), the warming effect of ozone is largely offset by the cooling effect of aerosols, resulting in a net cooling when the effects of aerosols, ozone, and land-use change are combined. (a, b) Adapted with permission from Figure SPM.2 in IPCC 2021;<sup>20</sup> (c) adapted with permission from Figure 7.8 in Forster et al. 2021<sup>2</sup> and Figure 2.11c in Gulev et al. 2021.<sup>10</sup>

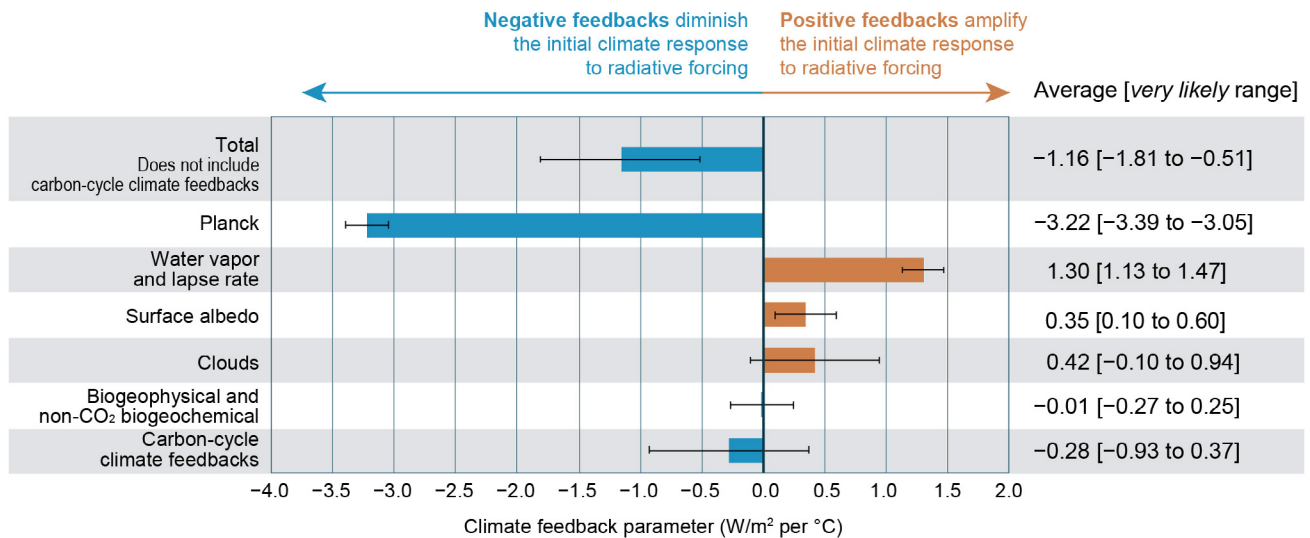
## Key Message 3.2

### The Estimated Range of Climate Sensitivity Has Narrowed by 50%

Recent improvements in the understanding of how climate feedbacks vary across timescales have narrowed the estimated *likely* range of warming expected from a doubling of atmospheric carbon dioxide by 50% to between 4.5°F and 7.2°F (*high confidence*).

The total climate response for a given forcing is an important indicator of the expected climate change impacts. This response is commonly characterized by the equilibrium climate sensitivity (ECS), defined as the change in global average surface temperature after the climate system reaches a steady state following a doubling of the atmospheric CO<sub>2</sub> concentration. A larger value of ECS indicates larger increases in global warming for a given increase in greenhouse gases. ECS depends both on the ERF from a doubling of CO<sub>2</sub> and the sum of climate feedbacks that can either amplify (a positive feedback) or dampen (a negative feedback) the temperature change. The primary feedbacks arise from increased emissions of longwave radiation that cools the warmer planet (Planck feedback); increases in atmospheric water vapor (a greenhouse gas); changes in the vertical profile of atmospheric temperature; reductions in the surface area covered by reflective snow and ice; and changes in cloudiness. Cloud feedbacks are the largest source of ECS uncertainty (Figure 3.2).<sup>2,21</sup> The response of the carbon cycle to climate warming contributes additional uncertainty (KM 3.4).

### Feedbacks in the Climate System



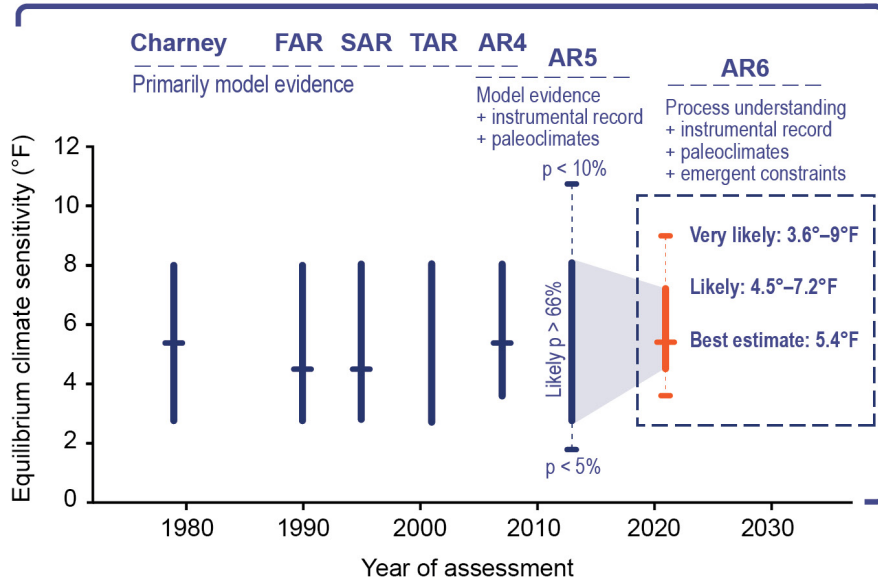
**Multiple feedback processes in the climate system amplify or partially diminish the response to radiative forcing; quantifying their values is necessary to determine the climate response to human activities.**

**Figure 3.2.** The graph shows assessed values of feedbacks acting in the climate system. The total feedback is the feedback that contributes to the assessed value of climate sensitivity. Bars denote the average feedback values, and uncertainties denoted by whiskers represent *very likely* ranges. Negative feedbacks are denoted by blue bars and positive feedbacks by orange bars. The feedback values are estimated by climate models based on the equilibrium change in Earth's energy balance in response to a doubling of carbon dioxide (CO<sub>2</sub>) with and without the feedback processes. W/m<sup>2</sup> is watts per square meter. Adapted with permission from Figure TS.17 in Arias et al. 2021.<sup>13</sup>

The key development since NCA4 is that the ECS uncertainty range has narrowed.<sup>2,21</sup> Recent assessments place ECS between 4.5°F and 7.2°F (2.5°C and 4.0°C), a 50% uncertainty reduction from previous assessments (Figure 3.3). It is *virtually certain* that ECS is greater than 2.7°F (1.5°C), guaranteeing significant climate change impacts from ongoing increases in CO<sub>2</sub> and other greenhouse gases.

### Advances in Understanding Climate Sensitivity and Climate Feedback

The reduced uncertainty in climate sensitivity and climate feedback...



...has been achieved through unprecedented quantitative synthesis of evidence from observed changes over recent decades, the industrial era, and paleoclimate.



#### Uncertainties in climate sensitivity and feedbacks have been reduced by synthesizing multiple lines of evidence.

**Figure 3.3.** The graph (left) shows estimates of equilibrium climate sensitivity (ECS; y-axis) and the considered lines of evidence as a function of the years (x-axis) in which various assessment reports were released. These assessments include the “Charney Report”—a study by an ad hoc US research group that was published in 1979—and the first through sixth assessment reports produced by the Intergovernmental Panel on Climate Change (IPCC), indicated here by the acronyms FAR, SAR, TAR, AR4, AR5, and AR6, respectively. NCA adopts the climate sensitivity values assessed by IPCC reports. Thick vertical bars indicate the *likely* range, and the horizontal tick marks on these bars, where present, indicate the best estimate (tick marks for the AR5 indicate a less than 5% probability of ECS being below 1.8°F and less than 10% probability of being greater than 10.8°F). The reduced estimated range of ECS in AR6 reflects advances in understanding of how climate feedbacks operate across timescales and an improved ability to combine physical constraints with observational data from recent decades, the industrial era, and paleoclimate records. The images of a satellite, the surface temperature time series, and a woolly mammoth (right) are emblematic of these three lines of evidence used to assess climate sensitivity. Adapted with permission from Figure TS.16a in Arias et al. 2021.<sup>13</sup>

This uncertainty reduction results from advances in combining observations and targeted modeling results from nearly independent lines of evidence, each of which generally agrees on the values of ECS. The lines of evidence include 1) observed present-day variations on monthly to interannual timescales from which cloud and other climate feedbacks are inferred; 2) observed temperature changes between the preindustrial period and present and associated relationships to ERF; and 3) estimated temperature and radiative forcing changes for multiple warm and cold periods in paleoclimate records.<sup>21</sup>

Advances since NCA4 include the following:

- Increased use of present-day observations to determine cloud and other climate feedbacks. Confidence in inferring feedbacks for centennial-scale climate changes from present-day variations on monthly to interannual timescales is bolstered by “emergent constraints” found in Coupled Model Intercomparison Project (CMIP) model ensembles (see App. 3).
- Increased use of very-high-resolution cloud-resolving models to determine expected changes in response to the warmer conditions
- Greater understanding of how changes in the spatial distribution of sea surface temperature over the historical period affected climate feedbacks
- Greater availability of reconstructed temperatures and ERF values for paleoclimate and greater confidence in how to account for the state-dependence of climate feedbacks and departures from equilibrium

The reduction of uncertainty in ECS was accompanied by reduced uncertainty in the cloud feedback. There is greater confidence that the sum of feedbacks over all cloud types is positive (i.e., a warming effect) and primarily results from increases in the altitude of high-level clouds and decreases in the amount of marine stratocumulus and continental low-level clouds. A previously identified negative feedback arising from the transition of cloud phase from ice to liquid as the planet warms<sup>22</sup> is now thought to be substantially smaller based on new observational evidence.<sup>23,24</sup>

Importantly, the new assessed range of ECS relies on observational analyses and selected modeling evidence but does not consider the ECS values from climate models directly. Models with ECS values outside of the assessed range are thought to have *unlikely* values of ECS. In particular, the CMIP6 models with ECS values greater than 9°F (5°C) may simulate an unrealistically early timing of reaching a given global warming level (GWL). Despite their unrealistic timings, these models may still be used to estimate the climate impacts occurring at a given GWL.<sup>25</sup>



## Key Message 3.3

### New Data and Analysis Methods Have Advanced Climate Science

A number of scientific developments have enabled deeper understanding of climate processes and their responses to human influence. Observational records have lengthened, and new observing systems have come online. New scenarios of socioeconomic development, and their associated emissions and land-use changes, drive updated climate projections from Earth system models. Large ensemble simulations from multiple models have enabled scientists to better distinguish anthropogenic climate change from natural climate variability. More targeted model evaluation techniques are using observations to narrow the estimated range of future climatic changes. Finally, advances in methods for extreme event attribution enabled scientists to estimate the contributions of human influence to some types of individual extreme events in near-real-time.

#### *Advances in Earth System Observations*

Surface and satellite observational products continue to provide deep insights into recent changes in the Earth system. New analyses based on long-term surface observations provide improved constraints on regional plant productivity and the moderating influences of water and nutrients (e.g., AmeriFlux sites and National Ecological Observatory Network [NEON] domains), on surface and subsurface runoff (e.g., USGS observing networks), on surface energy balance (e.g., Atmospheric Radiation Measurement [ARM] and other Baseline Surface Radiation Network [BSRN] sites), on uncertainty in near-surface temperatures (e.g., Goddard Institute for Space Studies Surface Temperature [GISTEMP]), and on atmospheric CO<sub>2</sub> and related gases (e.g., NOAA Earth System Research Laboratories Global Monitoring Laboratory [NOAA ESRL GML]). In situ measurements of ocean temperature, salinity, and key biogeochemical concentrations are provided by buoys, ship tracks, floats and drifters (NOAA Global Drifter Program [GDP]), and Sailables. Extended records from the Clouds and the Earth's Radiant Energy System (CERES) and Atmospheric Infrared Sounder (AIRS) satellite missions now provide increasing confidence in warming of the Earth's atmosphere and surface. Continued analysis of the now 30-year record of sea level heights from a series of satellite altimeters provides observations of a recent acceleration in sea level rise. However, continuing declines in the number of active in situ precipitation monitoring stations threaten to produce gaps in our precipitation observation record.<sup>26</sup>

Recently deployed observing systems promise a deeper understanding of Earth's physical systems and reduced uncertainty in climate projections. Recent NASA missions include the ECOSystem Spaceborne Thermal Radiometer Experiment on Space Station (ECOSTRESS) thermal imager, focused on vegetation temperature and response to climate stressors; the Global Ecosystem Dynamics Investigation (GEDI) ecosystem lidar, focused on the forest canopy; the Earth Surface Mineral Dust Source Investigation (EMIT) spectrometer; and the Surface Water and Ocean Topography (SWOT) mission in conjunction with the Centre National d'Études Spatiales, the Canadian Space Agency, and the United Kingdom Space Agency, focused on measuring surface water on land and ocean sea surface height. Other recently launched or forthcoming missions include NASA's Time-Resolved Observations of Precipitation structure and storm Intensity with a Constellation of Smallsats (TROPICS) and NOAA's Joint Polar Satellite System-2 (JPSS-2), focused on tropical cyclones and other extreme weather events. Additional frontiers in satellite-based climate monitoring include both hydrological (e.g., snow thickness) and atmospheric (e.g., clouds and atmospheric composition) properties. Besides satellite observations, NASA Jet Propulsion Laboratory's Airborne Snow Observatory (ASO) and its commercial successor have performed numerous snow surveys, enabling extremely detailed

maps of mountain snowpack. Also, recent efforts by USGS on the Next Generation Water Observing System (NGWOS) are enhancing the quality of real-time data on water quantity and quality from fixed and mobile instruments.

Combined with newer algorithms and data assimilation techniques, a growing number of observational data products enable tighter constraints for modern reanalysis datasets, such as Modern-Era Retrospective analysis for Research and Applications, Version 2 (MERRA2) and the European Centre for Medium-Range Weather Forecasts Reanalysis, Version 5 (ERA5). Improvements in the number and quality of observational data products have also enabled new process-oriented metrics and diagnostics (e.g., Leung et al. 2022;<sup>27</sup> Maloney et al. 2019;<sup>28</sup> Simpson et al. 2020<sup>29</sup>), which in turn enhance the validation of Earth system models (ESMs).

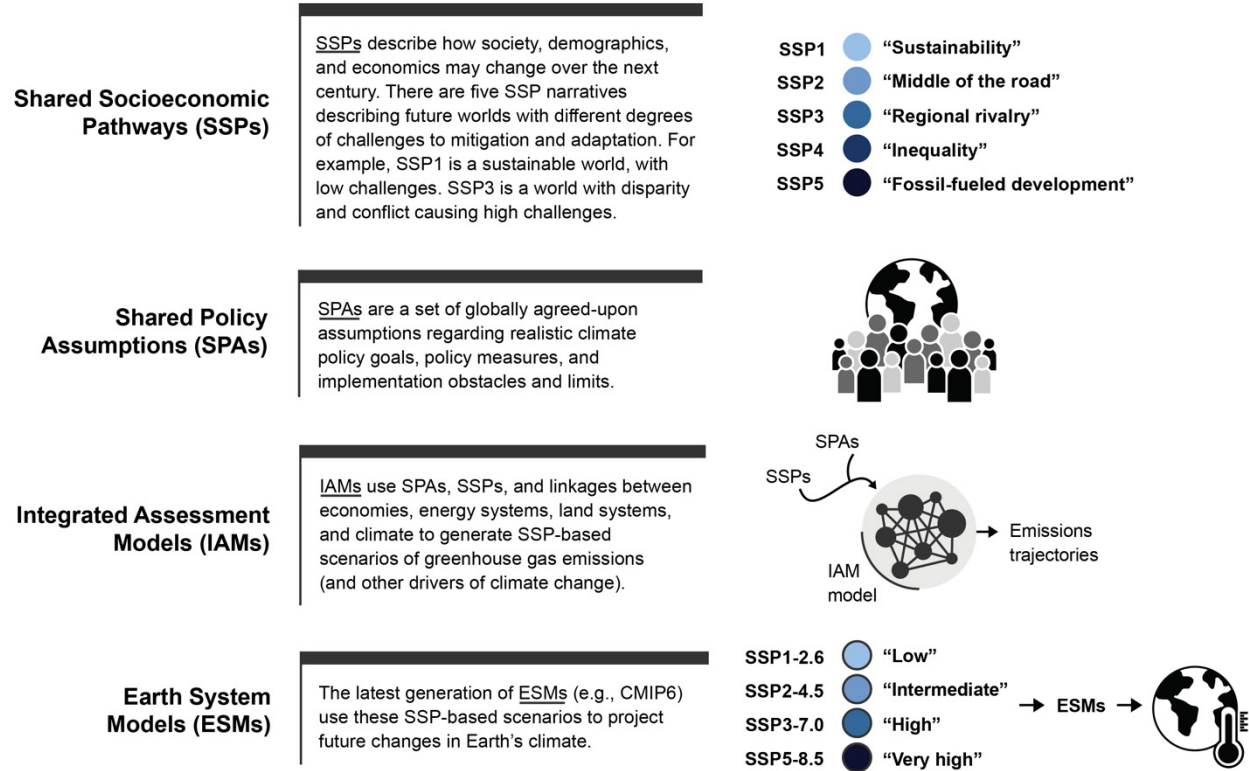
### **New Scenarios and Climate Projections**

A new generation of ESMs has produced an updated set of projections under many new policy-relevant scenarios. A number of ESMs have been run at significantly higher resolution (about 20–50 km) than the previous standard (about 100–200 km) for focused experiments to explore particular aspects of climatic changes, like tropical cyclones, that cannot be simulated by coarser-resolution models.

The Scenario Model Intercomparison Project (ScenarioMIP)<sup>30</sup> organized the main set of 21st-century projection experiments under the latest phase of the Coupled Model Intercomparison Project, CMIP6. These CMIP6 projections used newly developed scenarios based on Shared Socioeconomic Pathways (SSPs; Figure 3.4).<sup>31,32,33</sup> Five SSPs represent alternative plausible trajectories of 21st-century GDP and population growth and the pace and pervasiveness of socioeconomic and technological progress within individual nations and across the world (see Table 3 in the Guide to the Report). SSP-specific drivers are used in integrated assessment models (IAMs) to simulate the corresponding evolution of the energy system and the resulting greenhouse gas trajectories. These are in turn used by ESMs to drive their 21st-century projections. Some of these trajectories are also modified by imposing mitigation policies that meet specific warming targets (e.g., 1.5°C [2.7°F] or 2°C [3.6°F] above preindustrial levels) by the end of the century.<sup>34</sup> Figure 3.4 describes this process step-by-step.

Note that the mitigation assumptions in the various scenarios are not directly relatable to the mitigation discussion in Chapter 32, where the analysis is specifically centered on the current mitigation targets of the US in view of the Paris goals. The stringent goals of net-zero CO<sub>2</sub> emissions by 2050 that Chapter 32 discusses for the US are, however, consistent with the lowest scenario adopted in ScenarioMIP.

## SSP-Based Scenarios and Their Use in Climate Model Projections



**Projections of future climate involve a multistep process using scenarios about future socioeconomic developments, policy goals, and emissions to drive Earth system models.**

**Figure 3.4.** The graphic shows the chain of development leading to Earth system model experiments under CMIP6 ScenarioMIP, the most up-to-date 21st-century climate change projections. Five societal development pathways (the SSPs) were produced. Then, assumptions about climate mitigation policies that could be consistently applied to those socioeconomic futures were developed (the SPAs). Integrated assessment models took these baseline or mitigated pathways and produced alternative plausible trajectories of greenhouse gas emissions and land-use change. Earth system models used those emissions and land-use changes as inputs to produce the new CMIP6 scenarios of climate outcomes. Figure credit: Pacific Northwest National Laboratory, NOAA NCEI, and CISSSS NC.

The new scenarios are labeled “SSPX-Y,” where SSPX (with X ranging from 1 to 5) identifies the SSP used to produce the greenhouse gas trajectories and Y indicates the magnitude of the radiative forcing by 2100 in  $W/m^2$ . The main 21st-century trajectories from the CMIP6 ensemble are SSP1-2.6, SSP2-4.5, SSP3-7.0, and SSP5-8.5, along with SSP1-1.9, the lowest emissions trajectory, which is designed to stay below 1.5°C (2.7°F) of warming above preindustrial levels. These scenarios are intended to provide a representative set of plausible alternative pathways of greenhouse gas and aerosol emissions and land-use changes, according to alternative societal and economic development trends over the 21st century. Three new scenarios correspond to three of the Representative Concentration Pathway (RCP) scenarios used in CMIP5 in their overall forcing levels (SSP1-2.6 with RCP2.6, SSP2-4.5 with RCP4.5, and SSP5-8.5 with RCP8.5), albeit with different details in their composition of gases and land use. Scenario projections can be used to explore climate outcomes under a coherent future trajectory of greenhouse gases and other anthropogenic forcings.

An alternative perspective on the effects of climate change uses GWLs as an organizing principle. One can ask when a certain GWL will be reached for a given scenario and climate model, thus connecting the two perspectives. CMIP6 includes many experiments performed by many ESMs at about 100 km resolution.<sup>35</sup> A multimodel approach, the High Resolution Model Intercomparison Project (HighResMIP),<sup>36</sup> is featured for the first time in CMIP6 to systematically investigate the impact of horizontal resolution. Models par-

icipating in HighResMIP have resolutions between 20 and 50 km and show more realistic simulations of intense storms and resulting precipitation.<sup>37,38</sup> At these resolutions, they can explicitly represent tropical cyclones,<sup>39,40,41</sup> and their simulations support the conclusion of a global decrease in tropical cyclone frequency<sup>42</sup> together with an increase in intensity with warming. Their more refined topography also enhances their representation of local processes, such as the effects of warming on mountain snowpack—an important water source for the western United States.<sup>43</sup>

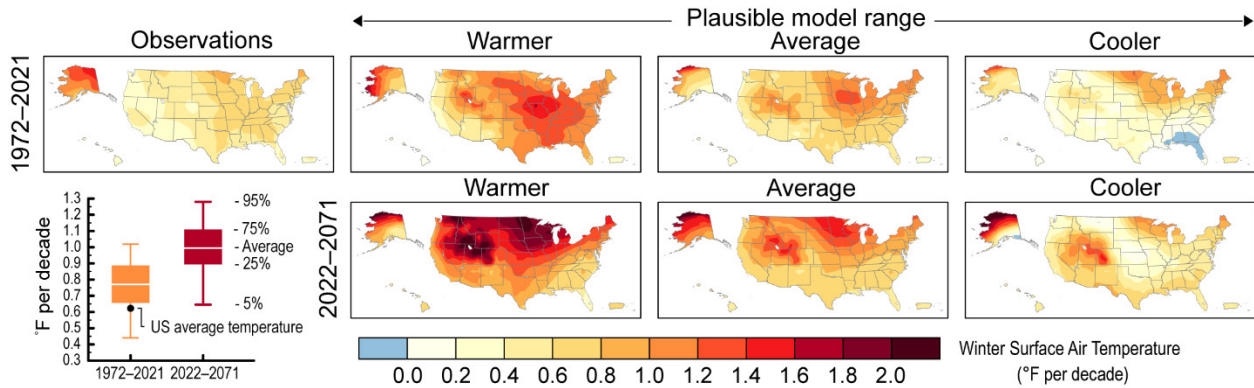
Storyline simulations are another strategy to develop future projections.<sup>44,45,46</sup> In one variation of this approach, ensembles of short initialized weather hindcast simulations under imposed warming conditions can provide actionable information at regional or local scales.<sup>47,48,49</sup> Longer multiyear simulations can also be performed to understand changes in the statistics of weather extremes and storm characteristics (e.g., Chen et al. 2023;<sup>50</sup> Gutmann et al. 2018<sup>51</sup>) or to explore future change in climatic extremes such as drought (e.g., Ullrich et al. 2018<sup>52</sup>).

### **Large Ensemble Simulations**

Many realizations of the past and future climate are generated from climate model simulations started from initial conditions that are slightly perturbed from one another. These small random perturbations, the so-called butterfly effect, can subsequently alter the chaotic sequence of weather and climate events and, hence, the future course of the variability simulated by the model. Recently, climate model experiments have been conducted using multiple climate models with small random perturbations at the start of the simulations. The advent of these initial-condition large ensembles (henceforth referred to as large ensembles) in climate modeling provides an explicit framework for quantifying the relative contributions of external drivers and natural variability to regional climate change by sampling different possible sequences of natural variability that share a common forced response.<sup>53</sup> The application of large ensembles to assess the possible range of climate trends at local and regional scales is a major advance in recent years (Figure 3.5). New experiments from multiple climate models that capture uncertainty due to natural variability, changes in variability, and model uncertainty have improved our ability to understand and quantify expected climatic changes and the relative contributions of human-caused climate change and natural climate variability at regional scales. A new insight from the large ensemble archive is that different models have different representations of natural climate variability and how such variability responds to anthropogenic climate change. For some variables, such as precipitation, variability consistently increases with global warming, and large ensembles provide important context for quantifying and understanding these changes.



## Winter Surface Air Temperature Trends in Large Ensemble Simulations



**Large ensemble simulations provide a plausible range of trends in winter surface air temperature combining the human-caused climate change and natural variability. The observed trend falls within the range simulated by the large ensemble for the historical period.**

**Figure 3.5.** This figure shows past and projected future trends (in °F per decade) in winter (December–February) average air temperature over the United States and its territories (except the US-Affiliated Pacific Islands [USA-PI]). The top row shows the observed trends during 1972–2021 (panel labeled “Observations”) and the plausible model range of trends simulated by the CESM2 100-member Large Ensemble during 1972–2021 (panels labeled “Warmer,” “Average,” and “Cooler”). Here, “warmer” means the ensemble member with the 5th largest US-average trend, “cooler” means the ensemble member with the 5th smallest US-average trend, and “average” means the average trend across all 100 ensemble members. Note that the model range results from the combined influences of simulated natural variability and human-caused climate change. The bottom row of maps shows the plausible model range of trends simulated by the Community Earth System Model 2 (CESM2) 100-member Large Ensemble projected for 2022–2071 under the SSP3-7.0 radiative forcing scenario (panels labeled “Warmer,” “Average,” and “Cooler”; see above for definitions). White areas on the maps are major lakes, including Great Salt Lake, Lake Okeechobee, and Lake Tahoe. Trend values in the USAPI (not shown) are very similar to those for the Hawaiian Islands. The box plot at the lower left shows the distribution of US-average trends simulated by the CESM2 100-member Large Ensemble for the period 1972–2021 (orange) and projected for the period 2022–2071 (red). The thin white line within each box denotes the average value, and the boundaries of the box show the 25th–75th percentile range. The black dot shows the observed US-average trend during 1972–2021, which lies within the plausible model range of trends. Figure credit: National Center for Atmospheric Research.

## Emergent Constraints on Future Projections

An approach to reduce uncertainty in climate change projections has matured over the past decade. It is known as “emergent constraints.”<sup>54</sup> The term refers to strong statistical relationships between highly uncertain future climate parameters and observable trends or variations in the current climate, along with a physical explanation of this relationship. Observations of the current climate are used to quantify the difference between simulated and observed values in a model simulation (referred to as model bias) and subsequently constrain the future climate parameters. Research on emergent constraints has targeted a wide variety of geophysical processes.<sup>55</sup> For example, projections of western US runoff in CMIP5 models can be constrained by the observed sensitivity of runoff to precipitation in the historical climate.<sup>56</sup> A linear relationship between the projected summer warming and the model warm bias over the central US in CMIP5 models can be used to correct the future temperature projections,<sup>57</sup> and the observed interhemispheric asymmetry of the intertropical convergence zone has been used to correct future projections of California winter precipitation.<sup>58</sup>

## Extreme Event Attribution

The science of evaluating the effects of human-caused climate change on extreme weather and climate events has advanced significantly. Human influence has changed the frequency and intensity of some types of extreme events, and it is now possible to quantify the influence of anthropogenic climate change on certain types of specific extreme events.

Extreme event attribution quantifies the current human influence on observed severe weather events, primarily through changes in magnitude and frequency.<sup>59</sup> Recent methodological advances have widened the classes of weather events analyzed and extended these analyses beyond single events to include hazards throughout an entire season (e.g., Herring et al. 2022,<sup>60</sup> 2019,<sup>61</sup> 2018;<sup>62</sup> Reed et al. 2022;<sup>63</sup> Wehner et al. 2019<sup>64</sup>). Confidence in attribution statements is increased when multiple methods, observations, and models lead to similar conclusions<sup>65</sup> and similar underlying trends are detected.<sup>66</sup>

Recent methodological advances include graphical methods to identify cause and effect pathways,<sup>67</sup> using physical insight to inform statistical models,<sup>68,69</sup> factual and counterfactual simulations,<sup>70</sup> and large ensembles.<sup>71</sup> The CMIP5/6 databases are often used in event attribution studies, but the relative coarseness of the model grids (100 km or more) limits applicability to large-scale events such as certain heatwaves<sup>72</sup> and winter storms.<sup>73</sup> Finer-scale events such as intense storms are often amenable to storyline hindcast simulations (see New Scenarios and Climate Projections above), using higher-resolution regional models to compare the “storm that was” with observed climate change to the “storm that might have been” without the human changes to the climate system.<sup>74,75</sup> However, by construction, such storyline analyses inform attribution statements about changes in the magnitude of an event not the frequency.

Attribution methods have advanced such that rapid statements can be made just weeks after an event<sup>76,77</sup> and even forecasted,<sup>78</sup> and these analyses could be made operational.<sup>79</sup> Despite recent progress, the human influence on some extreme weather events may not be attributable because of model limitations.<sup>80,81</sup>

Extreme event attribution has shown that some extreme events are happening with greater frequency, magnitude, and duration due to anthropogenic climate change. For example, climate change *very likely* made a 2016 extreme precipitation event in Louisiana heavier<sup>77</sup> and increased both precipitation<sup>82,83,84</sup> and flooding<sup>85</sup> during Hurricane Harvey. While these studies reveal how climate change affects extreme events, they also reveal that historical observations of climate are often insufficient for characterizing future risks.

### Key Message 3.4

#### Humans Are Changing Earth System Processes

Human activities cause changes throughout the Earth system, including the land surface, cryosphere, ocean and atmosphere, and carbon and water cycles. The magnitude, and for some processes the direction, of these changes can vary across regions, including within the US. These changes also occur against a background of substantial natural climate variability.

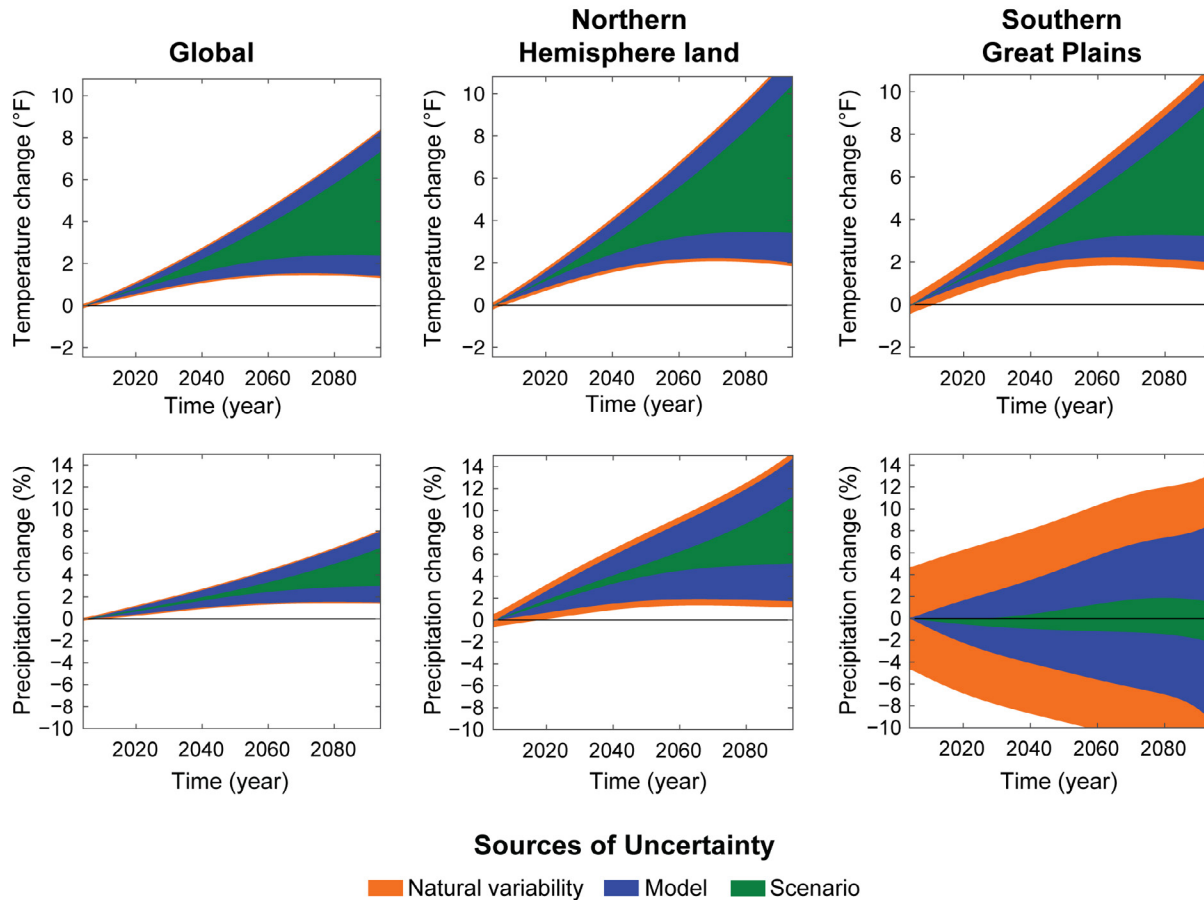
#### Natural Variability

At all spatial scales, the climate response is forced by anthropogenic drivers, which are *external* to the climate system. This response occurs against a background of *natural* climate variability (i.e., *internal* to the climate system). Such variability is generated by natural processes, for example, by atmosphere–ocean interaction (e.g., El Niño and La Niña events), atmosphere–land interaction, or chaotic variability within the atmosphere itself. Depending on the sequencing and magnitude of natural variability and the magnitude

of the climate change response, natural variability can mask the climate change signal, amplify it, or be overwhelmed by it. Natural variability therefore adds uncertainty to climate change projections. Because the sequencing of natural variability is largely unpredictable, this component of uncertainty in climate change projections is irreducible. This is in contrast with the uncertainty associated with the climate change response, which arises from lack of information about future greenhouse gas and aerosol emissions, as well as incomplete understanding of climate processes and associated limitations in terms of how well models reproduced observed changes. These are knowledge gaps that can, in principle, be filled (KM 3.2).

The magnitude of natural variability generally increases as spatial scales decrease (Figure 3.6). At the scale of a typical Earth system model (ESM) grid cell, natural variability is the dominant source of uncertainty in precipitation and temperature projections over much of the US. On continental scales, model and scenario uncertainties become more important.<sup>86</sup> Therefore, at the regional scales and the multidecadal time horizons relevant for adaptation planning, uncertainty due to natural variability can be a larger contributor to overall uncertainty in climate change than model or scenario uncertainties (Figure 3.6; e.g., Dong et al. 2021<sup>87</sup>). Furthermore, it is important to note that anthropogenic forcing also changes the variability of some Earth system processes, and these forced changes contribute to changes in the frequency, duration, and intensity of extreme events, such as heatwaves and heavy precipitation.

## Natural Variability and Climate Model and Scenario Uncertainties



The sources of uncertainty in climate projections vary depending on timescale and geographical scale and for different aspects of the climate system.

**Figure 3.6.** These charts show the relative importance of different sources of uncertainty (natural variability, model uncertainty, and scenario uncertainty) for projections of moving decadal average temperature (**top row**) and precipitation (**bottom row**) for the globe (**first column**), Northern Hemisphere land (**second column**), and the Southern Great Plains (**third column**) from 1999 to 2099 (decadal averages are plotted mid-decade; for example, the x-axis starts in 2004) relative to the reference period of 1995–2014, based on CMIP6 models. Model uncertainty is calculated as the variance across models' forced response estimates. Scenario uncertainty is calculated as the variance across multimodel averages for different scenarios. The shadings are constructed as a symmetric 90% range around the multimodel, multiscenario average projection. Figure credit: Cornell University, National Center for Atmospheric Research, and Pacific Northwest National Laboratory.

## Atmospheric Circulation Changes

Past and future climate changes in the United States are strongly modulated by atmospheric circulation features such as the semipermanent North Pacific and North Atlantic subtropical high-pressure systems, the Aleutian Low, the meandering jet stream stretching from the North Pacific to the North Atlantic, extratropical storm tracks and fronts, and the North American Monsoon. These regional- to continental-scale circulation features are in turn modulated by even-larger-scale overturning circulations such as the Hadley cell (see Perlwitz et al. 2017<sup>88</sup>). Regional circulation features over North America are also modulated by recurring remote patterns of variability such as the El Niño–Southern Oscillation (ENSO) and North Atlantic Oscillation and by variability due to the chaotic dynamics within the atmosphere (the so-called butterfly effect).



Anthropogenic forcing alters the vertical and horizontal energy and moisture distributions in the atmosphere. Atmospheric circulation is directly impacted by the resulting changes in the temperature gradient from the equator toward the poles (both in the lower and upper troposphere), the decrease in the rate that temperature falls with height above the surface, and increased latent heating.

A synthesis of observational and modeling studies estimates that the tropics have widened by about 0.5° of latitude per decade since 1979. Although climate models driven by external forcing simulate, on average, a larger expansion rate than observed, the observed rate is within the bounds of the model simulations.<sup>89</sup> The discrepancy between the observed and simulated rates of tropical widening is partly due to patterns of natural variability such as ENSO and the Pacific Decadal Oscillation, as well as natural atmospheric variability.<sup>90,91</sup>

Consistent with the tropical expansion, climate models project poleward shifts of the jet streams and storm tracks and poleward expansion of the subtropical dry zones with warming,<sup>88</sup> with associated impacts on the US. However, the Northern Hemisphere jet shifts are regionally and seasonally dependent (e.g., Oudar et al. 2020;<sup>92</sup> Zhou et al. 2022<sup>93</sup>). Simulations show a poleward jet shift in the central North Pacific with warming, along with an eastward jet extension that steers more Pacific storms toward California.<sup>94,95</sup> However, large uncertainty remains because the jet extension is also influenced by natural variability.<sup>87</sup> With global warming shifting the North American westerly jet poleward throughout the warm season, climate models project late-spring wetting and late-summer drying in the Midwest.<sup>96</sup> Poleward expansion of the North Atlantic subtropical high may intensify and extend the Great Plains low-level jet poleward, affecting warm-season precipitation in the Midwest.<sup>97</sup>

Besides changes connected to the tropical expansion, climate models project a weakening of the North American Monsoon with warming due to increased atmospheric stability.<sup>98</sup> Similar to other monsoon systems, the onset of North American Monsoon rainfall is projected to be delayed by warming.<sup>99,100,101</sup> In the North Pacific, warming is projected to reduce the frequency of atmospheric blocking during winter.<sup>102</sup>

### Water Cycle Changes

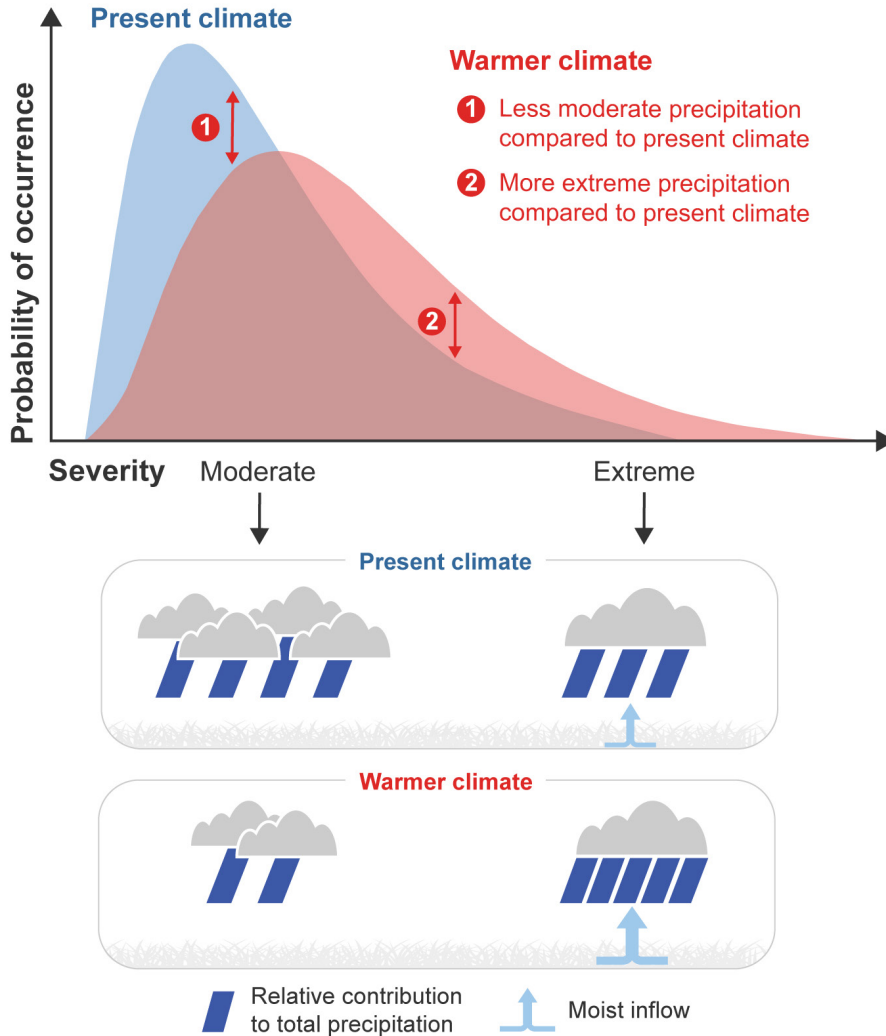
Many processes relevant to the water cycle have already begun to change and are projected to continue changing as the planet warms. These include the atmospheric circulation changes noted above as well as changes in atmospheric moisture, patterns of natural variability, the magnitude of variability of the water cycle, and the modulating role of vegetation on evaporation. These changes are driving changes in the intensity of precipitation in extreme events; snowfall, snowpack, and snow melt; and the seasonality of average precipitation and evaporation.

Seasonal and annual average precipitation and evaporation patterns have been changing with global warming. Precipitation from extreme events is projected to increase with warming (e.g., Neelin et al. 2017<sup>103</sup>). Heavy precipitation events constitute a large fraction of total precipitation and also a large fraction of the change in precipitation in both observations and projections.<sup>104,105,106,107</sup> However, it is possible to have increases in extreme precipitation but decreases in annual average precipitation at the same location due to large declines in non-extreme precipitation (Figure 3.7)<sup>98,108,109</sup> and overall changes in the variability of precipitation. Precipitation variability generally is projected to increase at all timescales and in most locations in response to anthropogenic forcing.<sup>110</sup> This implies increases in both heavy precipitation extremes and drought,<sup>111</sup> a phenomenon called whiplash.<sup>112</sup>

Water vapor factors into the intensity of precipitation extremes, such that increased water vapor due to warmer air temperatures alone would drive relatively uniform projected increases in precipitation extremes over much of the planet. Additionally, changes in circulation modulate the spatial pattern of extreme precipitation intensity change, increasing it in some regions and reducing it in others.<sup>113</sup> For extratropical cyclones

in summer, precipitation intensity increases, and more energetic convective storms are projected despite weakening circulation.<sup>114</sup> While understanding of these changes in extreme precipitation has improved, recent work has also highlighted the oftentimes large magnitude of natural variability in extreme precipitation (KM 3.5).

### Changes in the Contributions of Moderate and Extreme Events to Total Precipitation with Warming



**As the climate warms, extreme precipitation events become more intense and make up a larger fraction of total precipitation, while moderate events become less common.**

**Figure 3.7.** The graphic depicts example changes in the precipitation distribution at many locations as projected by climate models. **(top)** In general, warming shifts the distribution toward a greater probability of large events and a reduced probability of light to moderate events, with only a modest change in the average total precipitation over a season or year. **(bottom)** Greater levels of water vapor in the atmosphere in a warmer world drive more precipitation during storms, when moist air masses converge. The increased water vapor convergence, or moist inflow, in very stormy areas also transports more water vapor out of surrounding areas, reducing any light to moderate precipitation there. The changes in total precipitation are often modest, because they reflect this tug-of-war between opposing changes in heavy and light to moderate precipitation. Changes in circulation can also affect the changes in all parts of the precipitation distribution. Certainty in projected changes differs among the underlying processes: the increase in water vapor and associated increase in extremes is very certain, while the changes in circulation are less certain. Further discussion related to top panel can be found in Fischer and Knutti (2016).<sup>115</sup> Figure credit: Cornell University and University of California, Los Angeles.

Changes in precipitation seasonality can occur with or without changes in average annual total precipitation. Increases in the amplitude of the precipitation seasonal cycle may be expected, as precipitation increases proportionally to its present-day seasonal cycle. However, other changes in the seasonal cycle of precipitation have also been found. Examples of these changes include a sharpening of the seasonal cycle in California,<sup>112,116,117</sup> a substantial increase in late-spring precipitation and a substantial decrease in late-summer precipitation in the US Midwest,<sup>96</sup> and a delayed onset of rainfall in many monsoon regions.<sup>100,101</sup>

Even if precipitation increases in some regions in the future, one concern is that evaporation will increase with warming, leaving the land surface drier (also see Ch. 4). Model projections and observational analyses for the US suggest that the net effect will be for warming to increase evaporation and surface drying in much of the country.

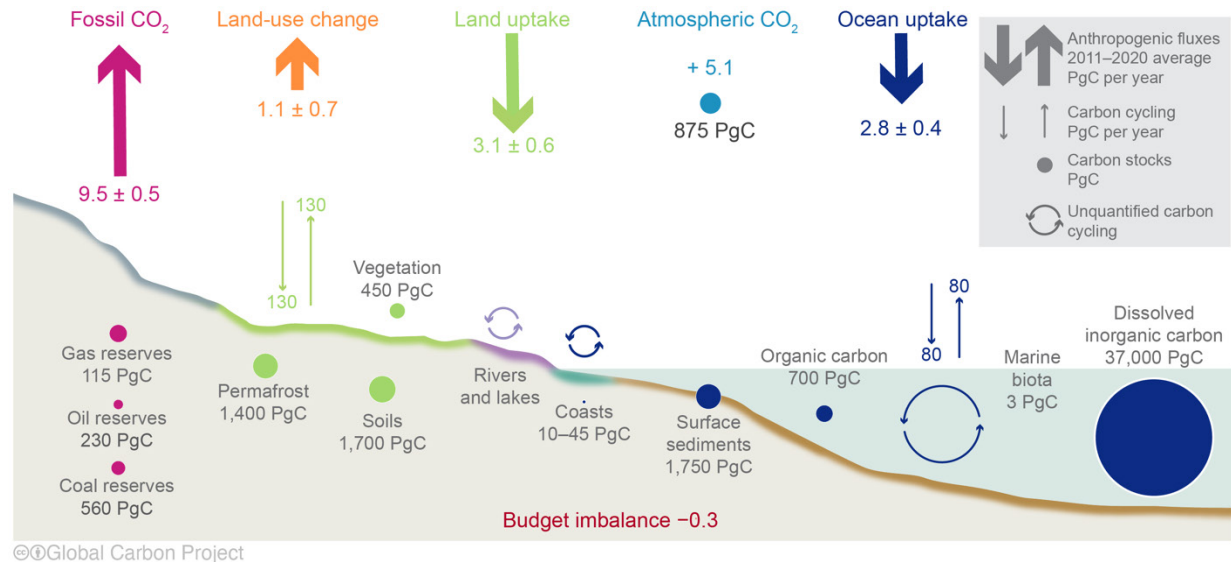
With warming temperatures, more precipitation falls as rain instead of snow. Snowpack in many mountainous regions of the US has already decreased on average over the last few decades; for example, the western US snowpack-driven reservoirs are already exhibiting changes.<sup>118</sup> These declines are expected to be exacerbated by greater increases in winter temperatures compared to summer temperatures in some regions due to snow albedo feedbacks. Another factor that decreases snowpack is the larger temperature increases at higher altitudes, which increase the frequency of multiyear snow droughts.<sup>119</sup> Decreases in warm-season streamflow have also been observed and projected because of the increase in evaporation with warmer temperatures.<sup>120,121,122</sup> Decreasing snowpack and increases in flooding are both concerns for water management. Increasing flooding is driven by the increasing intensity of extreme precipitation discussed above, by the shift from snowfall to rainfall, and potentially also by increases in rain-on-snow events, which can lead to rapid snowmelt (for one example, see Box 29.2).

### **Changes in the Carbon and Biogeochemical Cycles**

Understanding of the biogeochemical responses to human-caused greenhouse gas emissions has increased due to expanded observations and improvements in models. However, uncertainty in the future evolution of the global carbon cycle remains high (KM 2.3).

Terrestrial ecosystems and the oceans take up a little more than half of the CO<sub>2</sub> emitted from human activities, partially offsetting the climate effects of carbon emissions. From 2011 to 2020, annual emissions averaged  $10.6 \pm 1.2$  PgC, and the emitted carbon was ultimately distributed between the atmosphere (47%), vegetation and soils in terrestrial ecosystems (29%), and the oceans (24%; Figure 3.8).<sup>123</sup> Over the past six decades, the average fraction of anthropogenic CO<sub>2</sub> emissions that has accumulated in the atmosphere has remained nearly constant at 41%, even as fossil fuel emissions have rapidly increased.

## Carbon Dioxide Sources and Sinks



While the land and ocean take up some of the carbon dioxide from human activities, the rest continues to accumulate in the atmosphere every year.

**Figure 3.8.** The primary sources of anthropogenic carbon are fossil fuel and land-use change emissions (upward thick arrows). While the land biosphere and ocean continue to take up the same proportion of anthropogenic carbon every decade (downward thick arrows), atmospheric carbon dioxide (CO<sub>2</sub>) levels continue to rise as fossil fuel and land-use change emissions continue over time. Represented here is the budget of the global carbon cycle each year from estimates averaged globally for the decade 2011–2020, with flux estimates from Canadell et al. 2021.<sup>4</sup> Values are in Petagrams of carbon (PgC). Adapted from Friedlingstein et al. 2022<sup>123</sup> [CC BY 4.0].

An important question is whether the same fraction of fossil fuel emissions will continue to be offset by ocean and land biosphere uptake or whether the offset will slow or reverse over time. Answering this question depends on understanding feedbacks between the carbon cycle and climate change. The additional carbon sink on land is a consequence of multiple ecosystem processes, including increased photosynthesis responses to rising atmospheric CO<sub>2</sub>,<sup>124</sup> nitrogen deposition, fire suppression, and forest regrowth after disturbances such as land clearing for agriculture.<sup>125</sup> Large-scale observational constraints on increased vegetation productivity due to increased atmospheric CO<sub>2</sub> are uncertain.<sup>126</sup> Ocean waters take up an increasing amount of carbon due to chemical dissolution of CO<sub>2</sub> in seawater, biological fixation through photosynthesis, shell formation in some organisms, and subsequent transport of carbon into deeper waters.

As atmospheric CO<sub>2</sub> increases, plant productivity and soil carbon also increase and are partly responsible for increases in land carbon storage, which functions as a negative feedback on climate change. However, several processes could reduce terrestrial carbon uptake, including increasing temperature and drought frequency or intensity, limitation of other necessary nutrients, and land-use changes such as deforestation. In the Arctic, potentially large biogenic releases of CO<sub>2</sub> and CH<sub>4</sub> to the atmosphere due to permafrost thaw—the timing of which may be accelerated by increasing wildfire at high latitudes<sup>127</sup>—could be a potentially large positive climate feedback that may alter the effectiveness of climate mitigation strategies.<sup>128</sup> ESMS predict a total loss of near-surface permafrost by 2100 for intermediate (RCP4.5) and very high (RCP8.5) emissions scenarios, and permafrost carbon emissions are projected to outpace increased carbon uptake from higher vegetation productivity in a warmer Arctic.<sup>129</sup>

Uptake of CO<sub>2</sub>, an acid gas, by oceans leads to acidification of seawater through a series of chemical reactions that lower the pH and availability of carbonate ions in addition to other chemical changes (see



Chapter 2 for ocean acidification trend) that have been shown to be harmful to marine life.<sup>130</sup> Over time, uptake of carbon could slow as ocean waters become saturated with dissolved CO<sub>2</sub>.<sup>131</sup> Recent observations show that ocean carbon processes are starting to change in response to the growing ocean carbon sink, and these changes are expected to contribute to future weakening of the ocean carbon sink under medium to high emissions scenarios (similar to SSP2-4.5 and SSP5-8.5 of Figure 3.7 in Jiang et al. 2019<sup>132</sup>).<sup>133</sup>

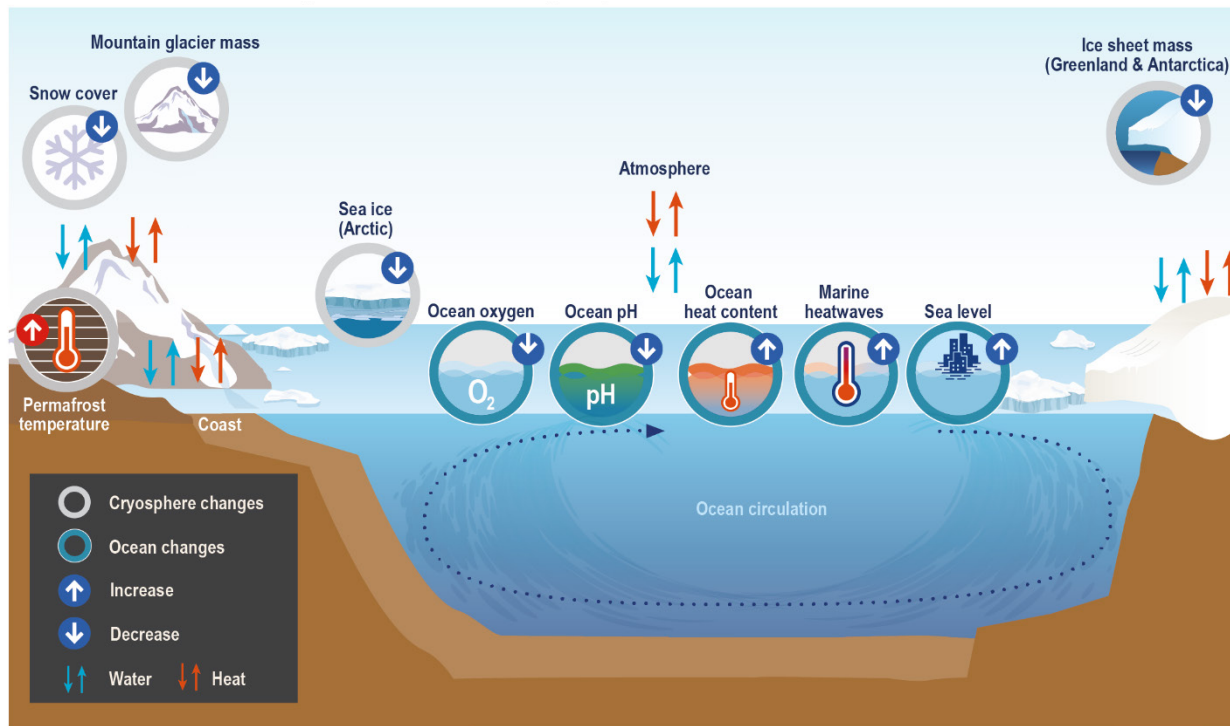
A comparison between the CMIP5 and CMIP6 generation of ESMs with respect to the representation of the CO<sub>2</sub> fertilization effect and carbon cycle–climate feedbacks suggests that uncertainties in these processes have remained large and virtually unchanged in recent years.<sup>134</sup> However, the latest generation of land models have improved representation of biogeochemical cycles,<sup>4</sup> and ocean models have exhibited improved representation of coupled physics and biogeochemical cycles.<sup>135</sup>

In the United States, the land carbon sink is dominated by forests, which have expanded in the last century due to fire exclusion in the West and to secondary forest regrowth following agricultural abandonment in the East. The growth of the North American forest biomass carbon sink is expected to become more saturated and less effective over time (Focus on Western Wildfires).<sup>125,136</sup> The climate change–wildfire relationship is also expected to play an increasingly dominant role in the strength of the US land carbon sink, requiring increased management of forests to meet carbon storage and other needs of society.<sup>137</sup> In addition, increasing temperature and moisture in some regions could lead to increased microbial emissions of CH<sub>4</sub> from wetlands and Arctic tundra.

### **Changes in the Ocean**

The ocean has a large capacity to store and release heat and has been able to absorb 91% of the excess heat attributed to greenhouse gas emissions.<sup>2</sup> The ocean both exchanges heat with the atmosphere and moves heat from the tropics toward polar regions, where warm surface ocean waters transform into cooler, high-density waters that sink (Figure 3.9),<sup>138</sup> taking high carbon concentrations with them.<sup>139</sup> The Atlantic Meridional Overturning Circulation (AMOC) is an important component of the global ocean circulation, transporting heat and carbon and affecting hydroclimate, hurricane activity, and coastal sea level. It is hypothesized from some proxy evidence that the AMOC has declined since the Industrial Revolution.<sup>140</sup> It remains uncertain whether observations support the anthropogenically forced weakening of the AMOC during the past four decades predicted by climate models.<sup>141</sup>

## Changes in Ocean, Cryosphere, and Coastal Processes



Climate change has multiple effects on the ocean, atmosphere, and cryosphere and their complex interactions.

**Figure 3.9.** The figure shows important physical processes that play a role in the ocean and cryosphere, along with their linkages. Associated climate change–related effects, including sea level rise, increasing ocean heat content, ocean acidification, marine heatwaves, and ice mass loss, are also shown. The arrows indicate an exchange taking place between ice, ocean, and atmosphere. Adapted with permission from Figure TS.2 in IPCC 2019.<sup>142</sup>

On short timescales (annual to decadal), ocean circulation dominates the pattern of changes in ocean heat content; although on longer timescales, the spatial pattern is primarily associated with the addition of excess heat into the ocean.<sup>143</sup> Since 2005, Argo profiling floats have provided observations of temperature and salinity changes in the global ocean to a depth of 2,000 m. These measurements show an increase in global ocean heat content, although there is geographic variability. On shorter timescales, marine heatwaves are periods of extreme high ocean temperature relative to the long-term average seasonal cycle.<sup>144</sup> Persistent marine heatwaves have been observed in the northeastern Pacific since around 2014,<sup>145,146,147</sup> with associated negative impacts on ocean ecosystems (Ch. 27; Figure 10.2).

### Changes in the Cryosphere

The cryosphere is the frozen part of the Earth system and includes ice sheets, glaciers, sea ice, permafrost, and snow (Figure 3.9). Observations of the cryosphere have expanded in recent years, including from satellites like Gravity Recovery and Climate Experiment Follow-On (GRACE-FO) and Ice, Cloud, and Land Elevation Satellite-2 (ICESat-2).<sup>148</sup> These and other complementary observations of the cryosphere show declines in ice sheet and glacier mass, snow cover, and Arctic sea ice.<sup>149</sup> Through efforts like the Ice Sheet Mass-Balance Inter-comparison Exercise (IMBIE),<sup>150</sup> there is clear evidence of loss of ice sheet mass from 1993 to 2020, and the rate of loss has increased for both the Greenland and Antarctic ice sheets. There is increased consensus regarding the behavior of many ice sheet processes. However, as the climate warms, the future response of the ice sheets and some associated processes are still uncertain.<sup>149</sup> Two specific processes, marine ice cliff instability<sup>151,152</sup> and marine ice sheet instability,<sup>153,154,155,156,157</sup> could lead to rapid

ice sheet loss over several decades, but the physical processes that would result in these instabilities and how they would progress once triggered remain uncertain. The decline in sea ice affects several critical functions: sea ice serves to regulate climate by reflecting solar radiation; inhibits ocean–atmosphere exchange of heat, momentum, and gases; and supports global deep–ocean circulation, polar species, and livelihoods of people in the Arctic.

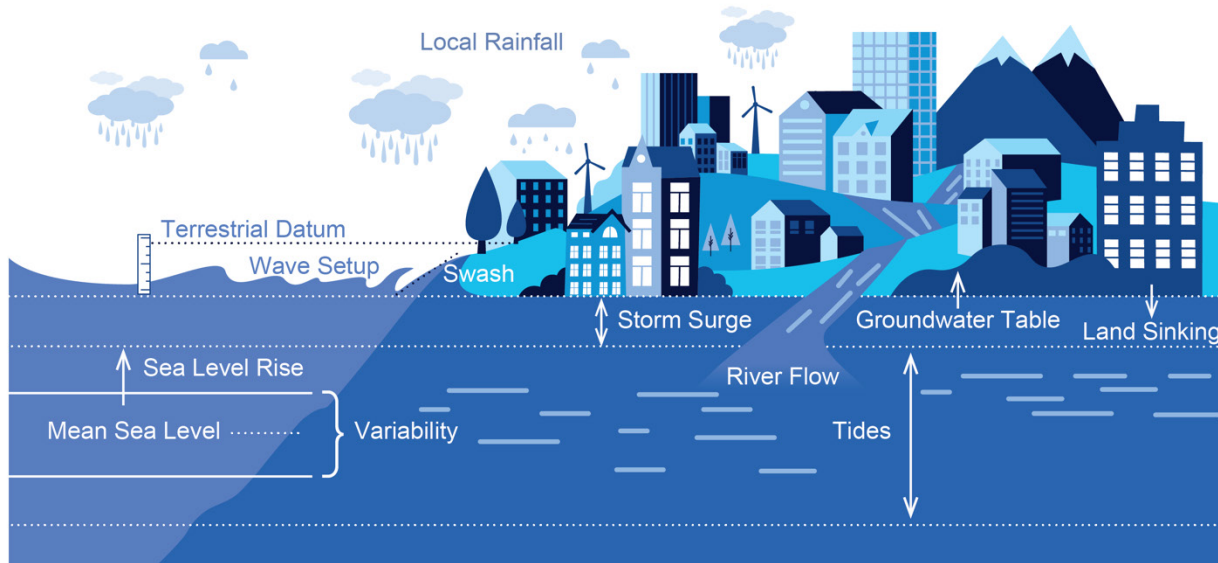
## Sea Level Rise

Over long time periods, the main drivers of changes in global mean sea level (GMSL) are thermal expansion due to heating of the ocean and the addition of water associated with melting ice from ice sheets and glaciers. Human-caused changes in the movement of water between ocean and land, including from groundwater depletion and water impoundment associated with dam building, have a minor impact on GMSL, although they can increase in importance for specific time periods.<sup>158</sup> The increase in GMSL during the 20th century estimated from tide-gauge records has been explained by the individual processes contributing to it.<sup>158</sup> The rate of the 20th-century increase in sea level was faster than in any other century in at least the last 3,000 years.<sup>159,160</sup> In the past two decades, the changes in GMSL measured by satellite altimetry have matched the expected sea level rise based on the combination of in situ measurements of the Argo profiling floats and the observations of water-mass change from the GRACE and GRACE-FO satellites. Data from the now three-decades-long satellite altimetry record shows that the rate of GMSL rise has been increasing, driven by accelerating contributions from the underlying processes.<sup>158,161,162</sup>

Sea level rise is not uniform across the globe. Relative sea level rise at any specific location responds to processes that are important at regional and local scales.<sup>149,163,164,165</sup> On short timescales and in short records, natural variations on interannual to decadal timescales can affect estimates of rates and accelerations. Over long time periods, there are three main causes of regional variations in relative sea level: 1) steric dynamic changes (the combination of thermal expansion and ocean dynamics that is driving global sea level rise); 2) gravitational, rotational, and deformational changes that result from water moving from the cryosphere to the ocean; and 3) vertical land movement (subsidence or uplift) due to glacial isostatic adjustment, tectonics, sediment compaction, groundwater and fossil fuel withdrawals, and other non-climatic factors.<sup>166,167</sup>

An improved understanding of the drivers of regional mean sea level rise and how processes combine to cause sea level change at the coast has led to better assessments of the frequency, duration, and timing of high-water levels and coastal flooding events (Figure 3.10).<sup>167</sup> Regional sea level change has been the main driver of changes in extreme water levels.<sup>167</sup> Due to ongoing regional relative sea level rise and narrowing of the gap between the typical high tide and flooding threshold, the frequency of high tide flooding has increased. Natural ocean variability, including that associated with tides and large-scale climate signals that did not necessarily result in flooding in the past, is expected to lead to a rapid increase in the amount of high tide flooding in the coming decades when combined with future sea level rise (see Ch. 9).<sup>167,168,169</sup>

## Coastal Flood Exposure



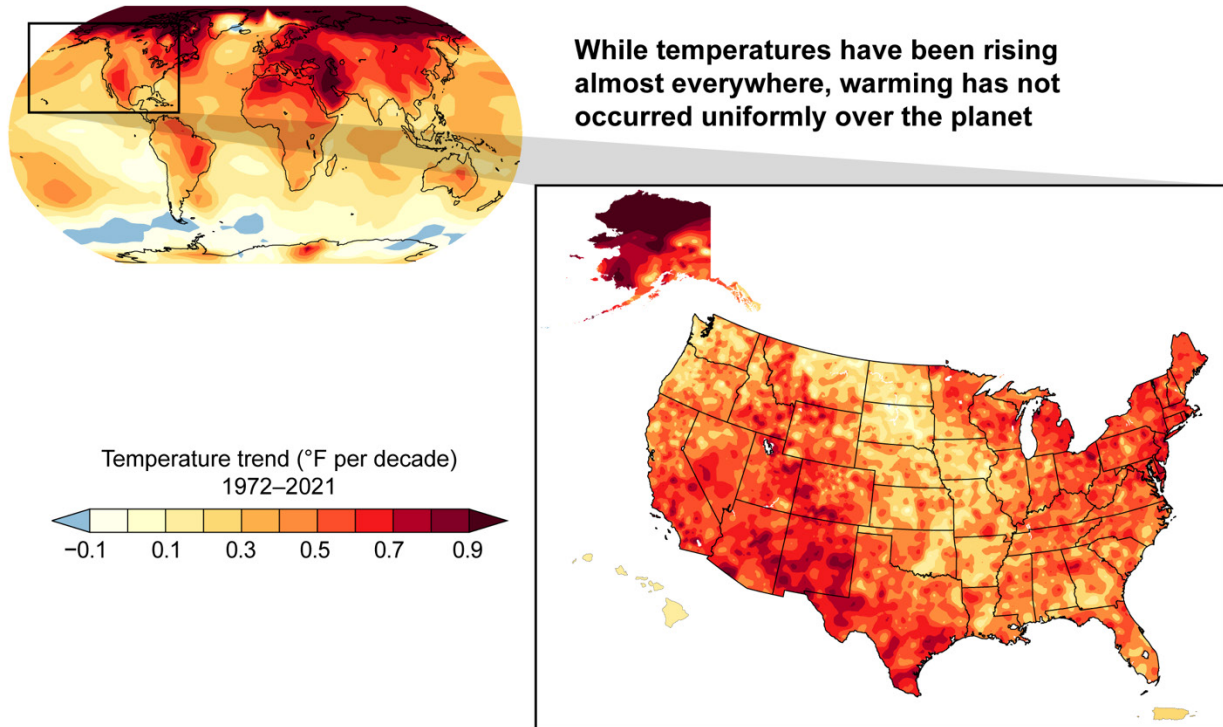
**Sea level rise is increasing the probability of coastal flooding and associated impacts.**

**Figure 3.10.** The schematic shows the physical factors affecting coastal flood exposure. Nearshore processes like storm surge, wave setup (the increase in water level due to the presence of breaking waves), and swash (wave runup and wave rundown) combine with other large-scale processes to drive impacts. Due to the clear and strong relative sea level rise signal—that is, the combination of global increases in sea level and the fact that land is sinking in many US coastal areas—the probability of flooding and impacts is increasing along most US coastlines. Source: Sweet et al. 2022.<sup>167</sup>

## Regional-Scale Changes

Many of the changes in Earth system processes discussed above can vary across a range of spatial scales. For example, at the continental scale (less than 10,000 km), the climate system's warming response to anthropogenic forcing is affected by differences in how quickly land and ocean areas warm, with land generally warming more quickly than the ocean. This is because land areas have a lower heat capacity and thus respond more quickly than the ocean to anthropogenic forcing, and because of the larger cooling effect of evaporation from the ocean surface. Therefore, North America generally warms more than adjacent oceans (Figure 3.11). The high latitudes of the Northern Hemisphere warm the most of any region, although the reasons for this are complex and may involve processes poorly captured by global climate models.<sup>170</sup> Precipitation responses, arising from the changes in the atmospheric circulation and water cycle processes discussed above, tend to be organized in latitude bands such as the tropics, subtropics, midlatitudes, and high latitudes.

## Regional Differences in Climate Response



**While temperatures have been rising almost everywhere, warming has not occurred uniformly over the planet.**

**Figure 3.11.** The maps show observed global (left) and overland US (right) trends (in °F per decade) in annual average near-surface temperature over the period 1972–2021. While temperatures have been increasing almost everywhere, warming has not occurred uniformly over either the planet or the US. Temperatures over land have been increasing faster than over the ocean, and the Arctic has been warming at more than twice the global average rate. Temperatures over the US have increased faster in Alaska, at high elevations, and in regions with significant seasonal snowpack. Figure credit: University of California, Los Angeles; University of California, Davis; NOAA NCEI; and CISS NC.

At the regional scale (less than 1,000 km), variations in land surface properties are associated with differences in the local climate responses to anthropogenic forcing. Examples from the US (Figure 3.11, US panel) include greater warming at snow margins in western US mountains,<sup>171</sup> greater warming in inland areas separated from the coast by California mountain ranges,<sup>172</sup> greater warming in extremely arid landscapes,<sup>173</sup> shifts of precipitation downwind in mountainous areas,<sup>174</sup> snowfall loss at higher elevations where temperatures increase above the freezing line,<sup>175,176</sup> changes in snowmelt-driven runoff as a function of elevation,<sup>177</sup> changes in snowfall over large lakes,<sup>178</sup> and changes in evaporation and soil moisture due to variations in vegetation. Regional variations in the changes of temperature and precipitation are also driven partly by the regional distributions of aerosols, which interact with clouds and radiation.<sup>179</sup> Downscaling techniques, which convert global model outputs from lower resolution (about 100 km) to high resolution (1–10 km), are often used to simulate these phenomena for adaptation planning (see App. 3).



## Key Message 3.5

### Humans Are Changing Weather and Climate Extremes

Human activities are affecting climate system processes in ways that alter the intensity, frequency, and/or duration of many weather and climate extremes, including extreme heat, extreme precipitation and flooding, agricultural and hydrological drought, and wildfire (*medium to high confidence*).

#### **Extreme Heat and Cold**

Changes in temperature extremes in recent decades are driven primarily by trends toward warmer conditions rather than any changes in variability.<sup>180</sup> Consequently, the frequency and intensity of cold extremes have declined over much of the United States while the frequency and intensity of extreme heat have increased.<sup>181</sup> Arctic warming may also drive increases in the occurrence and persistence of circulation anomalies that are related to extreme cold and heat,<sup>182</sup> although the evidence that these mechanisms have played a role in recent events is mixed.<sup>183,184</sup> Climate change may also be contributing to “false spring” events,<sup>185</sup> where early warming has caused early budbreak and flowering of plants, exposing them to damaging frost and freeze events.<sup>186</sup>

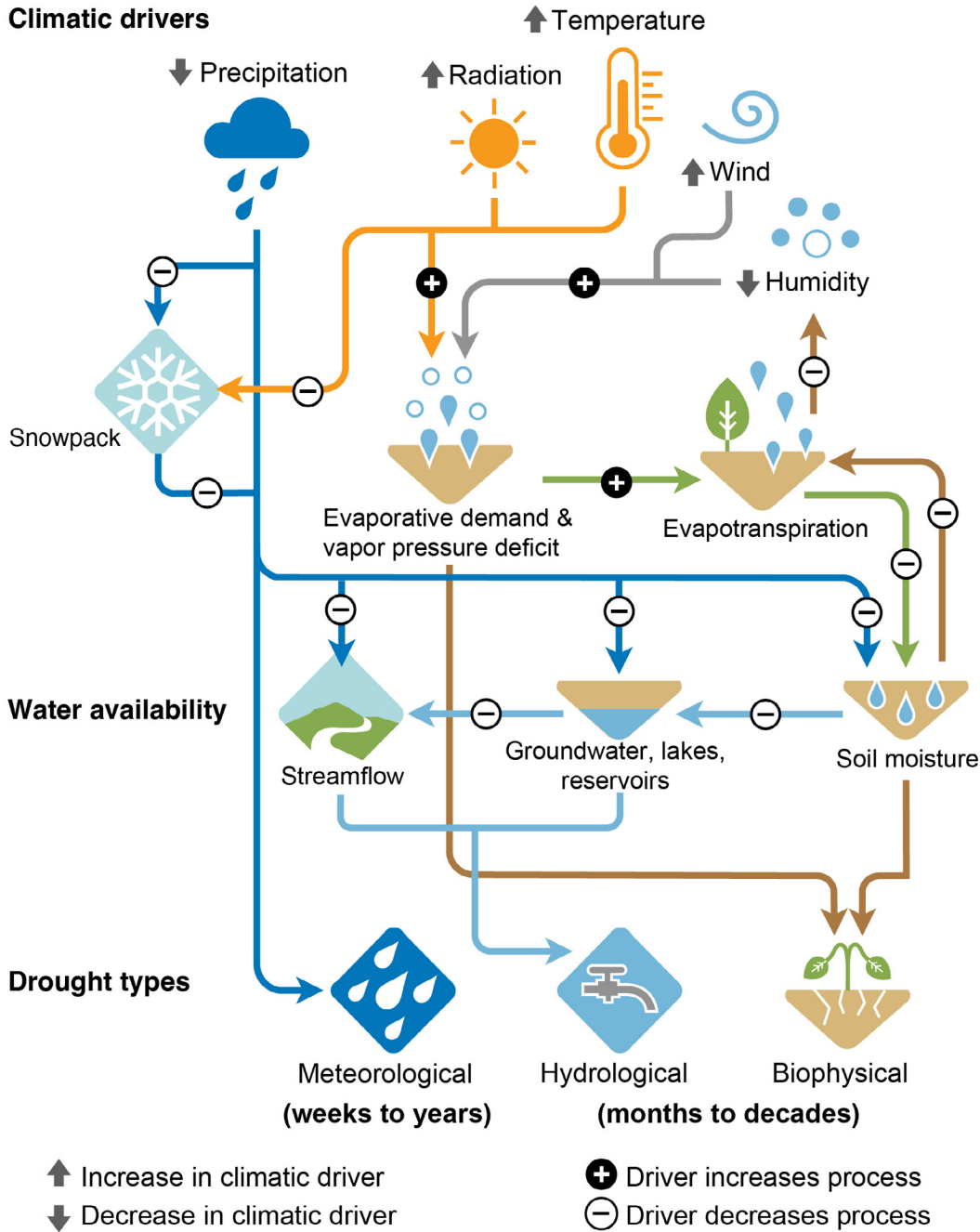
#### **Extreme Precipitation and Flooding**

Observed increases in extreme precipitation intensity at the continental scale in North America have been, for the first time, attributed to human influences.<sup>187</sup> With warming, it is expected, and has been documented, that more winter precipitation will fall as rain instead of snow,<sup>188</sup> although the projected intensity of most extreme snowstorms remains uncertain.<sup>189</sup> Projected increases in extreme precipitation events are larger in the winter season since warming in winter is larger, including events related to atmospheric rivers.<sup>190</sup> Precipitation associated with hurricanes increases with warming at least as much as water vapor,<sup>42</sup> and the heaviest events can increase at an even greater rate.<sup>63,191,192</sup> Where and when increases in extreme precipitation manifest in any given year or even decade is strongly subject to natural variability (see also KM 3.3). Notably, increases in extreme precipitation events do not always directly translate to increases in river flooding, in part because of the many processes at the land surface that affect flood events (KM 4.1; Figure 4.8).

#### **Drought**

Drought is broadly defined as a transient period of below-average water availability, typically expressed in terms of fluctuations in precipitation, soil moisture, or streamflow and runoff.<sup>193</sup> Drought is a complex phenomenon (Figure 3.12) that depends on fluctuations in moisture supply, direct losses of moisture to the atmosphere, and ecosystem and land surface processes.<sup>194,195,196</sup> Western North America experienced several decadal-scale droughts during the 20th century<sup>197</sup> and numerous multidecadal “megadroughts” prior to AD 1600<sup>198</sup> and is currently experiencing an ongoing megadrought largely unprecedented over the last 1,200 years.<sup>199,200</sup> See Chapter 6 for more information regarding the effect of changes in the water cycle over land.

### Climatic Drivers of Drought, Effects on Water Availability, and Impacts



**Climate change alters the hydrologic cycle and is expected to increase drought in some regions through various process pathways.**

**Figure 3.12.** Changes in climatic drivers (e.g., precipitation, temperature, wind, etc.) affect different aspects of the hydrologic cycle (e.g., evapotranspiration, snowpack, streamflow, soil moisture). In turn, these hydrologic shifts translate into changes in the severity, frequency, and risk of different drought types. Plus and minus signs denote the direction of change in the driver that would cause increases in drought. For example, where precipitation declines (down arrow), all drought types will increase because this reduces snowpack, streamflow, groundwater and reservoir storage, and soil moisture. Similarly, increasing temperatures (up arrow) are also expected to increase hydrological and biophysical drought by reducing snowpack and increasing evaporative losses from streams, surface reservoirs, and soils. Adapted with permission from Figure 8.6 in Douville et al. 2021.<sup>201</sup>

Observed and projected hydroclimatic changes in response to external forcing are highly season- and region-dependent over the US, especially in the West.<sup>202</sup> Natural variability also plays a prominent role in shaping hydroclimate on annual and decadal timescales,<sup>203</sup> as indicated by the decrease in total area coverage of low soil moisture over the US since 1915<sup>204</sup> and increasing Missouri River flows,<sup>205</sup> a region that is expected to become drier under climate change (e.g., Cook et al. 2015<sup>206</sup>). Climate change is expected to amplify drought, primarily through warming-induced increases in evaporative demand and surface water losses<sup>207,208</sup> and declines in snowfall and water stored in winter snowpack.<sup>43</sup> There is strong evidence that these processes are already amplifying hydrological drought severity in California,<sup>209,210,211</sup> the Pacific Northwest,<sup>212,213</sup> the Colorado River basin,<sup>121,214</sup> and across southwestern North America.<sup>200</sup> However, there are uncertainties in how these processes may present in the future. For example, changes in plant water use in response to increasing temperatures and rising atmospheric CO<sub>2</sub> are complex and poorly understood and may either ameliorate<sup>195</sup> or amplify<sup>215</sup> soil moisture and runoff droughts at the surface.

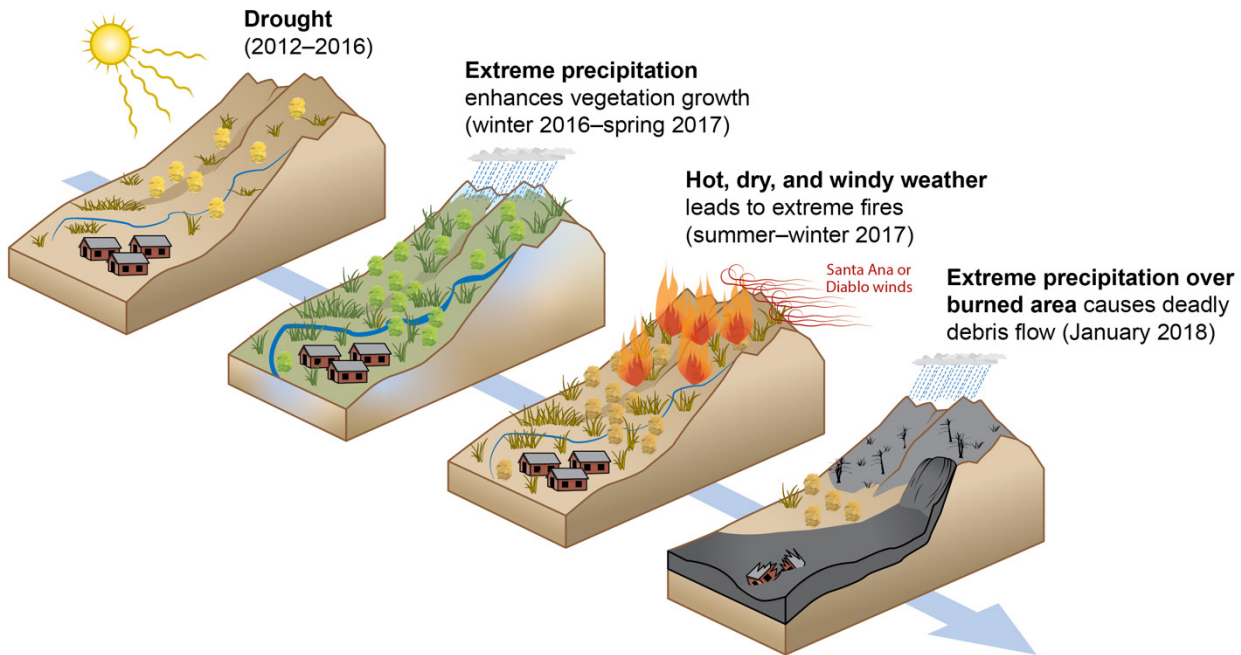
### Wildfire

The direct influence of climate change on modern and future wildfire activity arises from the effect of warming on fuel moisture content and flammability (Focus on Western Wildfires). Flammability is directly related to the vapor pressure deficit (VPD), an integrative measure of atmospheric aridity or dryness. High VPD is strongly associated with the hot and dry weather conditions conducive to the intensification and spread of wildfires, as well as with drier fuels at the surface. In recent decades, warmer temperatures, declines in humidity, and increases in VPD have caused large-scale increases in fire weather<sup>216</sup> and areas burned by wildfire<sup>217,218,219</sup> across the West. From 1984 to 2015, about half of the increase in burned area across the western United States is attributable to increases in fuel flammability caused by anthropogenic climate change. These climate change-driven increases in wildfire burned area are expected to continue into the coming decades, as fuel availability is not expected to be a limiting factor before 2050.<sup>220</sup>

### Compound Events

Compound events refer to the combination of multiple weather or climate events—which individually may not be extreme—that together pose risks to human or natural systems (see example in Figure 3.13)<sup>221,222,223</sup> and are described in further detail in Focus on Compound Events. Since climate change may affect the frequency and magnitude of the individual components of compound events in different ways, changes in compound events can be complex. Recent advances in statistical techniques used to describe compound events<sup>224,225,226,227</sup> offer rigorous ways to quantify changes. Progress has also been made in categorizing compound event types in this rapidly evolving field.<sup>223,228,229</sup>

### Consecutive Events Leading to and Resulting from Wildfires



**Consecutive events caused significant human health and economic impacts in Southern California from 2012 through 2018.**

**Figure 3.13.** A series of events in Southern California produced a cascade of impacts on human health and the economy. These include (from top left to bottom right): a prolonged drought from 2012 to 2016; above-average winter precipitation in 2017, enhancing growth of fuels; a dry, warm spring and summer, reducing moisture levels and drying existing vegetation; record-setting Santa Ana winds; fires occurring shortly thereafter; and rainfall over the burned area, leading to debris flow event in Montecito, CA. Adapted from AghaKouchak et al. 2020;<sup>230</sup> modified with permission from the Annual Review of Earth and Planetary Sciences, Volume 48 © 2020 by Annual Reviews, <http://www.annualreviews.org>.

# Traceable Accounts

## Process Description

Team members were selected from two sources: 1) the pool of nominations received via the public call for authors and 2) candidates identified by the chapter lead author, federal coordinating lead author, and agency coordinating authors from their extended networks and recommendations they received. The team was selected based on a thorough review of nomination packages received, with diversity of background and experience being a primary evaluation criterion for team makeup. Considering the areas of expertise needed for the chapter, as summarized below, selections were made to ensure diverse representation across multiple axes.

- Long-lived and short-lived climate forcers and biogeochemical cycles
- Land-use and land-cover change and biogeochemical cycles
- Climate response and internal variability
- Scenario development
- Climate feedbacks and response
- High-resolution modeling
- Regional climate change
- Climate model diagnostics and metrics
- Extreme event attribution
- Cryosphere and sea level rise
- Precipitation variability and extremes
- Drought and paleoclimate
- Hydrologic and heat extremes

Given that the scoping of this chapter is related solely to physical system processes and not impacts, risks, and vulnerabilities, it was determined early on in the process, and with the consent of the Federal Steering Committee, that stakeholder engagement meetings were not required for the data-gathering process. Authors communicated primarily through email and bimonthly (twice per month) team meetings to discuss chapter progress and any issues arising during the assessment of the literature.

## Key Message 3.1

### Human Activities Have Caused the Observed Global Warming

#### Description of Evidence Base

Evidence of human drivers of global warming is provided by identifying the human-induced components that perturb Earth's energy budget and by understanding how these have evolved over long timescales. The potential for surface warming due to increases in carbon dioxide (CO<sub>2</sub>) emitted from human activities was first identified in the 1800s,<sup>231,232,233</sup> and scientific understanding of the effect of anthropogenic CO<sub>2</sub> emissions on the climate strengthened with more than a century of advances in theoretical developments as well as through laboratory and in situ measurements.<sup>234</sup> The effect of other human drivers on climate, including non-CO<sub>2</sub> greenhouse gases (GHGs), land-use change, and aerosols, was also recognized by the 1970s. Assessment of multiple lines of evidence, including proxy records, ice core records, and direct observations,



provides unequivocal evidence of the role of human activities in increasing atmospheric levels of GHGs and aerosols over the industrial era. For the latest observational evidence of long-term changes in GHG abundances, the reader is referred to Figure TS.9 in the IPCC AR6 WGI Technical Summary,<sup>13</sup> which shows a strong increase in well-mixed greenhouse gases since the 19th century that is exceptional over the long term. Global average annual anthropogenic emissions of these gases reached the highest levels in human history over the present decade based on assessment of multiple lines of evidence.<sup>4</sup>

Human-induced emissions of GHGs alter the atmosphere's radiative balance and lead to a climate response. Earth system model simulations reproduce the observed global surface temperature trend only when human-induced climate drivers are included. Multimodel attribution experiments in support of the different phases of the Coupled Model Intercomparison Project (CMIP) have consistently shown the majority of the observed global warming to be human-induced, while that attributable to natural drivers is small.<sup>235</sup>

### Major Uncertainties and Research Gaps

Although there is *very high confidence* in the measured increases in atmospheric GHGs since preindustrial times, attributing these increases to anthropogenic emissions or natural emissions is subject to some uncertainty (e.g., Saunois et al. 2020;<sup>236</sup> Tans 2009<sup>237</sup>). Fossil fuel emissions of CO<sub>2</sub> have the lowest uncertainty because of the direct relationship between combustion and emissions. Since radiocarbon (<sup>14</sup>CO<sub>2</sub>) is absent in fossil fuels, measurements of atmospheric <sup>14</sup>CO<sub>2</sub> can be compared to CO<sub>2</sub> emissions inventories based on fuel consumption. Comparisons show agreements within the uncertainty bounds of the measurements.<sup>238</sup> However, there are discrepancies between different methods for quantifying CO<sub>2</sub> emissions and uptake related to land-use changes, the size of land uptake in the northern extratropics, and the strength of the ocean carbon uptake over the past decade.<sup>123</sup> For land-use change, a lack of historical land-cover information presents an important limitation. Likewise, inadequate coverage of datasets used to inform models of carbon exchanges between the biosphere and oceans and the atmosphere results in uncertainty for both process-based models and atmospheric inversions.

For methane (CH<sub>4</sub>) emissions and removals, uncertainties are potentially larger than for CO<sub>2</sub>. Emissions of CH<sub>4</sub> are usually the result of unintentional leakage from oil and gas infrastructure or the result of microbial processes that result from agriculture, livestock, or waste treatment. This unintentional leakage makes quantifying emissions using inventory methods difficult. However, measurements of the stable isotope of CH<sub>4</sub> (<sup>13</sup>CH<sub>4</sub>) imply that microbial sources are the primary drivers of recent atmospheric CH<sub>4</sub> growth, with smaller contributions from fossil fuel production. Measurements of <sup>13</sup>CH<sub>4</sub> provide insight into sources, because microbes prefer to use the lighter carbon isotope (<sup>12</sup>C) for metabolism, so an increase in microbial sources will mean isotopically lighter atmospheric CH<sub>4</sub>. Although the atmospheric record of CH<sub>4</sub> (<sup>13</sup>CH<sub>4</sub>) only extends over the last two decades, measurements from ice cores suggest that prior to the recent trend toward isotopically lighter atmospheric CH<sub>4</sub>, the trend was toward isotopically heavier CH<sub>4</sub>, as expected due to isotopically heavier fossil fuel emissions.

Other important sources of uncertainty include difficulty in constraining atmospheric chemical destruction and uncertainty in the distribution and processes determining natural emissions. Studies comparing bottom-up estimates of emissions using inventories and emissions models with estimates from atmospheric inversions highlight uncertainties in the estimates.<sup>236</sup> Other studies using atmospheric observations of stable isotopes of CH<sub>4</sub> have suggested that global fossil fuel emissions are, in all probability, higher than those estimated by inventories.<sup>5,239</sup>

### Description of Confidence and Likelihood

There is *very high confidence* that emissions of GHGs from human activities, fossil fuel use in particular, have unequivocally caused all global warming observed over the industrial era. There is also *very high confidence* that changes in natural climate drivers have had globally small and regionally variable long-term effects over

this period. Observations clearly show that concentrations of major GHGs have increased in the atmosphere since preindustrial times. Uncertainties in natural chemical removals and emissions can be significant. Sporadic changes in natural climate drivers, including solar activity and volcanic eruptions, temporarily influence surface temperatures. However, reconstructions and proxy records do not indicate any evidence of exceptional activity in these climate drivers over the past several hundred years.<sup>10</sup> In sum total, uncertainties in the magnitude and variability of climate drivers are not expected to change the central conclusion that anthropogenic emissions have caused the significant increases in GHGs.

## Key Message 3.2

### The Estimated Range of Climate Sensitivity Has Narrowed by 50%

#### Description of Evidence Base

The assessment of climate sensitivity and climate feedbacks follows that of Sherwood et al. (2020)<sup>21</sup> and Forster et al. (2021),<sup>2</sup> which were subject to review by peers and the community. In this Traceable Account, we provide a summary of the evidence base, major uncertainties, and a description of confidence and likelihood following these assessments. As also shown in Figure 3.3, the major change in these new assessments is to primarily base climate sensitivity estimates on observational data from multiple past periods combined with physical constraints, without directly using the values of climate sensitivity produced by climate models. Satellite observations of natural climate variability were used to provide global estimates of physical climate feedbacks,<sup>240,241</sup> as well as the cloud feedbacks for individual cloud types.<sup>24,242,243,244,245</sup> For many climate feedbacks, emergent constraints<sup>240,246,247</sup> support the practice of inferring long-term climate feedbacks from short-term climate feedbacks inferred from observations of present-day natural climate variability. For changes between the preindustrial period and present day, temperature analyses of in situ data provide confident estimates of global mean temperature changes.<sup>248,249</sup> Combining these temperature changes with estimates of effective radiative forcing for this period yields a preliminary estimate of climate sensitivity acting over the historical period. This preliminary estimate is now thought to be an underestimate of the climate sensitivity for CO<sub>2</sub> doubling because climate feedbacks are sensitive to the pattern of sea surface temperature warming, and the pattern of warming in the historical period differs markedly from that expected for doubling of CO<sub>2</sub>.<sup>173,250</sup> Inferring climate sensitivity from paleoclimate changes relies on accurate estimates of temperature and radiative forcing changes for well-studied stable periods in the past, such as the Last Glacial Maximum (~20,000 years ago),<sup>251</sup> the Mid-Pliocene Warm Period (~3 million years before present),<sup>252</sup> and the Paleocene–Eocene Thermal Maximum (~56 million years before present).<sup>253</sup> To estimate a present-day climate sensitivity from paleoclimatic data, estimates of changes in temperature and radiative forcing must be derived from proxy data. It is also necessary to consider how different ice sheet and continental configurations acted as forcing,<sup>254</sup> as well as the temperature dependence of climate feedbacks.<sup>255</sup>

Synthesizing the implications for climate sensitivity from this extremely diverse body of evidence is nontrivial. Synthesis requires the development of a common framework to treat evidence based on extensions to the forcing–feedback paradigm,<sup>2,21,256</sup> as well as the sustained multiyear interaction of scientists from diverse research communities. Mathematical methods used in synthesis vary from complex Bayesian methods<sup>21</sup> to simpler consistency arguments.<sup>2</sup>

#### Major Uncertainties and Research Gaps

A major uncertainty in the estimate of climate sensitivity involves the pattern of sea surface temperature warming in the Pacific for the long-term forced response to CO<sub>2</sub> doubling.<sup>21</sup> Over the last several decades, the observed pattern of warming has featured smaller warming or even cooling in the East Pacific,

increasing the amounts of low clouds and sunlight reflected back to space and thereby reducing the warming of Earth. It is thought that this pattern in the recent past is due to natural climate variability. It is expected that over the 21st century, the warming in the East Pacific will catch up to and exceed that in the West Pacific, matching the predictions of CMIP models for CO<sub>2</sub>-dominated warming. However, if the observed recent pattern of warming includes a component of the forced response to CO<sub>2</sub> that models fail to predict, then climate sensitivity values at the high end are less likely.

Other key climate sensitivity uncertainties<sup>21</sup> include 1) the scaling ratios between feedbacks estimated from the smaller short-term temperature variability and the larger climate change expected in the 21st century; 2) the cloud feedbacks from cloud types other than the well-studied marine low clouds; 3) the magnitude of aerosol forcing over the historical period, knowledge of which is critical for determining the component of historical warming from GHGs; 4) the abundance of dust and other aerosols in the Last Glacial Maximum; 5) the characterization by proxy records of temperature, trace gases, and other forcing agents for warm periods in the deep geological past; 6) the dependence of climate sensitivity on the background state; and 7) the accounting for Earth system effects when interpreting the consequences of the paleoclimate record for a climate sensitivity applicable to 21st-century warming.

### Description of Confidence and Likelihood

The *likely* ranges of climate sensitivity are derived from the synthesis of the evidence base through the framework of the forcing–feedback paradigm.<sup>2,21,256</sup> Confidence is *high* in the reduced range of climate sensitivity because its observational estimates are derived from three independent lines of evidence and because the three central estimates of climate sensitivity are in general agreement. The three lines of evidence are 1) evidence from natural climate variability in the present day, 2) evidence from the changes in climate from the preindustrial period to the present day, and 3) evidence from the changes in climate from various cold and warm periods in the paleoclimate record. Additional reasons for *high confidence* include a greater understanding of how physical climate feedbacks vary with the nature of changes for different timescales and a greater ability to synthesize diverse evidence from different periods in Earth’s past.

## Key Message 3.3

### New Data and Analysis Methods Have Advanced Climate Science

#### Description of Evidence Base

##### Advances in Earth System Observations

From temperature and precipitation observations that began in the 1800s through the earliest observations of CO<sub>2</sub> concentration taken on Mauna Loa from the late 1950s<sup>257</sup> and into the satellite era,<sup>258</sup> observations of the Earth system have been essential for constraining climate models and improving our understanding of the climate system. Since the last National Climate Assessment was released in 2018, several major advancements in understanding of the Earth system have arisen from observational platforms.

New observations using eddy covariance measurements from AmeriFlux and NEON and subsequent science are described in Novick et al. (2018)<sup>259</sup> and Chabbi and Loescher (2017),<sup>260</sup> respectively. A deeper understanding of the water cycle derived from subsurface and surface runoff from USGS is described in USGS (2019).<sup>261</sup> Improvements in estimating surface energy balance from ARM and other BSRN sites is described in Wild (2017).<sup>262</sup> Better constraints of uncertainty in near-surface temperatures from GISTEMP comes from Lenssen et al. (2019).<sup>248</sup> Understanding of atmospheric CO<sub>2</sub> and related gases comes from NOAA ESRL GML.<sup>263</sup> Understanding of ocean temperature, salinity, and key biogeochemical concentrations comes from buoys, ship tracks, floats, drifters,<sup>264,265</sup> and Saildrones.

Observational evidence to constrain Earth's heating rate from CERES and AIRS is described in Loeb et al. (2021)<sup>266</sup> and Susskind et al. (2019),<sup>267</sup> respectively. Improved evidence of sea level rise using satellite altimetry is documented in Li et al. (2022)<sup>268</sup> and Nerem et al. (2018).<sup>162</sup> Recently deployed NASA and NOAA satellite observing systems are documented in Fisher et al. (2020;<sup>269</sup> ECOSTRESS), Dubayah et al. (2020;<sup>270</sup> GEDI), Green et al. (2020;<sup>271</sup> EMIT), Zavadsky et al. (2017;<sup>272</sup> TROPICS), Goldberg and Zhou (2017;<sup>273</sup> JPSS-2), and Morrow et al. (2019;<sup>274</sup> SWOT). NASA JPL's ASO is described in Painter et al. (2016).<sup>275</sup> The USGS NGWOS system is described in Eberts et al. (2019).<sup>276</sup>

### New Scenarios and Climate Projections

The development of the set of new scenarios used by CMIP6 by the so-called parallel process<sup>277</sup> started while the CMIP5 simulations based on the Representative Concentration Pathways (RCPs) were produced, analyzed, and assessed in IPCC 2013<sup>278</sup> (the stage-setting essay for the new scenarios development is Ebi et al. 2014<sup>279</sup>). The new scenarios are based on plausible future alternative pathways of socioeconomic development (the Shared Socioeconomic Pathways [SSPs]) from which consistent GHG emissions trajectories unfold, as opposed to simply consisting of idealized trajectories of future GHGs. Idealized trajectories (like a 1% annual increase in CO<sub>2</sub> concentrations or an instantaneous doubling of CO<sub>2</sub> concentrations) are useful sensitivity experiments, but they cannot be considered plausible, being decoupled from assumptions about human-caused emissions. About 40 modeling centers from all over the world participated in CMIP6 and ScenarioMIP.<sup>280</sup>

### Large Ensemble Simulations

About a decade ago, the first initial-condition (“large”) ensembles were created (e.g., Deser et al. 2012,<sup>281</sup> 2012<sup>282</sup>) with a single model, followed by other models<sup>283</sup> and large ensembles with up to 100 simulations.<sup>284</sup> Currently there are large ensembles from many other climate models,<sup>53</sup> and the model intercomparison protocol for the most recent generation of simulations encouraged large ensembles of 10 realizations for all models.<sup>30</sup>

Large ensembles are used to estimate uncertainty from natural variability separately from the model uncertainty among climate models.<sup>86</sup> They have revealed the dependence of some aspects of natural variability, like precipitation, on climate state.<sup>110</sup> Large ensembles have also enabled the isolation of the response to different climate forcings, independent of natural variability and assessment of the linearity of these responses<sup>53</sup> or lack thereof.<sup>285</sup> They have also been used to assess whether El Niño–Southern Oscillation (ENSO) events and their impacts on precipitation and temperature over North America will change in the future<sup>286,287,288</sup> and to assess how large-scale atmospheric circulation patterns that affect US weather and climate may be altered by the effects of climate change.<sup>289</sup> Emerging applications of large ensembles include addressing questions related to the timing of when human-induced climate change signals exceed the natural variability of the climate,<sup>290</sup> risk assessment,<sup>291</sup> US water resources,<sup>292</sup> air pollution and associated health impacts,<sup>293,294</sup> and ecosystem stressors<sup>295</sup> (see Deser et al. 2020<sup>53</sup> for other examples).

### Emergent Constraints

Emergent constraints have been widely applied to reduce the simulated spread in the climate feedbacks that shape climate sensitivity.<sup>240,246,247</sup> Emergent constraints have also been applied to many other climate processes (see Hall et al. 2019<sup>55</sup> for a list). Williamson et al. (2021)<sup>296</sup> also provide a recent and comprehensive review of the emergent constraint literature and identify the various uncertainties in the physical and biogeochemical system responses that have been reduced in a credible way through the emergent constraint technique.

### Extreme Event Attribution

Since the landmark study of Stott et al. (2004),<sup>72</sup> which concluded that the chances of the 2003 European heatwave doubled due to anthropogenic climate change, many different author teams have analyzed a wide variety of extreme weather events to identify if there was a human influence. This large body of literature has been developed using many different approaches that have been surveyed by the author team. Of particular interest are a series of special supplements published since 2011 in the *Bulletin of the American Meteorological Society*.<sup>60,61,62,297,298,299,300,301,302,303</sup> Chapter authors have contributed to these reports and have published event attribution studies in the general literature.

Confidence in attributing the human influence, if any, on individual extreme weather events is increased when multiple independent author teams arrive at similar conclusions using different methods, observational estimates, and models, coupled with a thorough understanding of the physical processes of change. The copious amount of precipitation experienced in the greater Houston area during Hurricane Harvey provides a case in point, where three different teams concluded that anthropogenic climate change led to large attributable increases in storm total rainfall.<sup>82,83,84</sup> Confidence in this attribution has been further increased by the subsequent studies of other hurricanes, leading to similar conclusions.<sup>63,78,192,304</sup>

Confidence in an extreme event attribution statement hinges on reliable long-term observations.<sup>66</sup> Fortunately, much of the contiguous US (CONUS) is well observed since 1950 by the NOAA Global Historical Climate Network weather station measurements of temperature and precipitation. In many locations, reliable records span an entire century.<sup>305</sup>

Attribution is an exercise in causal inference; climate change attribution studies borrow techniques from the well-established epidemiology literature. Typical Pearl causal inference experiments involve two groups, a controlled (or placebo) group and a tested group.<sup>306</sup> As there is only one Earth, climate change attribution experiments can be performed only with numerical models. The limitations of climate models impose important caveats on any resulting attribution statements. The CMIP database of global climate models (GCMs) has been extensively used in attribution statements.<sup>307,308</sup> However, it is best suited for extreme events of larger spatial scales matching that of the CMIP models (e.g., heatwaves). More customized numerical experiments at higher resolution may be required for more localized extremes such as intense storms (including hurricanes).<sup>64</sup> Granger causal inference has also been applied to long observational records to make attribution statements without using climate models.<sup>67,309</sup> While a weaker form of causal inference due to the possibility of hidden covariates in the underlying statistical models (i.e., statistical model construction may bias findings), Granger causal inference can add to our understanding of changes in extreme event frequency and magnitude.

## Major Uncertainties and Research Gaps

### Advances in Earth System Observations

Unfortunately, not all quantities relevant to the Earth system can be easily observed. Although recent satellite missions such as GRACE<sup>310</sup> have been able to use gravitational measurements to constrain subsurface moisture, much of the subsurface remains poorly understood. Ongoing work has also suggested that deep-ocean heat content may have been underestimated,<sup>311</sup> a consequence of insufficient measurements of the deep ocean. Further, in situ measurements are generally more available within developed countries and in more easily accessed regions, resulting in significant observational gaps in the Southern Hemisphere (e.g., Guo et al. 2009<sup>312</sup>) and at high elevation.<sup>313,314</sup>

### New Scenarios and Climate Projections

Scenarios of future emissions and land-use change are developed as plausible alternatives, but no relative likelihood is attached to them. Some recent studies, however, have argued that the highest scenario,



SSP5-8.5, is no longer plausible without a reversal of current trends in the adoption of renewables and energy efficiency. The scenario development community is always testing the structural uncertainties of integrated assessment models and, therefore, the assumptions that produce the alternative emissions pathways. Timely updates of the baseline from which future projections are made, on the basis of current trends and observations of emissions, are necessary to maintain the plausibility of alternative pathways.

### Large Ensemble Simulations

Much remains to be done to obtain decision-relevant information at the scale of impacts—regional to local—with quantified uncertainty grounded in understanding of the natural variability, forcing, and structural sources of uncertainty. Identifying the forced pattern of response on local scales and separating it from natural variability is a continuing challenge, which has immediate implications for predictability, climate model evaluation, and the potential to narrow uncertainty in climate projections. Another key challenge is the so-called signal-to-noise paradox, which implies that models underestimate atmospheric predictability due to incomplete representations of key atmospheric and oceanic processes.<sup>315</sup> Thus, as models improve, there may be the potential to deliver more skillful climate predictions. Stakeholder and decision-maker input on what uncertainty is tolerable for specific applications, and what this means for the size of large ensembles, is another outstanding topic. The role of natural variability for many impacts, including air quality, has yet to be fully addressed. Finally, the implications of potential changes in natural variability for decadal prediction and predictability are still open questions. For example, what is the timescale of predictability? How predictable is  $x$  variable on  $y$  timescale?

### Emergent Constraints

Both Williamson et al. (2021)<sup>296</sup> and Hall et al. (2019)<sup>55</sup> identify major research gaps and uncertainties associated with the emergent constraint technique. Uncertainties include the following: 1) some proposed emergent constraints lack of out-of-sample testing in other model ensembles, 2) some proposed emergent constraints are characterized by a strong statistical relationship but lack a physical or theoretical framework to support the emergent relationship, and 3) some proposed emergent constraints lack observational data to constrain the future response, even assuming the emergent relationship is statistically robust and supported by a physical mechanism or theory. In addition, most emergent constraints have been applied to quantities of relevance to the global climate system. Going forward, it would be helpful to have more emergent constraints developed at the regional scale to reduce uncertainty in quantities of greatest relevance to the US or other regions.

### Extreme Event Attribution

Confidence in extreme attribution statement depends on both our understanding of the underlying physical mechanisms of change as well as on the fitness of our statistical and climate models.<sup>65</sup> This, of course, varies significantly depending on the nature of the extreme weather event. Attribution statements about the human influence on severe heatwaves and cold snaps are generally considered to be most confident.<sup>221</sup> Confidence in attribution statements about extreme precipitation vary greatly depending on storm type. Hurricane precipitation has been among the most-studied event, and recent assessment has concluded that modeling and satellite studies, as well as physical understanding, provide strong evidence that hurricane rainfall rates increased and will continue to increase due to anthropogenic climate change.<sup>221,316</sup> The Working Group I contribution to the Sixth Assessment Report of the Intergovernmental Panel on Climate Change (IPCC AR6 WGI) concluded that “event attribution studies and physical understanding indicate that human-induced climate change increases heavy precipitation associated with tropical cyclones (*high confidence*), but data limitations inhibit clear detection of past trends on the global scale.”<sup>220</sup> Partly based on CMIP5 models, the World Meteorological Organization’s Tropical Cyclone Expert Team<sup>42</sup> concluded: “For TC precipitation rates, there is at least medium-to-high confidence in an increase globally, with a median projected increase of 14%, or close to the rate of tropical water vapor increase with warming, at constant

relative humidity.” However recent higher-resolution modeling studies, particularly event attribution studies, find that hurricane precipitation increases at a rate substantially higher than that of water vapor alone, implying dynamical as well as thermodynamical changes (e.g., Reed et al. 2021,<sup>304</sup> 2022;<sup>63</sup> Risser and Wehner 2017;<sup>82</sup> van Oldenborgh et al. 2017;<sup>83</sup> Wang et al. 2018<sup>84</sup>). A recent satellite-based study reinforces this interpretation.<sup>316</sup> Atmospheric rivers and extratropical cyclones have received less attention, but it is expected that similar conclusions will be drawn as more studies are performed. Mesoscale convective systems (e.g., storms producing hail, tornadoes, and ice) are not so well studied due to both modeling and observational limitations of these specific local-scale events.

Changes in extreme wind events, such as produced by hurricanes, derechos, or Santa Ana-type events, are also poorly understood due to model limitations in realistically simulating these phenomena.

Extreme weather changes attributable to local thermodynamic processes are better understood than those due to changes in large-scale meteorological patterns due to uncertainty in changes in circulation patterns. Thus, attributable changes in meteorological drought (defined by rainfall deficits) caused by changing rainfall patterns from circulation are less well understood, especially for CONUS, than are attributable changes in agricultural and ecological drought (defined by increases in soil moisture deficit caused by warmer temperatures).<sup>196</sup>

Some events are so extreme that our statistical and climate models may not be fit for the purpose of quantifying the human influence, even if our understanding is such that we are confident that there is one. The 2021 heatwave in the Pacific Northwest is a good example. Temperatures experienced during this very rare compound extreme event are outside of the bounds of the fitted generalized extreme value statistical distributions typically used to ascertain changes in event frequency and magnitude. Also, it is unclear whether the standard ensemble of CMIP models can produce the specific large-scale meteorological patterns responsible for these record-breaking temperatures. For these very rare events, the recent development of large ensembles of climate models can increase our confidence in quantitative attribution statements in some instances.<sup>53</sup>

### Description of Confidence and Likelihood

The section is a description of factual results, so confidence and likelihood do not apply.

## Key Message 3.4

### Humans Are Changing Earth System Processes

#### Description of Evidence Base

##### Natural Variability

In the last decade, there has been increasing recognition of the role of regional-scale natural variability in the past and future evolution of climate, as well as the fact that regional natural variability signals can be competitive with forced anthropogenic signals (e.g., Deser 2020<sup>317</sup>). The mechanisms by which the climate system generates such large levels of natural variability are well documented and understood. Examples of such modes of variability relevant to North American climate include ENSO, the Pacific Decadal Oscillation, the Pacific North American pattern, and the northern annular mode. Many of these patterns have limited predictability beyond a timescale of about two weeks, leading to an irreducible uncertainty in the actual evolution of climate. A caveat here relates to the ENSO phenomenon, which has some seasonal to interannual predictability. We also note that modes of variability themselves can also be affected by anthropogenic forcing, and these signals may be predictable.<sup>318</sup> This idea of irreducible uncertainty applies to

future projections only. It is not meant to cast doubt on anthropogenic climate change that has already been detected in the observational record despite natural variability.<sup>221,235</sup>

### Atmospheric Circulation Changes

Many aspects of atmospheric circulation changes have been studied using observations (global reanalysis) and model simulations. Important large-scale circulation features that influence US regional climate include the jet stream, storm tracks, the Aleutian low, the North Pacific and North Atlantic subtropical highs, North American Monsoon circulation, and others, which are strongly influenced by the overturning Hadley circulation in the tropics. In turn, large-scale circulation, such as the North Atlantic subtropical high, influences mesoscale circulation features, such as the Great Plains low-level jet that affects precipitation in the central and midwestern US. Hence, understanding how the Hadley circulation changes with warming is important for understanding changes in large-scale and mesoscale circulations affecting US regional climate. Staten et al. (2018)<sup>89</sup> and Grise et al. (2019)<sup>90</sup> synthesized previous studies documenting the poleward shift in the subsiding branches of the Hadley circulation since 1979. Both studies found that methodological differences in how the Hadley circulation is calculated can partly explain the discrepancy between the rate of tropical expansion derived from global reanalyses and model historical simulations found in previous studies. However, both studies also highlighted the challenge in detecting changes in the tropical expansion and attributing them to anthropogenic warming because of the large natural variability, particularly for the poleward expansion in the Northern Hemisphere that is more relevant to large-scale circulations affecting North America.

Besides the tropical expansion, many studies analyzed model simulations and projections of changes in large-scale circulations—such as the jet stream,<sup>87,93,95,319</sup> storm tracks,<sup>320</sup> extratropical cyclones,<sup>189,321</sup> and the North Atlantic subtropical high,<sup>100,322</sup>—and compared observed and model-simulated historical trends in sea level pressure.<sup>323</sup> Many of these studies used multimodel and large ensemble simulations to first determine if a robust signal of change is found and, if so, the mechanisms for how warming may influence the circulation features; the impacts of the circulation changes to precipitation are also often investigated. Model experiments allowing isolation of the direct radiative effect of CO<sub>2</sub>, which is a fast process, versus the effect of sea surface temperature warming, which is a slower process, have also contributed to improving understanding of how increasing GHGs affect atmospheric circulation.

### Water Cycle Changes

A sizeable and expanding literature describes past and projected future changes in processes relevant to Earth's water cycle.<sup>201,324</sup> Much of the literature on the water cycle separates its projected past and future changes into two components: one proportional to the change in water vapor—the “thermodynamic” response—and another that depends on atmospheric circulation and other factors—the “dynamic” response. Water vapor changes increase at roughly constant relative humidity with warming,<sup>325</sup> with variations over land and during different phases of the response<sup>326</sup> that are relevant to the US. Changes in circulation also modulate the spatial pattern of extreme precipitation intensity change, increasing it in some regions and reducing it in others,<sup>113</sup> which is the main driver of the variations in magnitude and sign of precipitation change seasonally and regionally. Precipitation variability generally is projected to increase at all timescales and in most locations in response to GHG-driven warming.<sup>110</sup> This implies increases in both heavy precipitation extremes and drought,<sup>111</sup> a phenomenon called whiplash.<sup>112</sup>

### Changes in the Carbon and Biogeochemical Cycles

Observations show that about half of annually emitted CO<sub>2</sub> from human activities is absorbed by the terrestrial biosphere and oceans.<sup>327</sup> The observational record of atmospheric CO<sub>2</sub> growth and estimates of fossil fuel emissions based on economic fuel statistics are used to estimate the residual total uptake of carbon by the terrestrial ecosystem and the ocean. Determining the amount of uptake for land and oceans

is more complicated and uncertain. For the oceans, upscaled global measurements of the partial pressure of CO<sub>2</sub> (pCO<sub>2</sub>) in seawater and total carbon in organic and inorganic compounds dissolved in interior ocean waters are used to estimate current and cumulative carbon sinks (e.g., Rödenbeck et al. 2015;<sup>328</sup> Takahashi et al. 2009<sup>329</sup>).

On land, direct measurements of atmosphere–land biosphere fluxes are used to understand carbon sources and sinks and their variability on daily to interannual timescales.<sup>330</sup>

### Changes in Ocean, Cryosphere, and Sea Level

Over the course of the 20th century, sea level rise occurring on global scales estimated from reconstruction created from tide-gauge records has been explained by the individual processes contributing to it.<sup>158</sup> These process contributions were estimated from a combination of direct observations and observation-driven reconstructions. Using modern observation systems, global sea level rise from satellite altimetry between 2002 and 2017 has been explained using the in situ measurements of the Argo profiling floats and the observations of water-mass change from the GRACE and GRACE-FO satellites,<sup>331</sup> demonstrating closure of the global sea level budget. As seen in both tide-gauge and satellite records, the rate of global mean sea level rise has been increasing, driven by accelerating contributions from the underlying processes.<sup>158,161,162</sup>

At the regional level, similar studies have assessed the rates of sea level rise and performed similar budget studies as those conducted on global scales. The combination of models, reconstructions, and observations allows for accounting of all the relevant processes, and an understanding of the drivers of total sea level rise has been demonstrated on regional scales across a range of different timescales in several studies (e.g., Frederikse et al. 2017;<sup>332</sup> Harvey et al. 2021;<sup>333</sup> Rietbroek et al. 2016;<sup>334</sup> Walker et al. 2021<sup>160</sup>). The current relative sea level observation network measures the dominant processes contributing to regional sea level, and this has supported more dedicated, process-level studies on sea level rise.

### Regional-Scale Changes

It has been well established since the earliest climate change assessments (e.g., IPCC 1990;<sup>335</sup> National Research Council 1979<sup>336</sup>) that the local climate change response in a particular variable can differ substantially from the corresponding globally averaged response. For the latest versions of the geographical distributions of the response in particular variables to anthropogenic forcing, and the corresponding globally averaged response, the reader is referred to examples seen in Figures SPM.5, SPM.8, TS.6 of the IPCC AR6 WGI.<sup>13,20</sup>

## Major Uncertainties and Research Gaps

### Natural Variability

Because of the limited duration of the observational record, the magnitude of natural variability on decadal timescales and longer is not as well quantified as shorter-timescale variability. For example, the true natural variability of the climate system on decadal to centennial timescales could be larger than what we estimate from GCMs, which would further increase the irreducible uncertainty stemming from natural variability.

### Atmospheric Circulation Changes

While advances have been made in reconciling the previously reported differences in tropical expansion rates in observations and model simulations, uncertainties remain, especially in future projections of tropical expansion in the Northern Hemisphere because of the large natural variability and the relatively small poleward expansion in response to increasing GHGs.<sup>90</sup> Some studies also highlighted several important sources of uncertainty in projecting midlatitude atmospheric circulation changes related to model biases (e.g., Dong et al. 2021<sup>58</sup>), a tug-of-war between opposing mechanisms (e.g., Shaw and Voigt 2015<sup>319</sup>), and natural variability (e.g., Deser et al. 2020;<sup>53</sup> Dong et al. 2021<sup>87</sup>). For historical century-scale

regional trends in sea level pressure, large differences were found between different observational estimates from gridded datasets and reanalysis reconstructions.<sup>323</sup>

As discussed in KM 3.4, large-scale circulation changes are influenced by meridional and vertical temperature gradients; thus, Arctic amplification (the enhancement of near-surface air temperature change over the Arctic relative to lower latitudes), besides changes in the tropical Hadley circulation, may also influence midlatitude atmospheric circulations such as blocking, with potential implications for cold extremes. However, significant challenges remain in connecting Arctic amplification to midlatitude circulation changes due to the complex nonlinear dynamics of the jet stream.<sup>337,338</sup>

### Water Cycle Changes

Of note is the role of climate variability in many aspects of the water cycle (especially for changes at the regional scale): natural variability is known (with *high confidence*, from observations, theory, and simulations) to be large for many aspects of the water cycle, and this can result in a low ceiling to the likelihood that can be placed on any specific realization of the future or past water cycle, even in situations where confidence in understanding is high (see above, “Large Ensemble Simulations” in KM 3.3, and Douville et al. 2021<sup>201</sup>). For this reason, it is particularly important for the water cycle to focus on the probability of what could happen in the future and the probability that observed changes that have already occurred are due to forced changes (as opposed to natural variability), rather than focusing on specific deterministic trajectories of what has already happened or will happen in the future. Furthermore, forced changes in variability that are expected for precipitation and other aspects of the water cycle complicate this picture further, more than for other variables such as temperature.

For extreme precipitation in particular, an outstanding question is whether, and if so how much, the thermodynamic and dynamic components of extreme precipitation change are coupled.<sup>339</sup> This would imply a positive feedback mechanism that could amplify extreme precipitation increases beyond the thermodynamic increase.

One uncertainty is the role of vegetation in modulating changes in evapotranspiration, which can in turn influence other factors including soil moisture, streamflow, and wildfire. In addition to changing evaporation from soil, plants also influence total evaporation through competing effects. In response to increased atmospheric CO<sub>2</sub> concentrations, plant stomata do not need to open as much to take in CO<sub>2</sub> for photosynthesis, which can reduce the amount of water they lose through transpiration, thus decreasing total evapotranspiration.<sup>340</sup> Conversely, an overall increase in the amount of vegetation can amplify evaporative losses and surface drying.<sup>215,341,342</sup> It is not yet clear which of these mechanisms will predominate, although model projections and observational analyses for the US suggest that the net effect will be for warming to increase evaporation and surface drying in much of the country.<sup>199,200,207,208,343</sup>

A key gap in understanding the hydrologic cycle and how it can change is the enormous range of scales in space and time on which relevant processes operate, from the scale of nanometers (cloud condensation nuclei), to the scale of cloud systems and watersheds (1 km to 1,000s of km), to the whole globe (evaporation and precipitation constitute a large fraction of energy flow between the surface and atmosphere). No observing system can capture, and no numerical model can represent, all of these processes at once, which is a key challenge for understanding and projecting the water cycle and its change. Continuing to increase the range of scales that can be captured by consistent, continuous observing systems and represented within a single model is one promising path toward decreasing some of the uncertainty in the future water cycle.<sup>201</sup>



### Changes in the Carbon and Biogeochemical Cycles

Carbon fluxes, especially from the terrestrial biosphere are spatially heterogeneous and can undergo large temporal changes as well. Observations used to estimate carbon fluxes are sparsely distributed, and data records are often too short to be used to characterize interannual variability and trends. Models of ocean circulation and biogeochemistry and detailed models of plant growth and dynamics can be used to upscale carbon fluxes using observations for guidance, but there is significant uncertainty in many processes, such as the effects of nutrient limitation on plants and phytoplankton and responses to climate changes. Machine learning approaches have also been used to upscale flux observations (e.g., Jung et al. 2020<sup>344</sup>). Inverse modeling combines information from atmospheric observations, atmospheric transport models, and best-available estimates of carbon fluxes from land and ocean via models to produce carbon flux estimates; however, these modeling systems are also limited by sparse data. Major regions that are important for understanding the global carbon budget, such as the tropics and Siberia, do not have adequate observational coverage, and this lack makes accurate estimates of land and ocean fluxes difficult to achieve.

All of the above-mentioned issues, and the large uncertainty associated with future emissions, make predicting the future evolution of the carbon cycle difficult. Uncertainties in future climate drivers such as temperature, precipitation, and cloudiness result in uncertainty in how land and ocean biogeochemistry will evolve in the future. Furthermore, the difficulties in modeling nutrient availability and limitation, as well as disturbances such as fires, insect and disease outbreaks, severe weather, and human land-use change, introduce more uncertainties that affect predictions of how the carbon cycle and climate change will interact. The mobilization to the atmosphere of CO<sub>2</sub> and CH<sub>4</sub> from enhanced decomposition of the huge reserves of carbon in Arctic soils represents a potentially important positive carbon cycle–climate feedback, but it is particularly difficult to model due to difficult-to-quantify processes like cryoturbation and local erosion and thermokarst processes.<sup>345</sup> Current carbon cycle models that are coupled to climate models disagree widely on the future response of carbon exchanges between the oceans, land biosphere, and atmosphere to continued fossil fuel emissions. The range of responses has not appreciably changed since the previous model intercomparison (CMIP5).<sup>134</sup>

### Changes in Ocean, Cryosphere, and Sea Level

Many of the components of the modern sea level observation network—particularly space-based platforms—are limited in their coverage of coastal regions. The US coastlines have better coverage from tide gauges than other parts of the world, although large gaps between tide gauges are still present. This is also true of measurements of coastal subsidence that generally originate from point-measurements from the Global Positioning System, although satellite-based interferometric synthetic aperture radar (InSAR) provides a possible solution (e.g., Shirzaei et al. 2021<sup>346</sup>). The connection between open-ocean sea level change and the sea level change experienced at the coast is still an active research area.

As a result of observations and improved modeling efforts, there is increased consensus regarding the behavior of many of the ice sheet processes. However, the future response of the ice sheets as the climate continues to warm, and of some of the associated processes, is still uncertain. It has been hypothesized that two possible processes in particular, known as the marine ice cliff instability<sup>151,152</sup> and the marine ice sheet instability,<sup>153,155,156</sup> could lead to rapid ice sheet loss over the course of several decades. The physical processes that would result in these instabilities and how they would progress once triggered remain uncertain. Resolving these uncertainties would require continued and additional observations of the ice sheets—and ocean and atmosphere that surround them. Additionally, advances in ice sheet modeling that potentially leverage these observations are a priority to narrow future estimates of ice mass loss.

### Regional-Scale Changes

Although the idea that the regional climate change response differs from the globally averaged response is not controversial, there remain major uncertainties in the magnitudes of climate change responses at any given location. This reflects large differences in local outcomes across the GCM projections, as well as large differences in the local response when those GCMs are downscaled to higher resolution.

### Description of Confidence and Likelihood

The section is a description of general results, so confidence and likelihood do not apply.

## Key Message 3.5

### Humans Are Changing Weather and Climate Extremes

#### Description of Evidence Basis

The theoretical basis of changes in extreme temperature and precipitation are well established. As temperature increases, a shift in the distribution implies that high temperatures become more frequent. Extreme precipitation occurs in saturated atmospheres. The Clausius–Clapeyron relationship, identified in the 19th century—specifying that saturation-specific humidity increases by between 6% and 7% per one degree Celsius of warming at typical surface air temperatures—dictates that available moisture during extreme storms increases with warming. The efficiency with which different types of storms precipitate that available moisture varies, as does the response in precipitation efficiency to warming. Limited event attribution studies and other high-resolution modeling studies find that extreme precipitation can increase at a rate greater than that indicated by Clausius–Clapeyron.

The effect of warming on drought varies between drought definitions. Understanding of changes in meteorological drought is limited by understanding of the atmospheric circulation changes that affect storm track and frequency. On the other hand, changes in agricultural drought are sensitive to changes in evapotranspiration, which increases sharply with increased temperatures.<sup>221</sup>

#### Major Uncertainties and Research Gaps

Land surface and vegetation processes have substantial impacts on climate extremes through the modulation of energy fluxes between the surface and atmosphere and surface water partitioning.<sup>347</sup> For example, dry surface conditions (e.g., a drought) and urbanization can both amplify heat extremes,<sup>348,349</sup> while wetter soils can increase the risk of precipitation events causing large floods.<sup>350,351</sup> However, few long-term data on these processes are available at large scales,<sup>348</sup> and their representation in climate models is often highly simplified.<sup>352</sup> Further, despite the fact that many extremes are strongly tied to atmospheric circulation anomalies (e.g., atmospheric ridge events), changes in these dynamics remain highly uncertain. While changes in sea ice and meridional temperature gradients may be linked to increases in the frequency and persistence of midlatitude circulation patterns associated with extreme events (e.g., Coumou et al. 2018<sup>353</sup>), studies suggest that these changes have not yet emerged from background natural variability.<sup>354</sup> Confidence in model-based assessments of changes in frequency or intensity of extreme events can be enhanced in cases where a detectable anthropogenic trend in an extreme, or closely related metric, has been found. However, this is not the case for some extreme event types, including those related to long-term changes in circulation.

The ensembles of tropical cyclone-permitting (~20 km) model simulations are small both in the number of realizations and of independent climate models, which limits understanding of tropical storm statistics. Even fewer long convection-permitting (<4 km) regional model simulations are available, limiting our understanding of how mesoscale convection systems and similar intense storms will respond to warming.

The effect of warming on the processes leading to rapid intensification is also poorly understood. While theory and high-resolution modeling find that winds in the most intense storms become stronger, detection and attribution of such changes has not yet been accomplished, as the most common metric—the Saffir–Simpson wind speed—is an instantaneous point-wise maximum and very noisy.

Finally, climate change may be moving us into an era of large or unprecedented extremes that fall far outside the range of historical variability, particularly regarding temperature (e.g., Overland 2021<sup>355</sup>). In such cases, many statistical approaches may be insufficient and make it difficult, with any confidence, to conduct detection and attribution analyses.<sup>76</sup>

### Description of Confidence Likelihood

Anthropogenic forcing has increased the frequency, duration, and intensity of extreme heat across most land areas (*high confidence*),<sup>20,356</sup> with some evidence that extreme cold events have also declined (*medium confidence*).<sup>308</sup> These changes are driven by average shifts in the temperature distributions toward warmer conditions that are significant and robust across most of the world.<sup>180</sup> Heavy precipitation events have increased in some regions (*high confidence*)<sup>20</sup> because of the strong dependence of the water-holding capacity of the atmosphere on temperatures (e.g., Kunkel et al. 2013<sup>357</sup>). Coastal flood risk has increased, and is projected to continue to increase, because of sea level rise (*high confidence*; e.g., Vousdoukas et al. 2018<sup>358</sup>). Notably, while the most extreme river floods are expected to increase in severity because of increases in heavy precipitation (*high confidence*), more general trends are mixed because flood risk also depends on policies and land surface processes.<sup>201</sup> Soil moisture droughts are also increasing in frequency and severity in many regions (*medium to high confidence*)<sup>20</sup> through the direct effects of warming on snow, evapotranspiration, and plant water use.<sup>43,215,342</sup> There is also *high confidence* that the intensity and frequency of precipitation droughts are increasing in Mediterranean-climate regions.<sup>359,360,361,362</sup> Climate change increases fuel flammability through higher temperatures and lower humidity and has increased the area burned by wildfires in western US (*high confidence*)<sup>217,219</sup> and Australia.<sup>363</sup> Despite these climate change-driven regional increases, however, global burn area has declined in recent years as a consequence of agricultural expansion and intensification, especially in savanna and grassland ecosystems.<sup>364</sup>

While tropical cyclones are the most studied extreme storm type with high-resolution (~25 km) global models, more such simulations are required to develop a theory about cyclogenesis and intensity changes with climate change. While attribution studies find that extreme precipitation over land in major tropical cyclones *very likely* scales with temperature increases at rates greater than the Clausius–Clapeyron rate, average total tropical storm precipitation scales at least at Clausius–Clapeyron rates,<sup>42</sup> but confidence is limited as there are limited high-resolution projections. It is also *likely* that precipitation increases over land will differ from those over oceans.

## References

1. Boucher, O., D. Randall, P. Artaxo, C. Bretherton, G. Feingold, P. Forster, V.-M. Kerminen, Y. Kondo, H. Liao, U. Lohmann, P. Rasch, S.K. Satheesh, S. Sherwood, B. Stevens, and X.Y. Zhang, 2013: Ch. 7. Clouds and aerosols. In: *Climate Change 2013: The Physical Science Basis. Contribution of Working Group I to the Fifth Assessment Report of the Intergovernmental Panel on Climate Change*. Stocker, T.F., D. Qin, G.-K. Plattner, M. Tignor, S.K. Allen, J. Boschung, A. Nauels, Y. Xia, V. Bex, and P.M. Midgley, Eds. Cambridge University Press, Cambridge, UK and New York, NY, 571–658. <https://doi.org/10.1017/cbo9781107415324.016>
2. Forster, P., T. Storelvmo, K. Armour, W. Collins, J.-L. Dufresne, D. Frame, D.J. Lunt, T. Mauritsen, M.D. Palmer, M. Watanabe, M. Wild, and H. Zhang, 2021: Ch. 7. The Earth's energy budget, climate feedbacks, and climate sensitivity. In: *Climate Change 2021: The Physical Science Basis. Contribution of Working Group I to the Sixth Assessment Report of the Intergovernmental Panel on Climate Change*. Masson-Delmotte, V., P. Zhai, A. Pirani, S.L. Connors, C. Péan, S. Berger, N. Caud, Y. Chen, L. Goldfarb, M.I. Gomis, M. Huang, K. Leitzell, E. Lonnoy, J.B.R. Matthews, T.K. Maycock, T. Waterfield, O. Yelekçi, R. Yu, and B. Zhou, Eds. Cambridge University Press, Cambridge, UK and New York, NY, USA, 923–1054. <https://doi.org/10.1017/9781009157896.009>
3. Fahey, D.W., S. Doherty, K.A. Hibbard, A. Romanou, and P.C. Taylor, 2017: Ch. 2. Physical drivers of climate change. In: *Climate Science Special Report: Fourth National Climate Assessment, Volume I*. Wuebbles, D.J., D.W. Fahey, K.A. Hibbard, D.J. Dokken, B.C. Stewart, and T.K. Maycock, Eds. U.S. Global Change Research Program, Washington, DC, USA, 73–113. <https://doi.org/10.7930/j0513wcr>
4. Canadell, J.G., P.M.S. Monteiro, M.H. Costa, L. Cotrim da Cunha, P.M. Cox, A.V. Eliseev, S. Henson, M. Ishii, S. Jaccard, C. Koven, A. Lohila, P.K. Patra, S. Piao, J. Rogelj, S. Syampungani, S. Zaehle, and K. Zickfeld, 2021: Ch. 5. Global carbon and other biogeochemical cycles and feedbacks. In: *Climate Change 2021: The Physical Science Basis. Contribution of Working Group I to the Sixth Assessment Report of the Intergovernmental Panel on Climate Change*. Masson-Delmotte, V., P. Zhai, A. Pirani, S.L. Connors, C. Péan, S. Berger, N. Caud, Y. Chen, L. Goldfarb, M.I. Gomis, M. Huang, K. Leitzell, E. Lonnoy, J.B.R. Matthews, T.K. Maycock, T. Waterfield, O. Yelekçi, R. Yu, and B. Zhou, Eds. Cambridge University Press, Cambridge, UK and New York, NY, USA, 673–816. <https://doi.org/10.1017/9781009157896.007>
5. Lan, X., S. Basu, S. Schwietzke, L.M.P. Bruhwiler, E.J. Dlugokencky, S.E. Michel, O.A. Sherwood, P.P. Tans, K. Thoning, G. Etiope, Q. Zhuang, L. Liu, Y. Oh, J.B. Miller, G. Pétron, B.H. Vaughn, and M. Crippa, 2021: Improved constraints on global methane emissions and sinks using  $\delta^{13}\text{C}-\text{CH}_4$ . *Global Biogeochemical Cycles*, **35** (6), e2021GB007000. <https://doi.org/10.1029/2021gb007000>
6. Schaefer, H., S.E.M. Fletcher, C. Veidt, K.R. Lassey, G.W. Brailsford, T.M. Bromley, E.J. Dlugokencky, S.E. Michel, J.B. Miller, I. Levin, D.C. Lowe, R.J. Martin, B.H. Vaughn, and J.W.C. White, 2016: A 21st-century shift from fossil-fuel to biogenic methane emissions indicated by  $^{13}\text{C}-\text{CH}_4$ . *Science*, **352** (6281), 80–84. <https://doi.org/10.1126/science.aad2705>
7. Szopa, S., V. Naik, B. Adhikary, P. Artaxo, T. Berntsen, W.D. Collins, S. Fuzzi, L. Gallardo, A. Kiendler-Scharr, Z. Klimont, H. Liao, N. Unger, and P. Zanis, 2021: Ch. 6. Short-lived climate forcers. In: *Climate Change 2021: The Physical Science Basis. Contribution of Working Group I to the Sixth Assessment Report of the Intergovernmental Panel on Climate Change*. Masson-Delmotte, V., P. Zhai, A. Pirani, S.L. Connors, C. Péan, S. Berger, N. Caud, Y. Chen, L. Goldfarb, M.I. Gomis, M. Huang, K. Leitzell, E. Lonnoy, J.B.R. Matthews, T.K. Maycock, T. Waterfield, O. Yelekçi, R. Yu, and B. Zhou, Eds. Cambridge University Press, Cambridge, UK and New York, NY, USA, 817–922. <https://doi.org/10.1017/9781009157896.008>
8. Tian, H., R. Xu, J.G. Canadell, R.L. Thompson, W. Winiwarter, P. Suntharalingam, E.A. Davidson, P. Ciais, R.B. Jackson, G. Janssens-Maenhout, M.J. Prather, P. Regnier, N. Pan, S. Pan, G.P. Peters, H. Shi, F.N. Tubiello, S. Zaehle, F. Zhou, A. Arneeth, G. Battaglia, S. Berthet, L. Bopp, A.F. Bouwman, E.T. Buitenhuis, J. Chang, M.P. Chipperfield, S.R.S. Dangal, E. Dlugokencky, J.W. Elkins, B.D. Eyre, B. Fu, B. Hall, A. Ito, F. Joos, P.B. Krummel, A. Landolfi, G.G. Laruelle, R. Lauerwald, W. Li, S. Lienert, T. Maavara, M. MacLeod, D.B. Millet, S. Olin, P.K. Patra, R.G. Prinn, P.A. Raymond, D.J. Ruiz, G.R. van der Werf, N. Vuichard, J. Wang, R.F. Weiss, K.C. Wells, C. Wilson, J. Yang, and Y. Yao, 2020: A comprehensive quantification of global nitrous oxide sources and sinks. *Nature*, **586** (7828), 248–256. <https://doi.org/10.1038/s41586-020-2780-0>
9. Forster, P., V. Ramaswamy, P. Artaxo, T. Berntsen, R. Betts, D.W. Fahey, J. Haywood, J. Lean, D.C. Lowe, G. Myhre, J. Nganga, R. Prinn, G. Raga, M. Schulz, and R. Van Dorland, 2007: Ch. 2. Changes in atmospheric constituents and in radiative forcing. In: *Climate Change 2007: The Physical Science Basis. Contribution of Working Group I to the Fourth Assessment Report of the Intergovernmental Panel on Climate Change*. Solomon, S., D. Qin, M. Manning, Z. Chen, M. Marquis, K.B. Averyt, M. Tignor, and H.L. Miller, Eds. Cambridge University Press, Cambridge, UK and New York, NY, USA. [https://archive.ipcc.ch/publications\\_and\\_data/ar4/wg1/en/ch2.html](https://archive.ipcc.ch/publications_and_data/ar4/wg1/en/ch2.html)



10. Gulev, S.K., P.W. Thorne, J. Ahn, F.J. Dentener, C.M. Domingues, S. Gerland, D. Gong, D.S. Kaufman, H.C. Nnamchi, J. Quaas, J.A. Rivera, S. Sathyendranath, S.L. Smith, B. Trewin, K. von Schuckmann, and R.S. Vose, 2021: Ch. 2. Changing state of the climate system. In: *Climate Change 2021: The Physical Science Basis. Contribution of Working Group I to the Sixth Assessment Report of the Intergovernmental Panel on Climate Change*. Masson-Delmotte, V., P. Zhai, A. Pirani, S.L. Connors, C. Péan, S. Berger, N. Caud, Y. Chen, L. Goldfarb, M.I. Gomis, M. Huang, K. Leitzell, E. Lonnoy, J.B.R. Matthews, T.K. Maycock, T. Waterfield, O. Yelekçi, R. Yu, and B. Zhou, Eds. Cambridge University Press, Cambridge, UK and New York, NY, USA, 287–422. <https://doi.org/10.1017/9781009157896.004>
11. Myhre, G., D. Shindell, F.-M. Bréon, W. Collins, J. Fuglestedt, J. Huang, D. Koch, J.-F. Lamarque, D. Lee, B. Mendoza, T. Nakajima, A. Robock, G. Stephens, T. Takemura, and H. Zhang, 2013: Ch. 8. Anthropogenic and natural radiative forcing. In: *Climate Change 2013: The Physical Science Basis. Contribution of Working Group I to the Fifth Assessment Report of the Intergovernmental Panel on Climate Change*. Stocker, T.F., D. Qin, G.-K. Plattner, M. Tignor, S.K. Allen, J. Boschung, A. Nauels, Y. Xia, V. Bex, and P.M. Midgley, Eds. Cambridge University Press, Cambridge, UK and New York, NY, USA, 659–740. <https://www.ipcc.ch/report/ar5/wg1/>
12. Quaas, J., H. Jia, C. Smith, A.L. Albright, W. Aas, N. Bellouin, O. Boucher, M. Doutriaux-Boucher, P.M. Forster, D. Grosvenor, S. Jenkins, Z. Klimont, N.G. Loeb, X. Ma, V. Naik, F. Paulot, P. Stier, M. Wild, G. Myhre, and M. Schulz, 2022: Robust evidence for reversal of the trend in aerosol effective climate forcing. *Atmospheric Chemistry and Physics*, **22** (18), 12221–12239. <https://doi.org/10.5194/acp-22-12221-2022>
13. Arias, P.A., N. Bellouin, E. Coppola, R.G. Jones, G. Krinner, J. Marotzke, V. Naik, M.D. Palmer, G.-K. Plattner, J. Rogelj, M. Rojas, J. Sillmann, T. Storelvmo, P.W. Thorne, B. Trewin, K. Achuta Rao, B. Adhikary, R.P. Allan, K. Armour, G. Bala, R. Barimalala, S. Berger, J.G. Canadell, C. Cassou, A. Cherchi, W. Collins, W.D. Collins, S.L. Connors, S. Corti, F. Cruz, F.J. Dentener, C. Dereczynski, A. Di Luca, A. Diongue Niang, F.J. Doblas-Reyes, A. Dosio, H. Douville, F. Engelbrecht, V. Eyring, E. Fischer, P. Forster, B. Fox-Kemper, J.S. Fuglestedt, J.C. Fyfe, N.P. Gillett, L. Goldfarb, I. Gorodetskaya, J.M. Gutierrez, R. Hamdi, E. Hawkins, H.T. Hewitt, P. Hope, A.S. Islam, C. Jones, D.S. Kaufman, R.E. Kopp, Y. Kosaka, J. Kossin, S. Krakovska, J.-Y. Lee, J. Li, T. Mauritsen, T.K. Maycock, M. Meinshausen, S.-K. Min, P.M.S. Monteiro, T. Ngo-Duc, F. Otto, I. Pinto, A. Pirani, K. Raghavan, R. Ranasinghe, A.C. Ruane, L. Ruiz, J.-B. Sallée, B.H. Samset, S. Sathyendranath, S.I. Seneviratne, A.A. Sörensson, S. Szopa, I. Takayabu, A.-M. Tréguier, B. van den Hurk, R. Vautard, K. von Schuckmann, S. Zaehle, X. Zhang, and K. Zickfeld, 2021: Technical summary. In: *Climate Change 2021: The Physical Science Basis. Contribution of Working Group I to the Sixth Assessment Report of the Intergovernmental Panel on Climate Change*. Masson-Delmotte, V., P. Zhai, A. Pirani, S.L. Connors, C. Péan, S. Berger, N. Caud, Y. Chen, L. Goldfarb, M.I. Gomis, M. Huang, K. Leitzell, E. Lonnoy, J.B.R. Matthews, T.K. Maycock, T. Waterfield, O. Yelekçi, R. Yu, and B. Zhou, Eds. Cambridge University Press, Cambridge, UK and New York, NY, USA, 33–144. <https://doi.org/10.1017/9781009157896.002>
14. Chen, L. and P.A. Dirmeyer, 2019: Global observed and modelled impacts of irrigation on surface temperature. *International Journal of Climatology*, **39** (5), 2587–2600. <https://doi.org/10.1002/joc.5973>
15. Bonan, G.B., 2008: Forests and climate change: Forcings, feedbacks, and the climate benefits of forests. *Science*, **320** (5882), 1444–1449. <https://doi.org/10.1126/science.1155121>
16. Prevedello, J.A., G.R. Winck, M.M. Weber, E. Nichols, and B. Sinervo, 2019: Impacts of forestation and deforestation on local temperature across the globe. *PLoS ONE*, **14** (3), e0213368. <https://doi.org/10.1371/journal.pone.0213368>
17. Friberg, J., B.G. Martinsson, M.K. Sporre, S.M. Andersson, C.A.M. Brenninkmeijer, M. Hermann, P.F.J. van Velthoven, and A. Zahn, 2015: Influence of volcanic eruptions on midlatitude upper tropospheric aerosol and consequences for cirrus clouds. *Earth and Space Science*, **2** (7), 285–300. <https://doi.org/10.1002/2015ea000110>
18. Schmidt, A., M.J. Mills, S. Ghan, J.M. Gregory, R.P. Allan, T. Andrews, C.G. Bardeen, A. Conley, P.M. Forster, A. Gettelman, R.W. Portmann, S. Solomon, and O.B. Toon, 2018: Volcanic radiative forcing from 1979 to 2015. *Journal of Geophysical Research: Atmospheres*, **123** (22), 12491–12508. <https://doi.org/10.1029/2018jd028776>
19. Zhu, J. and J.E. Penner, 2020: Radiative forcing of anthropogenic aerosols on cirrus clouds using a hybrid ice nucleation scheme. *Atmospheric Chemistry and Physics*, **20** (13), 7801–7827. <https://doi.org/10.5194/acp-20-7801-2020>
20. IPCC, 2021: Summary for policymakers. In: *Climate Change 2021: The Physical Science Basis. Contribution of Working Group I to the Sixth Assessment Report of the Intergovernmental Panel on Climate Change*. Masson-Delmotte, V., P. Zhai, A. Pirani, S.L. Connors, C. Péan, S. Berger, N. Caud, Y. Chen, L. Goldfarb, M.I. Gomis, M. Huang, K. Leitzell, E. Lonnoy, J.B.R. Matthews, T.K. Maycock, T. Waterfield, O. Yelekçi, R. Yu, and B. Zhou, Eds. Cambridge University Press, Cambridge, UK and New York, NY, USA, 3–32. <https://doi.org/10.1017/9781009157896.001>



21. Sherwood, S.C., M.J. Webb, J.D. Annan, K.C. Armour, P.M. Forster, J.C. Hargreaves, G. Hegerl, S.A. Klein, K.D. Marvel, E.J. Rohling, M. Watanabe, T. Andrews, P. Braconnot, C.S. Bretherton, G.L. Foster, Z. Hausfather, A.S. von der Heydt, R. Knutti, T. Mauritsen, J.R. Norris, C. Proistosescu, M. Rugenstein, G.A. Schmidt, K.B. Tokarska, and M.D. Zelinka, 2020: An assessment of Earth's climate sensitivity using multiple lines of evidence. *Reviews of Geophysics*, **58** (4), e2019RG000678. <https://doi.org/10.1029/2019rg000678>
22. Mitchell, J.F.B., C.A. Senior, and W.J. Ingram, 1989: CO<sub>2</sub> and climate: A missing feedback? *Nature*, **341** (6238), 132–134. <https://doi.org/10.1038/341132a0>
23. Ceppi, P., D.T. McCoy, and D.L. Hartmann, 2016: Observational evidence for a negative shortwave cloud feedback in middle to high latitudes. *Geophysical Research Letters*, **43** (3), 1331–1339. <https://doi.org/10.1002/2015gl067499>
24. Terai, C.R., S.A. Klein, and M.D. Zelinka, 2016: Constraining the low-cloud optical depth feedback at middle and high latitudes using satellite observations. *Journal of Geophysical Research: Atmospheres*, **121** (16), 9696–9716. <https://doi.org/10.1002/2016jd025233>
25. Hausfather, Z., K. Marvel, G.A. Schmidt, J.W. Nielsen-Gammon, and M. Zelinka, 2022: Climate simulations: Recognize the 'hot model' problem. *Nature*, **605** (7908), 26–29. <https://doi.org/10.1038/d41586-022-01192-2>
26. Sun, Q., C. Miao, Q. Duan, H. Ashouri, S. Sorooshian, and K.-L. Hsu, 2018: A review of global precipitation data sets: Data sources, estimation, and intercomparisons. *Reviews of Geophysics*, **56** (1), 79–107. <https://doi.org/10.1002/2017RG000574>
27. Leung, L.R., W.R. Boos, J.L. Catto, C. A. DeMott, G.M. Martin, J.D. Neelin, T.A. O'Brien, S. Xie, Z. Feng, N.P. Klingaman, Y.-H. Kuo, R.W. Lee, C. Martinez-Villalobos, S. Vishnu, M.D.K. Priestley, C. Tao, and Y. Zhou, 2022: Exploratory precipitation metrics: Spatiotemporal characteristics, process-oriented, and phenomena-based. *Journal of Climate*, **35** (12), 3659–3686. <https://doi.org/10.1175/jcli-d-21-0590.1>
28. Maloney, E.D., A. Gettelman, Y. Ming, J.D. Neelin, D. Barrie, A. Mariotti, C.-C. Chen, D.R.B. Coleman, Y.-H. Kuo, B. Singh, H. Annamalai, A. Berg, J.F. Booth, S.J. Camargo, A. Dai, A. Gonzalez, J. Hafner, X. Jiang, X. Jing, D. Kim, A. Kumar, Y. Moon, C.M. Naud, A.H. Sobel, K. Suzuki, F. Wang, J. Wang, A.A. Wing, X. Xu, and M. Zhao, 2019: Process-oriented evaluation of climate and weather forecasting models. *Bulletin of the American Meteorological Society*, **100** (9), 1665–1686. <https://doi.org/10.1175/bams-d-18-0042.1>
29. Simpson, I.R., J. Bacmeister, R.B. Neale, C. Hannay, A. Gettelman, R.R. Garcia, P.H. Lauritzen, D.R. Marsh, M.J. Mills, B. Medeiros, and J.H. Richter, 2020: An evaluation of the large-scale atmospheric circulation and its variability in CESM2 and other CMIP models. *Journal of Geophysical Research: Atmospheres*, **125** (13), e2020JD032835. <https://doi.org/10.1029/2020jd032835>
30. O'Neill, B.C., C. Tebaldi, D.P. van Vuuren, V. Eyring, P. Friedlingstein, G. Hurtt, R. Knutti, E. Kriegler, J.F. Lamarque, J. Lowe, G.A. Meehl, R. Moss, K. Riahi, and B.M. Sanderson, 2016: The Scenario Model Intercomparison Project (ScenarioMIP) for CMIP6. *Geoscientific Model Development*, **9** (9), 3461–3482. <https://doi.org/10.5194/gmd-9-3461-2016>
31. O'Neill, B.C., E. Kriegler, K. Riahi, K.L. Ebi, S. Hallegatte, T.R. Carter, R. Mathur, and D.P. van Vuuren, 2014: A new scenario framework for climate change research: The concept of Shared Socioeconomic Pathways. *Climatic Change*, **122** (3), 387–400. <https://doi.org/10.1007/s10584-013-0905-2>
32. Riahi, K., D.P. van Vuuren, E. Kriegler, J. Edmonds, B.C. O'Neill, S. Fujimori, N. Bauer, K. Calvin, R. Dellink, O. Fricko, W. Lutz, A. Popp, J.C. Cuaresma, S. Kc, M. Leimbach, L. Jiang, T. Kram, S. Rao, J. Emmerling, K. Ebi, T. Hasegawa, P. Havlik, F. Humpenöder, L.A. Da Silva, S. Smith, E. Stehfest, V. Bosetti, J. Eom, D. Gernaat, T. Masui, J. Rogelj, J. Strefler, L. Drouet, V. Krey, G. Luderer, M. Harmsen, K. Takahashi, L. Baumstark, J.C. Doelman, M. Kainuma, Z. Klimont, G. Marangoni, H. Lotze-Campen, M. Obersteiner, A. Tabeau, and M. Tavoni, 2017: The Shared Socioeconomic Pathways and their energy, land use, and greenhouse gas emissions implications: An overview. *Global Environmental Change*, **42**, 153–168. <https://doi.org/10.1016/j.gloenvcha.2016.05.009>
33. van Vuuren, D.P., E. Kriegler, B.C. O'Neill, K.L. Ebi, K. Riahi, T.R. Carter, J. Edmonds, S. Hallegatte, T. Kram, R. Mathur, and H. Winkler, 2014: A new scenario framework for climate change research: Scenario matrix architecture. *Climatic Change*, **122** (3), 373–386. <https://doi.org/10.1007/s10584-013-0906-1>
34. Kriegler, E., J. Edmonds, S. Hallegatte, K.L. Ebi, T. Kram, K. Riahi, H. Winkler, and D.P. van Vuuren, 2014: A new scenario framework for climate change research: The concept of shared climate policy assumptions. *Climatic Change*, **122** (3), 401–414. <https://doi.org/10.1007/s10584-013-0971-5>

35. Eyring, V., S. Bony, G.A. Meehl, C.A. Senior, B. Stevens, R.J. Stouffer, and K.E. Taylor, 2016: Overview of the Coupled Model Intercomparison Project Phase 6 (CMIP6) experimental design and organization. *Geoscientific Model Development*, **9** (5), 1937–1958. <https://doi.org/10.5194/gmd-9-1937-2016>
36. Haarsma, R.J., M.J. Roberts, P.L. Vidale, C.A. Senior, A. Bellucci, Q. Bao, P. Chang, S. Corti, N.S. Fučkar, V. Guemas, J. von Hardenberg, W. Hazeleger, C. Kodama, T. Koenigk, L.R. Leung, J. Lu, J.J. Luo, J. Mao, M.S. Mizielinski, R. Mizuta, P. Nobre, M. Satoh, E. Scoccimarro, T. Semmler, J. Small, and J.S. von Storch, 2016: High Resolution Model Intercomparison Project (HighResMIP v1.0) for CMIP6. *Geoscientific Model Development*, **9** (11), 4185–4208. <https://doi.org/10.5194/gmd-9-4185-2016>
37. Jiayang, G., M. Shoshiro, M.J. Roberts, R. Haarsma, D. Putrasahan, C.D. Roberts, E. Scoccimarro, L. Terray, B. Vannière, and P.L. Vidale, 2020: Influence of model resolution on bomb cyclones revealed by HighResMIP-PRIMAVERA simulations. *Environmental Research Letters*, **15** (8), 084001. <https://doi.org/10.1088/1748-9326/ab88fa>
38. Wehner, M., J. Lee, M. Risser, P. Ullrich, P. Gleckler, and W.D. Collins, 2021: Evaluation of extreme sub-daily precipitation in high-resolution global climate model simulations. *Philosophical Transactions of the Royal Society A: Mathematical, Physical and Engineering Sciences*, **379** (2195), 20190545. <https://doi.org/10.1098/rsta.2019.0545>
39. Roberts, M.J., J. Camp, J. Seddon, P.L. Vidale, K. Hodges, B. Vanniere, J. Mecking, R. Haarsma, A. Bellucci, E. Scoccimarro, L.-P. Caron, F. Chauvin, L. Terray, S. Valcke, M.-P. Moine, D. Putrasahan, C. Roberts, R. Senan, C. Zarzycki, and P. Ullrich, 2020: Impact of model resolution on tropical cyclone simulation using the HighResMIP-PRIMAVERA multimodel ensemble. *Journal of Climate*, **33** (7), 2557–2583. <https://doi.org/10.1175/jcli-d-19-0639.1>
40. Roberts, M.J., J. Camp, J. Seddon, P.L. Vidale, K. Hodges, B. Vannière, J. Mecking, R. Haarsma, A. Bellucci, E. Scoccimarro, L.-P. Caron, F. Chauvin, L. Terray, S. Valcke, M.-P. Moine, D. Putrasahan, C.D. Roberts, R. Senan, C. Zarzycki, P. Ullrich, Y. Yamada, R. Mizuta, C. Kodama, D. Fu, Q. Zhang, G. Danabasoglu, N. Rosenbloom, H. Wang, and L. Wu, 2020: Projected future changes in tropical cyclones using the CMIP6 HighResMIP multimodel ensemble. *Geophysical Research Letters*, **47** (14), e2020GL088662. <https://doi.org/10.1029/2020gl088662>
41. Wehner, M.F., K.A. Reed, B. Loring, D. Stone, and H. Krishnan, 2018: Changes in tropical cyclones under stabilized 1.5 and 2.0 °C global warming scenarios as simulated by the Community Atmospheric Model under the HAPPI protocols. *Earth System Dynamics*, **9** (1), 187–195. <https://doi.org/10.5194/esd-9-187-2018>
42. Knutson, T., S.J. Camargo, J.C.L. Chan, K. Emanuel, C.H. Ho, J. Kossin, M. Mohapatra, M. Satoh, M. Sugi, K. Walsh, and L. Wu, 2020: Tropical cyclones and climate change assessment: Part II: Projected response to anthropogenic warming. *Bulletin of the American Meteorological Society*, **101** (3), 303–322. <https://doi.org/10.1175/bams-d-18-0194.1>
43. Siirila-Woodburn, E.R., A.M. Rhoades, B.J. Hatchett, L.S. Huning, J. Szinai, C. Tague, P.S. Nico, D.R. Feldman, A.D. Jones, W.D. Collins, and L. Kaatz, 2021: A low-to-no snow future and its impacts on water resources in the western United States. *Nature Reviews Earth & Environment*, **2** (11), 800–819. <https://doi.org/10.1038/s43017-021-00219-y>
44. Albano, C.M., M.I. McCarthy, M.D. Dettinger, and S.A. McAffee, 2021: Techniques for constructing climate scenarios for stress test applications. *Climatic Change*, **164** (3), 33. <https://doi.org/10.1007/s10584-021-02985-6>
45. Shepherd, T.G., 2016: A common framework for approaches to extreme event attribution. *Current Climate Change Reports*, **2** (1), 28–38. <https://doi.org/10.1007/s40641-016-0033-y>
46. Shepherd, T.G., 2019: Storyline approach to the construction of regional climate change information. *Proceedings of the Royal Society A: Mathematical, Physical and Engineering Sciences*, **475** (2225), 20190013. <https://doi.org/10.1098/rspa.2019.0013>
47. Garrido-Perez, J.M., C. Ordóñez, D. Barriopedro, R. García-Herrera, J.L. Schnell, and D.E. Horton, 2022: A storyline view of the projected role of remote drivers on summer air stagnation in Europe and the United States. *Environmental Research Letters*, **17** (1), 014026. <https://doi.org/10.1088/1748-9326/ac4290>
48. Michaelis, A.C., A. Gershunov, A. Weyant, M.A. Fish, T. Shulgina, and F.M. Ralph, 2022: Atmospheric river precipitation enhanced by climate change: A case study of the storm that contributed to California's Oroville Dam crisis. *Earth's Future*, **10** (3), e2021EF002537. <https://doi.org/10.1029/2021ef002537>
49. Patricola, C.M., M.F. Wehner, E. Bercos-Hickey, F.V. Maciel, C. May, M. Mak, O. Yip, A.M. Roche, and S. Leal, 2022: Future changes in extreme precipitation over the San Francisco Bay Area: Dependence on atmospheric river and extratropical cyclone events. *Weather and Climate Extremes*, **36**, 100440. <https://doi.org/10.1016/j.wace.2022.100440>

50. Chen, X., L.R. Leung, Y. Gao, Y. Liu, and M. Wigmosta, 2023: Sharpening of cold-season storms over the western United States. *Nature Climate Change*, **13** (2), 167–173. <https://doi.org/10.1038/s41558-022-01578-0>
51. Gutmann, E.D., R.M. Rasmussen, C. Liu, K. Ikeda, C.L. Bruyere, J.M. Done, L. Garrè, P. Friis-Hansen, and V. Veldore, 2018: Changes in hurricanes from a 13-yr convection-permitting pseudo-Global warming simulation. *Journal of Climate*, **31** (9), 3643–3657. <https://doi.org/10.1175/jcli-d-17-0391.1>
52. Ullrich, P.A., Z. Xu, A.M. Rhoades, M.D. Dettinger, J.F. Mount, A.D. Jones, and P. Vahmani, 2018: California's drought of the future: A midcentury recreation of the exceptional conditions of 2012–2017. *Earth's Future*, **6** (11), 1568–1587. <https://doi.org/10.1029/2018ef001007>
53. Deser, C., F. Lehner, K.B. Rodgers, T. Ault, T.L. Delworth, P.N. DiNezio, A. Fiore, C. Frankignoul, J.C. Fyfe, D.E. Horton, J.E. Kay, R. Knutti, N.S. Lovenduski, J. Marotzke, K.A. McKinnon, S. Minobe, J. Randerson, J.A. Screen, I.R. Simpson, and M. Ting, 2020: Insights from Earth system model initial-condition large ensembles and future prospects. *Nature Climate Change*, **10** (4), 277–286. <https://doi.org/10.1038/s41558-020-0731-2>
54. Eyring, V., P.M. Cox, G.M. Flato, P.J. Gleckler, G. Abramowitz, P. Caldwell, W.D. Collins, B.K. Gier, A.D. Hall, F.M. Hoffman, G.C. Hurtt, A. Jahn, C.D. Jones, S.A. Klein, J.P. Krasting, L. Kwiatkowski, R. Lorenz, E. Maloney, G.A. Meehl, A.G. Pendergrass, R. Pincus, A.C. Ruane, J.L. Russell, B.M. Sanderson, B.D. Santer, S.C. Sherwood, I.R. Simpson, R.J. Stouffer, and M.S. Williamson, 2019: Taking climate model evaluation to the next level. *Nature Climate Change*, **9** (2), 102–110. <https://doi.org/10.1038/s41558-018-0355-y>
55. Hall, A., P. Cox, C. Huntingford, and S. Klein, 2019: Progressing emergent constraints on future climate change. *Nature Climate Change*, **9** (4), 269–278. <https://doi.org/10.1038/s41558-019-0436-6>
56. Lehner, F., A.W. Wood, J.A. Vano, D.M. Lawrence, M.P. Clark, and J.S. Mankin, 2019: The potential to reduce uncertainty in regional runoff projections from climate models. *Nature Climate Change*, **9** (12), 926–933. <https://doi.org/10.1038/s41558-019-0639-x>
57. Lin, Y., W. Dong, M. Zhang, Y. Xie, W. Xue, J. Huang, and Y. Luo, 2017: Causes of model dry and warm bias over central U.S. and impact on climate projections. *Nature Communications*, **8** (1), 881. <https://doi.org/10.1038/s41467-017-01040-2>
58. Dong, L., L.R. Leung, J. Lu, and F. Song, 2021: Double-ITCZ as an emergent constraint for future precipitation over Mediterranean climate regions in the north hemisphere. *Geophysical Research Letters*, **48** (3), e2020GL091569. <https://doi.org/10.1029/2020gl091569>
59. National Academies of Sciences, Engineering, and Medicine, 2016: *Attribution of Extreme Weather Events in the Context of Climate Change*. National Academies Press, Washington, DC, 186 pp. <https://doi.org/10.17226/21852>
60. Herring, S.C., N. Christidis, A. Hoell, and P.A. Stott, 2022: Explaining extreme events of 2020 from a climate perspective. *Bulletin of the American Meteorological Society*, **103** (3), S1–S117. <https://doi.org/10.1175/bams-explainingextremeevents2020.1>
61. Herring, S.C., N. Christidis, A. Hoell, M.P. Hoerling, and P.A. Stott, 2019: Explaining extreme events of 2017 from a climate perspective. *Bulletin of the American Meteorological Society*, **100** (1), S1–S117. <https://doi.org/10.1175/bams-explainingextremeevents2017.1>
62. Herring, S.C., N. Christidis, A. Hoell, J.P. Kossin, C.J. Schreck, III, and P.A. Stott, 2018: Explaining extreme events of 2016 from a climate perspective. *Bulletin of the American Meteorological Society*, **99** (1), S1–S157. <https://doi.org/10.1175/bams-explainingextremeevents2016.1>
63. Reed, K.A., M.F. Wehner, and C.M. Zarzycki, 2022: Attribution of 2020 hurricane season extreme rainfall to human-induced climate change. *Nature Communications*, **13** (1), 1905. <https://doi.org/10.1038/s41467-022-29379-1>
64. Wehner, M.F., C. Zarzycki, and C. Patricola, 2019: Ch. 12. Estimating the human influence on tropical cyclone intensity as the climate changes. In: *Hurricane Risk*. Collins, J.M. and K. Walsh, Eds. Springer, Cham, Switzerland, 235–260. [https://doi.org/10.1007/978-3-030-02402-4\\_12](https://doi.org/10.1007/978-3-030-02402-4_12)
65. Otto, F.E.L., L.J. Harrington, D. Frame, E. Boyd, K.C. Lauta, M. Wehner, B. Clarke, E. Raju, C. Boda, M. Hauser, R.A. James, and R.G. Jones, 2020: Toward an inventory of the impacts of human-induced climate change. *Bulletin of the American Meteorological Society*, **101** (11), E1972–E1979. <https://doi.org/10.1175/bams-d-20-0027.1>
66. Knutson, T., 2017: Detection and attribution methodologies overview. In: *Climate Science Special Report: Fourth National Climate Assessment*. Wuebbles, D.J., D.W. Fahey, K.A. Hibbard, D.J. Dokken, B.C. Stewart, and T.K. Maycock, Eds. U.S. Global Change Research Program, Washington, DC, USA, 443–451. <https://doi.org/10.7930/j0319t2j>

67. Ebert-Uphoff, I. and Y. Deng, 2015: Ch. 11. Using causal discovery algorithms to learn about our planet's climate. In: *Machine Learning and Data Mining Approaches to Climate Science*. Lakshmanan, V., E. Gilleland, A. McGovern, and M. Tingley, Eds. Springer, Cham, Switzerland, 113–126. [https://doi.org/10.1007/978-3-319-17220-0\\_11](https://doi.org/10.1007/978-3-319-17220-0_11)
68. Risser, M., W. Collin, M. Wehner, T. O'Brien, C. Paciorek, J.P. O'Brien, C. Patricola, H. Huang, P. Ullrich, and B. Loring, 2021: A method for detection and attribution of regional precipitation change using Granger causality application to the United States historical record. *Climate Dynamics*. <https://doi.org/10.21203/rs.3.rs-785460/v1>
69. Risser, M.D., W.D. Collins, M.F. Wehner, T.A. O'Brien, C.J. Paciorek, J.P. O'Brien, C.M. Patricola, H. Huang, P.A. Ullrich, and B. Loring, 2023: A framework for detection and attribution of regional precipitation change: Application to the United States historical record. *Climate Dynamics*, **60**, 705–741. <https://doi.org/10.1007/s00382-022-06321-1>
70. Perkins-Kirkpatrick, S.E., D.A. Stone, D.M. Mitchell, S. Rosier, A.D. King, Y.T.E. Lo, J. Pastor-Paz, D. Frame, and M. Wehner, 2022: On the attribution of the impacts of extreme weather events to anthropogenic climate change. *Environmental Research Letters*, **17** (2), 024009. <https://doi.org/10.1088/1748-9326/ac44c8>
71. van der Wiel, K., N. Wanders, F.M. Selten, and M.F.P. Bierkens, 2019: Added value of large ensemble simulations for assessing extreme river discharge in a 2 °C warmer world. *Geophysical Research Letters*, **46** (4), 2093–2102. <https://doi.org/10.1029/2019gl081967>
72. Stott, P.A., D.A. Stone, and M.R. Allen, 2004: Human contribution to the European heatwave of 2003. *Nature*, **432** (7017), 610–614. <https://doi.org/10.1038/nature03089>
73. Kam, J., S.-K. Min, Y.-H. Kim, B.-H. Kim, and J.-S. Kug, 2022: Anthropogenic contribution to the record-breaking warm and wet winter 2019/20 over northwest Russia. *Bulletin of the American Meteorological Society*, **103** (3), S38–S43. <https://doi.org/10.1175/bams-d-21-0148.1>
74. Pall, P., C.M. Patricola, M.F. Wehner, D.A. Stone, C.J. Paciorek, and W.D. Collins, 2017: Diagnosing conditional anthropogenic contributions to heavy Colorado rainfall in September 2013. *Weather and Climate Extremes*, **17**, 1–6. <https://doi.org/10.1016/j.wace.2017.03.004>
75. Takayabu, I., K. Hibino, H. Sasaki, H. Shiogama, N. Mori, Y. Shibutani, and T. Takemi, 2015: Climate change effects on the worst-case storm surge: A case study of Typhoon Haiyan. *Environmental Research Letters*, **10** (6), 064011. <https://doi.org/10.1088/1748-9326/10/6/064011>
76. Philip, S.Y., S.F. Kew, G.J. van Oldenborgh, F.S. Anslow, S.I. Seneviratne, R. Vautard, D. Coumou, K.L. Ebi, J. Arrighi, R. Singh, M. van Aalst, C. Pereira Marghidan, M. Wehner, W. Yang, S. Li, D.L. Schumacher, M. Hauser, R. Bonnet, L.N. Luu, F. Lehner, N. Gillett, J. Tradowsky, G.A. Vecchi, C. Rodell, R.B. Stull, R. Howard, and F.E.L. Otto, 2021: Rapid attribution analysis of the extraordinary heat wave on the Pacific coast of the US and Canada in June 2021. *Earth System Dynamics*, **13** (4), 1689–1713. <https://doi.org/10.5194/esd-13-1689-2022>
77. van der Wiel, K., S.B. Kapnick, G.J. van Oldenborgh, K. Whan, S. Philip, G.A. Vecchi, R.K. Singh, J. Arrighi, and H. Cullen, 2017: Rapid attribution of the August 2016 flood-inducing extreme precipitation in south Louisiana to climate change. *Hydrology and Earth System Sciences*, **21** (2), 897–921. <https://doi.org/10.5194/hess-21-897-2017>
78. Reed, K.A., A.M. Stansfield, M.F. Wehner, and C.M. Zarzycki, 2020: Forecasted attribution of the human influence on Hurricane Florence. *Science Advances*, **6** (1), 9253. <https://doi.org/10.1126/sciadv.aaw9253>
79. Wehner, M.F. and K.A. Reed, 2022: Operational extreme weather event attribution can quantify climate change loss and damages. *PLoS Climate*, **1** (2), e0000013. <https://doi.org/10.1371/journal.pclm.0000013>
80. van Oldenborgh, G.J., K. van der Wiel, S. Kew, S. Philip, F. Otto, R. Vautard, A. King, F. Lott, J. Arrighi, R. Singh, and M. van Aalst, 2021: Pathways and pitfalls in extreme event attribution. *Climatic Change*, **166** (1), 13. <https://doi.org/10.1007/s10584-021-03071-7>
81. van Oldenborgh, G.J., M.F. Wehner, R. Vautard, F.E.L. Otto, S.I. Seneviratne, P.A. Stott, G.C. Hegerl, S.Y. Philip, and S.F. Kew, 2022: Attributing and projecting heatwaves is hard: We can do better. *Earth's Future*, **10** (6), e2021EF002271. <https://doi.org/10.1029/2021ef002271>
82. Risser, M.D. and M.F. Wehner, 2017: Attributable human-induced changes in the likelihood and magnitude of the observed extreme precipitation during Hurricane Harvey. *Geophysical Research Letters*, **44** (24), 12457–12464. <https://doi.org/10.1002/2017gl075888>
83. van Oldenborgh, G.J., K. van der Wiel, A. Sebastian, R. Singh, J. Arrighi, F. Otto, K. Haustein, S. Li, G. Vecchi, and H. Cullen, 2017: Attribution of extreme rainfall from Hurricane Harvey, August 2017. *Environmental Research Letters*, **12** (12), 124009. <https://doi.org/10.1088/1748-9326/aa9ef2>



84. Wang, S.Y.S., L. Zhao, J.-H. Yoon, P. Klotzbach, and R.R. Gillies, 2018: Quantitative attribution of climate effects on Hurricane Harvey's extreme rainfall in Texas. *Environmental Research Letters*, **13** (5), 054014. <https://doi.org/10.1088/1748-9326/aabb85>
85. Wehner, M. and C. Sampson, 2021: Attributable human-induced changes in the magnitude of flooding in the Houston, Texas region during Hurricane Harvey. *Climatic Change*, **166** (1), 1–13. <https://doi.org/10.1007/s10584-021-03114-z>
86. Lehner, F., C. Deser, N. Maher, J. Marotzke, E.M. Fischer, L. Brunner, R. Knutti, and E. Hawkins, 2020: Partitioning climate projection uncertainty with multiple large ensembles and CMIP5/6. *Earth System Dynamics*, **11** (2), 491–508. <https://doi.org/10.5194/esd-11-491-2020>
87. Dong, L., L.R. Leung, F. Song, and J. Lu, 2021: Uncertainty in El Niño-like warming and California precipitation changes linked by the Interdecadal Pacific Oscillation. *Nature Communications*, **12** (1), 6484. <https://doi.org/10.1038/s41467-021-26797-5>
88. Perlwitz, J., T. Knutson, J.P. Kossin, and A.N. LeGrande, 2017: Ch. 5. Large-scale circulation and climate variability. In: *Climate Science Special Report: Fourth National Climate Assessment, Volume I*. Wuebbles, D.J., D.W. Fahey, K.A. Hibbard, D.J. Dokken, B.C. Stewart, and T.K. Maycock, Eds. U.S. Global Change Research Program, Washington, DC, USA, 161–184. <https://doi.org/10.7930/j0rv0kvq>
89. Staten, P.W., J. Lu, K.M. Grise, S.M. Davis, and T. Birner, 2018: Re-examining tropical expansion. *Nature Climate Change*, **8** (9), 768–775. <https://doi.org/10.1038/s41558-018-0246-2>
90. Grise, K.M., S.M. Davis, I.R. Simpson, D.W. Waugh, Q. Fu, R.J. Allen, K.H. Rosenlof, C.C. Ummenhofer, K.B. Karnauskas, A.C. Maycock, X.-W. Quan, T. Birner, and P.W. Staten, 2019: Recent tropical expansion: Natural variability or forced response? *Journal of Climate*, **32** (5), 1551–1571. <https://doi.org/10.1175/jcli-d-18-0444.1>
91. Simpson, I., 2018: Natural variability in the width of the tropics. *US CLIVAR Variations*, **16** (2), 14–20. <https://usclivar.org/newsletters>
92. Oudar, T., J. Cattiaux, and H. Douville, 2020: Drivers of the northern extratropical eddy-driven jet change in CMIP5 and CMIP6 models. *Geophysical Research Letters*, **47** (8), e2019GL086695. <https://doi.org/10.1029/2019gl086695>
93. Zhou, W., L.R. Leung, and J. Lu, 2022: Seasonally and regionally dependent shifts of the atmospheric westerly jets under global warming. *Journal of Climate*, **35** (16), 5433–5447. <https://doi.org/10.1175/jcli-d-21-0723.1>
94. Dong, L. and L.R. Leung, 2021: Winter precipitation changes in California under global warming: Contributions of CO<sub>2</sub>, uniform SST warming, and SST change patterns. *Geophysical Research Letters*, **48** (5), e2020GL091736. <https://doi.org/10.1029/2020gl091736>
95. Neelin, J.D., B. Langenbrunner, J.E. Meyerson, A. Hall, and N. Berg, 2013: California winter precipitation change under global warming in the Coupled Model Intercomparison Project phase 5 ensemble. *Journal of Climate*, **26** (17), 6238–6256. <https://doi.org/10.1175/jcli-d-12-00514.1>
96. Zhou, W., L.R. Leung, and J. Lu, 2022: Seasonally dependent future changes in the U.S. Midwest hydroclimate and extremes. *Journal of Climate*, **35** (1), 17–27. <https://doi.org/10.1175/jcli-d-21-0012.1>
97. Song, F., L.R. Leung, J. Lu, and L. Dong, 2018: Future changes in seasonality of the North Pacific and North Atlantic subtropical highs. *Geophysical Research Letters*, **45** (21), 11959–11968. <https://doi.org/10.1029/2018gl079940>
98. Pascale, S., W.R. Boos, S. Bordoni, T.L. Delworth, S.B. Kapnick, H. Murakami, G.A. Vecchi, and W. Zhang, 2017: Weakening of the North American monsoon with global warming. *Nature Climate Change*, **7** (11), 806–812. <https://doi.org/10.1038/nclimate3412>
99. Cook, B.I. and R. Seager, 2013: The response of the North American Monsoon to increased greenhouse gas forcing. *Journal of Geophysical Research: Atmospheres*, **118** (4), 1690–1699. <https://doi.org/10.1002/jgrd.50111>
100. Song, F., L.R. Leung, J. Lu, and L. Dong, 2018: Seasonally dependent responses of subtropical highs and tropical rainfall to anthropogenic warming. *Nature Climate Change*, **8** (9), 787–792. <https://doi.org/10.1038/s41558-018-0244-4>
101. Song, F., L.R. Leung, J. Lu, L. Dong, W. Zhou, B. Harrop, and Y. Qian, 2021: Emergence of seasonal delay of tropical rainfall during 1979–2019. *Nature Climate Change*, **11** (7), 605–612. <https://doi.org/10.1038/s41558-021-01066-x>



102. Davini, P. and F. D'Andrea, 2020: From CMIP3 to CMIP6: Northern Hemisphere atmospheric blocking simulation in present and future climate. *Journal of Climate*, **33** (23), 10021–10038. <https://doi.org/10.1175/jcli-d-19-0862.1>
103. Neelin, J.D., S. Sahany, S.N. Stechmann, and D.N. Bernstein, 2017: Global warming precipitation accumulation increases above the current-climate cutoff scale. *Proceedings of the National Academy of Sciences of the United States of America*, **114** (6), 1258–1263. <https://doi.org/10.1073/pnas.1615333114>
104. Groisman, P.Y., R.W. Knight, D.R. Easterling, T.R. Karl, G.C. Hegerl, and V.N. Razuvaev, 2005: Trends in intense precipitation in the climate record. *Journal of Climate*, **18** (9), 1326–1350. <https://doi.org/10.1175/jcli3339.1>
105. Karl, T.R. and R.W. Knight, 1998: Secular trends of precipitation amount, frequency, and intensity in the United States. *Bulletin of the American Meteorological Society*, **79** (2), 231–241. DOI:10.1175/1520-0477(1998)079<0231:STO PAF>2.0.CO;2. [https://journals.ametsoc.org/view/journals/bams/79/2/1520-0477\\_1998\\_079\\_0231\\_stopaf\\_2\\_0\\_co\\_2.xml](https://journals.ametsoc.org/view/journals/bams/79/2/1520-0477_1998_079_0231_stopaf_2_0_co_2.xml)
106. Pendergrass, A.G. and R. Knutti, 2018: The uneven nature of daily precipitation and its change. *Geophysical Research Letters*, **45** (21), 11980–11988. <https://doi.org/10.1029/2018gl080298>
107. Semenov, V. and L. Bengtsson, 2002: Secular trends in daily precipitation characteristics: Greenhouse gas simulation with a coupled AOGCM. *Climate Dynamics*, **19** (2), 123–140. <https://doi.org/10.1007/s00382-001-0218-4>
108. Pascale, S., S.B. Kapnick, S. Bordoni, and T.L. Delworth, 2018: The influence of CO<sub>2</sub> forcing on North American monsoon moisture surges. *Journal of Climate*, **31** (19), 7949–7968. <https://doi.org/10.1175/jcli-d-18-0007.1>
109. Polade, S.D., A. Gershunov, D.R. Cayan, M.D. Dettinger, and D.W. Pierce, 2017: Precipitation in a warming world: Assessing projected hydro-climate changes in California and other Mediterranean climate regions. *Scientific Reports*, **7** (1), 10783. <https://doi.org/10.1038/s41598-017-11285-y>
110. Pendergrass, A.G., R. Knutti, F. Lehner, C. Deser, and B.M. Sanderson, 2017: Precipitation variability increases in a warmer climate. *Scientific Reports*, **7** (1), 17966. <https://doi.org/10.1038/s41598-017-17966-y>
111. Ukkola, A.M., M.G. De Kauwe, M.L. Roderick, G. Abramowitz, and A.J. Pitman, 2020: Robust future changes in meteorological drought in CMIP6 projections despite uncertainty in precipitation. *Geophysical Research Letters*, **47** (1), e2020GL087820. <https://doi.org/10.1029/2020gl087820>
112. Swain, D.L., B. Langenbrunner, J.D. Neelin, and A. Hall, 2018: Increasing precipitation volatility in twenty-first-century California. *Nature Climate Change*, **8** (5), 427–433. <https://doi.org/10.1038/s41558-018-0140-y>
113. Pfahl, S., P.A. O'Gorman, and E.M. Fischer, 2017: Understanding the regional pattern of projected future changes in extreme precipitation. *Nature Climate Change*, **7** (6), 423–427. <https://doi.org/10.1038/nclimate3287>
114. Gertler, C.G. and P.A. O'Gorman, 2019: Changing available energy for extratropical cyclones and associated convection in Northern Hemisphere summer. *Proceedings of the National Academy of Sciences of the United States of America*, **116** (10), 4105–4110. <https://doi.org/10.1073/pnas.1812312116>
115. Fischer, E.M. and R. Knutti, 2016: Observed heavy precipitation increase confirms theory and early models. *Nature Climate Change*, **6** (11), 986–991. <https://doi.org/10.1038/nclimate3110>
116. Dong, L., L.R. Leung, J. Lu, and F. Song, 2019: Mechanisms for an amplified precipitation seasonal cycle in the U.S. West Coast under global warming. *Journal of Climate*, **32** (15), 4681–4698. <https://doi.org/10.1175/jcli-d-19-0093.1>
117. Luković, J., J.C.H. Chiang, D. Blagojević, and A. Sekulić, 2021: A later onset of the rainy season in California. *Geophysical Research Letters*, **48** (4), e2020GL090350. <https://doi.org/10.1029/2020gl090350>
118. Mote, P.W., S. Li, D.P. Lettenmaier, M. Xiao, and R. Engel, 2018: Dramatic declines in snowpack in the western US. *Npj Climate and Atmospheric Science*, **1** (1), 1–6. <https://doi.org/10.1038/s41612-018-0012-1>
119. Marshall, A.M., J.T. Abatzoglou, T.E. Link, and C.J. Tennant, 2019: Projected changes in interannual variability of peak snowpack amount and timing in the western United States. *Geophysical Research Letters*, **46** (15), 8882–8892. <https://doi.org/10.1029/2019gl083770>
120. Lehner, F., E.R. Wahl, A.W. Wood, D.B. Blatchford, and D. Llewellyn, 2017: Assessing recent declines in Upper Rio Grande runoff efficiency from a paleoclimate perspective. *Geophysical Research Letters*, **44** (9), 4124–4133. <https://doi.org/10.1002/2017gl073253>

121. Milly, P.C.D. and K.A. Dunne, 2020: Colorado River flow dwindles as warming-driven loss of reflective snow energizes evaporation. *Science*, **367** (6483), 1252–1255. <https://doi.org/10.1126/science.aay9187>
122. Woodhouse, C.A., G.T. Pederson, K. Morino, S.A. McAfee, and G.J. McCabe, 2016: Increasing influence of air temperature on upper Colorado River streamflow. *Geophysical Research Letters*, **43** (5), 2174–2181. <https://doi.org/10.1002/2015gl067613>
123. Friedlingstein, P., M.W. Jones, M. O’Sullivan, R.M. Andrew, D.C.E. Bakker, J. Hauck, C. Le Quéré, G.P. Peters, W. Peters, J. Pongratz, S. Sitch, J.G. Canadell, P. Ciais, R.B. Jackson, S.R. Alin, P. Anthoni, N.R. Bates, M. Becker, N. Bellouin, L. Bopp, T.T.T. Chau, F. Chevallier, L.P. Chini, M. Cronin, K.I. Currie, B. Decharme, L.M. Djeutchouang, X. Dou, W. Evans, R.A. Feely, L. Feng, T. Gasser, D. Gilfillan, T. Gkritzalis, G. Grassi, L. Gregor, N. Gruber, Ö. Gürses, I. Harris, R.A. Houghton, G.C. Hurtt, Y. Iida, T. Ilyina, I.T. Luijckx, A. Jain, S.D. Jones, E. Kato, D. Kennedy, K. Klein Goldewijk, J. Knauer, J.I. Korsbakken, A. Körtzinger, P. Landschützer, S.K. Lauvset, N. Lefèvre, S. Lienert, J. Liu, G. Marland, P.C. McGuire, J.R. Melton, D.R. Munro, J.E.M.S. Nabel, S.I. Nakaoka, Y. Niwa, T. Ono, D. Pierrot, B. Poulter, G. Rehder, L. Resplandy, E. Robertson, C. Rödenbeck, T.M. Rosan, J. Schwinger, C. Schwingshackl, R. Séférian, A.J. Sutton, C. Sweeney, T. Tanhua, P.P. Tans, H. Tian, B. Tilbrook, F. Tubiello, G.R. van der Werf, N. Vuichard, C. Wada, R. Wanninkhof, A.J. Watson, D. Willis, A.J. Wiltshire, W. Yuan, C. Yue, X. Yue, S. Zaehle, and J. Zeng, 2022: Global carbon budget 2021. *Earth System Science Data*, **14** (4), 1917–2005. <https://doi.org/10.5194/essd-14-1917-2022>
124. Chen, C., W.J. Riley, I.C. Prentice, and T.F. Keenan, 2022: CO<sub>2</sub> fertilization of terrestrial photosynthesis inferred from site to global scales. *Proceedings of the National Academy of Sciences of the United States of America*, **119** (10), e2115627119. <https://doi.org/10.1073/pnas.2115627119>
125. Pugh, T.A.M., M. Lindeskog, B. Smith, B. Poulter, A. Arneth, V. Haverd, and L. Calle, 2019: Role of forest regrowth in global carbon sink dynamics. *Proceedings of the National Academy of Sciences of the United States of America*, **116** (10), 4382–4387. <https://doi.org/10.1073/pnas.1810512116>
126. Walker, A.P., M.G. De Kauwe, A. Bastos, S. Belmecheri, K. Georgiou, R.F. Keeling, S.M. McMahon, B.E. Medlyn, D.J.P. Moore, R.J. Norby, S. Zaehle, K.J. Anderson-Teixeira, G. Battipaglia, R.J.W. Brienen, K.G. Cabugao, M. Cailleret, E. Campbell, J.G. Canadell, P. Ciais, M.E. Craig, D.S. Ellsworth, G.D. Farquhar, S. Fatichi, J.B. Fisher, D.C. Frank, H. Graven, L. Gu, V. Haverd, K. Heilman, M. Heimann, B.A. Hungate, C.M. Iversen, F. Joos, M. Jiang, T.F. Keenan, J. Knauer, C. Körner, V.O. Leshyk, S. Leuzinger, Y. Liu, N. MacBean, Y. Malhi, T.R. McVicar, J. Penuelas, J. Pongratz, A.S. Powell, T. Riutta, M.E.B. Sabot, J. Schleucher, S. Sitch, W.K. Smith, B. Sulman, B. Taylor, C. Terrer, M.S. Torn, K.K. Treseder, A.T. Trugman, S.E. Trumbore, P.J. van Mantgem, S.L. Voelker, M.E. Whelan, and P.A. Zuidema, 2021: Integrating the evidence for a terrestrial carbon sink caused by increasing atmospheric CO<sub>2</sub>. *New Phytologist*, **229** (5), 2413–2445. <https://doi.org/10.1111/nph.16866>
127. Chen, Y., D.M. Romps, J.T. Seeley, S. Veraverbeke, W.J. Riley, Z.A. Mekonnen, and J.T. Randerson, 2021: Future increases in Arctic lightning and fire risk for permafrost carbon. *Nature Climate Change*, **11** (5), 404–410. <https://doi.org/10.1038/s41558-021-01011-y>
128. Bruhwiler, L., S. Basu, J.H. Butler, A. Chatterjee, E. Dlugokencky, M.A. Kenney, A. McComiskey, S.A. Montzka, and D. Stanitski, 2021: Observations of greenhouse gases as climate indicators. *Climatic Change*, **165** (1), 12. <https://doi.org/10.1007/s10584-021-03001-7>
129. Miner, K.R., M.R. Turetsky, E. Malina, A. Bartsch, J. Tamminen, A.D. McGuire, A. Fix, C. Sweeney, C.D. Elder, and C.E. Miller, 2022: Permafrost carbon emissions in a changing Arctic. *Nature Reviews Earth and Environment*, **3** (1), 55–67. <https://doi.org/10.1038/s43017-021-00230-3>
130. Busch, D.S. and P. McElhany, 2016: Estimates of the direct effect of seawater pH on the survival rate of species groups in the California Current ecosystem. *PLoS ONE*, **11** (8), e0160669. <https://doi.org/10.1371/journal.pone.0160669>
131. Heinze, C., S. Meyer, N. Goris, L. Anderson, R. Steinfeldt, N. Chang, C. Le Quéré, and D.C.E. Bakker, 2015: The ocean carbon sink—Impacts, vulnerabilities and challenges. *Earth System Dynamics*, **6** (1), 327–358. <https://doi.org/10.5194/esd-6-327-2015>
132. Jiang, L.-Q., B.R. Carter, R.A. Feely, S.K. Lauvset, and A. Olsen, 2019: Surface ocean pH and buffer capacity: Past, present and future. *Scientific Reports*, **9** (1), 18624. <https://doi.org/10.1038/s41598-019-55039-4>
133. Schlunegger, S., K.B. Rodgers, J.L. Sarmiento, T. Ilyina, J.P. Dunne, Y. Takano, J.R. Christian, M.C. Long, T.L. Frölicher, R. Slater, and F. Lehner, 2020: Time of emergence and large ensemble intercomparison for ocean biogeochemical trends. *Global Biogeochemical Cycles*, **34** (8), e2019GB006453. <https://doi.org/10.1029/2019gb006453>

134. Arora, V.K., A. Katavouta, R.G. Williams, C.D. Jones, V. Brovkin, P. Friedlingstein, J. Schwinger, L. Bopp, O. Boucher, P. Cadule, M.A. Chamberlain, J.R. Christian, C. Delire, R.A. Fisher, T. Hajima, T. Ilyina, E. Joetzjer, M. Kawamiya, C.D. Koven, J.P. Krasting, R.M. Law, D.M. Lawrence, A. Lenton, K. Lindsay, J. Pongratz, T. Raddatz, R. Séférian, K. Tachiiri, J.F. Tjiputra, A. Wiltshire, T. Wu, and T. Ziehn, 2020: Carbon–concentration and carbon–climate feedbacks in CMIP6 models and their comparison to CMIP5 models. *Biogeosciences*, **17** (16), 4173–4222. <https://doi.org/10.5194/bg-17-4173-2020>
135. Séférian, R., S. Berthet, A. Yool, J. Palmiéri, L. Bopp, A. Tagliabue, L. Kwiatkowski, O. Aumont, J. Christian, J. Dunne, M. Gehlen, T. Ilyina, J.G. John, H. Li, M.C. Long, J.Y. Luo, H. Nakano, A. Romanou, J. Schwinger, C. Stock, Y. Santana-Falcón, Y. Takano, J. Tjiputra, H. Tsujino, M. Watanabe, T. Wu, F. Wu, and A. Yamamoto, 2020: Tracking improvement in simulated marine biogeochemistry between CMIP5 and CMIP6. *Current Climate Change Reports*, **6** (3), 95–119. <https://doi.org/10.1007/s40641-020-00160-0>
136. Zhu, K., J. Zhang, S. Niu, C. Chu, and Y. Luo, 2018: Limits to growth of forest biomass carbon sink under climate change. *Nature Communications*, **9** (1), 2709. <https://doi.org/10.1038/s41467-018-05132-5>
137. Hessburg, P.F., S.J. Prichard, R.K. Hagmann, N.A. Povak, and F.K. Lake, 2021: Wildfire and climate change adaptation of western North American forests: A case for intentional management. *Ecological Applications*, **31** (8), e02432. <https://doi.org/10.1002/eap.2432>
138. Talley, L., 2013: Closure of the global overturning circulation through the Indian, Pacific, and Southern Oceans: Schematics and transports. *Oceanography*, **26**, 80–97. <https://doi.org/10.5670/oceanog.2013.07>
139. Gruber, N., D. Clement, B.R. Carter, R.A. Feely, S. van Heuven, M. Hoppema, M. Ishii, R.M. Key, A. Kozyr, S.K. Lauvset, C. Lo Monaco, J.T. Mathis, A. Murata, A. Olsen, F.F. Perez, C.L. Sabine, T. Tanhua, and R. Wanninkhof, 2019: The oceanic sink for anthropogenic CO<sub>2</sub> from 1994 to 2007. *Science*, **363** (6432), 1193–1199. <https://doi.org/10.1126/science.aau5153>
140. Caesar, L., S. Rahmstorf, A. Robinson, G. Feulner, and V. Saba, 2018: Observed fingerprint of a weakening Atlantic Ocean overturning circulation. *Nature*, **556** (7700), 191–196. <https://doi.org/10.1038/s41586-018-0006-5>
141. Jackson, L.C. and R.A. Wood, 2020: Fingerprints for early detection of changes in the AMOC. *Journal of Climate*, **33** (16), 7027–7044. <https://doi.org/10.1175/jcli-d-20-0034.1>
142. IPCC, 2019: *IPCC Special Report on the Ocean and Cryosphere in a Changing Climate*. Pörtner, H.-O., D.C. Roberts, V. Masson-Delmotte, P. Zhai, M. Tignor, E. Poloczanska, K. Mintenbeck, A. Alegria, M. Nicolai, A. Okem, J. Petzold, B. Rama, and N.M. Weyer, Eds. Cambridge University Press, Cambridge, UK and New York, NY, USA, 755 pp. <https://doi.org/10.1017/9781009157964>
143. Zanna, L., S. Khatiwala, J.M. Gregory, J. Ison, and P. Heimbach, 2019: Global reconstruction of historical ocean heat storage and transport. *Proceedings of the National Academy of Sciences of the United States of America*, **116** (4), 1126–1131. <https://doi.org/10.1073/pnas.1808838115>
144. Hobday, A.J., L.V. Alexander, S.E. Perkins, D.A. Smale, S.C. Straub, E.C.J. Oliver, J.A. Benthuysen, M.T. Burrows, M.G. Donat, M. Feng, N.J. Holbrook, P.J. Moore, H.A. Scannell, A. Sen Gupta, and T. Wernberg, 2016: A hierarchical approach to defining marine heatwaves. *Progress in Oceanography*, **141**, 227–238. <https://doi.org/10.1016/j.pocean.2015.12.014>
145. Amaya, D.J., A.J. Miller, S.-P. Xie, and Y. Kosaka, 2020: Physical drivers of the summer 2019 North Pacific marine heatwave. *Nature Communications*, **11** (1), 1903. <https://doi.org/10.1038/s41467-020-15820-w>
146. Di Lorenzo, E. and N. Mantua, 2016: Multi-year persistence of the 2014/15 North Pacific marine heatwave. *Nature Climate Change*, **6**, 1042–1047. <https://doi.org/10.1038/nclimate3082>
147. Gentemann, C.L., M.R. Fewings, and M. García-Reyes, 2017: Satellite sea surface temperatures along the West Coast of the United States during the 2014–2016 northeast Pacific marine heat wave. *Geophysical Research Letters*, **44** (1), 312–319. <https://doi.org/10.1002/2016gl071039>
148. Markus, T., T. Neumann, A. Martino, W. Abdalati, K. Brunt, B. Csatho, S. Farrell, H. Fricker, A. Gardner, D. Harding, M. Jasinski, R. Kwok, L. Magruder, D. Lubin, S. Luthcke, J. Morison, R. Nelson, A. Neuenschwander, S. Palm, S. Popescu, C.K. Shum, B.E. Schutz, B. Smith, Y. Yang, and J. Zwally, 2017: The Ice, Cloud, and land Elevation Satellite-2 (ICESat-2): Science requirements, concept, and implementation. *Remote Sensing of Environment*, **190**, 260–273. <https://doi.org/10.1016/j.rse.2016.12.029>

149. Fox-Kemper, B., H.T. Hewitt, C. Xiao, G. Aðalgeirsdóttir, S.S. Drijfhout, T.L. Edwards, N.R. Golledge, M. Hemer, R.E. Kopp, G. Krinner, A. Mix, D. Notz, S. Nowicki, I.S. Nurhati, L. Ruiz, J.-B. Sallée, A.B.A. Slangen, and Y. Yu, 2021: Ch. 9. Ocean, cryosphere and sea level change. In: *Climate Change 2021: The Physical Science Basis. Contribution of Working Group I to the Sixth Assessment Report of the Intergovernmental Panel on Climate Change*. Masson-Delmotte, V., P. Zhai, A. Pirani, S.L. Connors, C. Péan, S. Berger, N. Caud, Y. Chen, L. Goldfarb, M.I. Gomis, M. Huang, K. Leitzell, E. Lonnoy, J.B.R. Matthews, T.K. Maycock, T. Waterfield, O. Yelekçi, R. Yu, and B. Zhou, Eds. Cambridge University Press, Cambridge, UK and New York, NY, USA, 1211–1362. <https://doi.org/10.1017/9781009157896.011>
150. The Imbie Team, 2020: Mass balance of the Greenland ice sheet from 1992 to 2018. *Nature*, **579** (7798), 233–239. <https://doi.org/10.1038/s41586-019-1855-2>
151. DeConto, R.M. and D. Pollard, 2016: Contribution of Antarctica to past and future sea-level rise. *Nature*, **531** (7596), 591–597. <https://doi.org/10.1038/nature17145>
152. DeConto, R.M., D. Pollard, R.B. Alley, I. Velicogna, E. Gasson, N. Gomez, S. Sadai, A. Condrón, D.M. Gilford, E.L. Ashe, R.E. Kopp, D. Li, and A. Dutton, 2021: The Paris Climate Agreement and future sea-level rise from Antarctica. *Nature*, **593** (7857), 83–89. <https://doi.org/10.1038/s41586-021-03427-0>
153. Hoffman, M.J., X. Asay-Davis, S.F. Price, J. Fyke, and M. Perego, 2019: Effect of subshelf melt variability on sea level rise contribution from Thwaites Glacier, Antarctica. *Journal of Geophysical Research: Earth Surface*, **124** (12), e2019JF005155. <https://doi.org/10.1029/2019jf005155>
154. Joughin, I., B.E. Smith, and B. Medley, 2014: Marine ice sheet collapse potentially under way for the Thwaites Glacier Basin, West Antarctica. *Science*, **344** (6185), 735–738. <https://doi.org/10.1126/science.1249055>
155. Morlighem, M., E. Rignot, T. Binder, D. Blankenship, R. Drews, G. Eagles, O. Eisen, F. Ferraccioli, R. Forsberg, P. Fretwell, V. Goel, J.S. Greenbaum, H. Gudmundsson, J. Guo, V. Helm, C. Hofstede, I. Howat, A. Humbert, W. Jokat, N.B. Karlsson, W.S. Lee, K. Matsuoka, R. Millan, J. Mouginot, J. Paden, F. Pattyn, J. Roberts, S. Rosier, A. Ruppel, H. Seroussi, E.C. Smith, D. Steinhage, B. Sun, M.R. van den Broeke, T.D. van Ommen, M. van Wessel, and D.A. Young, 2020: Deep glacial troughs and stabilizing ridges unveiled beneath the margins of the Antarctic ice sheet. *Nature Geoscience*, **13** (2), 132–137. <https://doi.org/10.1038/s41561-019-0510-8>
156. Robel, A.A., H. Seroussi, and G.H. Roe, 2019: Marine ice sheet instability amplifies and skews uncertainty in projections of future sea-level rise. *Proceedings of the National Academy of Sciences of the United States of America*, **116** (30), 14887–14892. <https://doi.org/10.1073/pnas.1904822116>
157. Waibel, M.S., C.L. Hulbe, C.S. Jackson, and D.F. Martin, 2018: Rate of mass loss across the instability threshold for Thwaites Glacier determines rate of mass loss for entire basin. *Geophysical Research Letters*, **45** (2), 809–816. <https://doi.org/10.1002/2017gl076470>
158. Frederikse, T., F. Landerer, L. Caron, S. Adhikari, D. Parkes, V.W. Humphrey, S. Dangendorf, P. Hogarth, L. Zanna, L. Cheng, and Y.-H. Wu, 2020: The causes of sea-level rise since 1900. *Nature*, **584** (7821), 393–397. <https://doi.org/10.1038/s41586-020-2591-3>
159. Kemp, A.C., A.J. Wright, R.J. Edwards, R.L. Barnett, M.J. Brain, R.E. Kopp, N. Cahill, B.P. Horton, D.J. Charman, A.D. Hawkes, T.D. Hill, and O. van de Plassche, 2018: Relative sea-level change in Newfoundland, Canada during the past 13000 years. *Quaternary Science Reviews*, **201**, 89–110. <https://doi.org/10.1016/j.quascirev.2018.10.012>
160. Walker, J.S., R.E. Kopp, T.A. Shaw, N. Cahill, N.S. Khan, D.C. Barber, E.L. Ashe, M.J. Brain, J.L. Clear, D.R. Corbett, and B.P. Horton, 2021: Common Era sea-level budgets along the U.S. Atlantic coast. *Nature Communications*, **12** (1), 1841. <https://doi.org/10.1038/s41467-021-22079-2>
161. Dangendorf, S., C. Hay, F.M. Calafat, M. Marcos, C.G. Piecuch, K. Berk, and J. Jensen, 2019: Persistent acceleration in global sea-level rise since the 1960s. *Nature Climate Change*, **9** (9), 705–710. <https://doi.org/10.1038/s41558-019-0531-8>
162. Nerem, R.S., B.D. Beckley, J.T. Fasullo, B.D. Hamlington, D. Masters, and G.T. Mitchum, 2018: Climate-change-driven accelerated sea-level rise detected in the altimeter era. *Proceedings of the National Academy of Sciences of the United States of America*, **115** (9), 2022–2025. <https://doi.org/10.1073/pnas.1717312115>



163. Hamlington, B.D., A.S. Gardner, E. Ivins, J.T.M. Lenaerts, J.T. Reager, D.S. Trossman, E.D. Zaron, S. Adhikari, A. Arendt, A. Aschwanden, B.D. Beckley, D.P.S. Bekaert, G. Blewitt, L. Caron, D.P. Chambers, H.A. Chandanpurkar, K. Christianson, B. Csatho, R.I. Cullather, R.M. DeConto, J.T. Fasullo, T. Frederikse, J.T. Freymueller, D.M. Gilford, M. Giroto, W.C. Hammond, R. Hock, N. Holschuh, R.E. Kopp, F. Landerer, E. Larour, D. Menemenlis, M. Merrifield, J.X. Mitrovica, R.S. Nerem, I.J. Nias, V. Nieves, S. Nowicki, K. Pangaluru, C.G. Piecuch, R.D. Ray, D.R. Rounce, N.-J. Schlegel, H. Seroussi, M. Shirzaei, W.V. Sweet, I. Velicogna, N. Vinogradova, T. Wahl, D.N. Wiese, and M.J. Willis, 2020: Understanding of contemporary regional sea-level change and the implications for the future. *Reviews of Geophysics*, **58** (3), e2019RG000672. <https://doi.org/10.1029/2019rg000672>
164. Kopp, R.E., R.M. Horton, C.M. Little, J.X. Mitrovica, M. Oppenheimer, D.J. Rasmussen, B.H. Strauss, and C. Tebaldi, 2014: Probabilistic 21st and 22nd century sea-level projections at a global network of tide-gauge sites. *Earth's Future*, **2** (8), 383–406. <https://doi.org/10.1002/2014ef000239>
165. Sweet, W.V., R.E. Kopp, C.P. Weaver, J. Obeysekera, R.M. Horton, E.R. Thieler, and C. Zervas, 2017: Global and Regional Sea Level Rise Scenarios for the United States. NOAA Technical Report NOS CO-OPS 083. National Oceanic and Atmospheric Administration, National Ocean Service, Silver Spring, MD, 75 pp. <https://repository.library.noaa.gov/view/noaa/18399>
166. Gregory, J.M., S.M. Griffies, C.W. Hughes, J.A. Lowe, J.A. Church, I. Fukimori, N. Gomez, R.E. Kopp, F. Landerer, G.L. Cozannet, R.M. Ponte, D. Stammer, M.E. Tamisiea, and R.S.W. van de Wal, 2019: Concepts and terminology for sea level: Mean, variability and change, both local and global. *Surveys in Geophysics*, **40** (6), 1251–1289. <https://doi.org/10.1007/s10712-019-09525-z>
167. Sweet, W.V., B.D. Hamlington, R.E. Kopp, C.P. Weaver, P.L. Barnard, D. Bekaert, W. Brooks, M. Craghan, G. Dusek, T. Frederikse, G. Garner, A.S. Genz, J.P. Krasting, E. Larour, D. Marcy, J.J. Marra, J. Obeysekera, M. Osler, M. Pendleton, D. Roman, L. Schmied, W. Veatch, K.D. White, and C. Zuzak, 2022: Global and Regional Sea Level Rise Scenarios for the United States: Updated Mean Projections and Extreme Water Level Probabilities Along U.S. Coastlines. NOAA Technical Report NOS 01. National Oceanic and Atmospheric Administration, National Ocean Service, Silver Spring, MD, 111 pp. <https://oceanservice.noaa.gov/hazards/sealevelrise/sealevelrise-tech-report-sections.html>
168. Thompson, P.R., M.J. Widlansky, B.D. Hamlington, M.A. Merrifield, J.J. Marra, G.T. Mitchum, and W. Sweet, 2021: Rapid increases and extreme months in projections of United States high-tide flooding. *Nature Climate Change*, **11** (7), 584–590. <https://doi.org/10.1038/s41558-021-01077-8>
169. Yin, J., S.M. Griffies, M. Winton, M. Zhao, and L. Zanna, 2020: Response of storm-related extreme sea level along the U.S. Atlantic coast to combined weather and climate forcing. *Journal of Climate*, **33** (9), 3745–3769. <https://doi.org/10.1175/jcli-d-19-0551.1>
170. Bintanja, R., E.C. van der Linden, and W. Hazeleger, 2012: Boundary layer stability and Arctic climate change: A feedback study using EC-Earth. *Climate Dynamics*, **39** (11), 2659–2673. <https://doi.org/10.1007/s00382-011-1272-1>
171. Walton, D.B., A. Hall, N. Berg, M. Schwartz, and F. Sun, 2017: Incorporating snow albedo feedback into downscaled temperature and snow cover projections for California's Sierra Nevada. *Journal of Climate*, **30** (4), 1417–1438. <https://doi.org/10.1175/jcli-d-16-0168.1>
172. Sun, F., A. Hall, M. Schwartz, D.B. Walton, and N. Berg, 2016: Twenty-first-century snowfall and snowpack changes over the Southern California mountains. *Journal of Climate*, **29** (1), 91–110. <https://doi.org/10.1175/jcli-d-15-0199.1>
173. Zhou, C., M.D. Zelinka, and S.A. Klein, 2016: Impact of decadal cloud variations on the Earth's energy budget. *Nature Geoscience*, **9** (12), 871–874. <https://doi.org/10.1038/ngeo2828>
174. Siler, N. and G. Roe, 2014: How will orographic precipitation respond to surface warming? An idealized thermodynamic perspective. *Geophysical Research Letters*, **41** (7), 2606–2613. <https://doi.org/10.1002/2013gl059095>
175. López-Moreno, J.I., S. Goyette, S.M. Vicente-Serrano, and M. Beniston, 2011: Effects of climate change on the intensity and frequency of heavy snowfall events in the Pyrenees. *Climatic Change*, **105** (3), 489–508. <https://doi.org/10.1007/s10584-010-9889-3>
176. Ohba, M. and H. Kawase, 2020: Rain-on-snow events in Japan as projected by a large ensemble of regional climate simulations. *Climate Dynamics*, **55** (9), 2785–2800. <https://doi.org/10.1007/s00382-020-05419-8>
177. Huang, X., D.L. Swain, and A.D. Hall, 2020: Future precipitation increase from very high resolution ensemble downscaling of extreme atmospheric river storms in California. *Science Advances*, **6** (29), 1323. <https://doi.org/10.1126/sciadv.aba1323>



178. Gula, J. and W.R. Peltier, 2012: Dynamical downscaling over the Great Lakes Basin of North America using the WRF regional climate model: The impact of the Great Lakes system on regional greenhouse warming. *Journal of Climate*, **25** (21), 7723–7742. <https://doi.org/10.1175/jcli-d-11-00388.1>
179. Liu, L., D. Shawki, A. Voulgarakis, M. Kasoar, B.H. Samset, G. Myhre, P.M. Forster, Ø. Hodnebrog, J. Sillmann, S.G. Aalbergsjø, O. Boucher, G. Faluvegi, T. Iversen, A. Kirkevåg, J.-F. Lamarque, D. Olivié, T. Richardson, D. Shindell, and T. Takemura, 2018: A PDRMIP multimodel study on the impacts of regional aerosol forcings on global and regional precipitation. *Journal of Climate*, **31** (11), 4429–4447. <https://doi.org/10.1175/jcli-d-17-0439.1>
180. Baldwin, J.W., J.B. Dessy, G.A. Vecchi, and M. Oppenheimer, 2019: Temporally compound heat wave events and global warming: An emerging hazard. *Earth's Future*, **7** (4), 411–427. <https://doi.org/10.1029/2018ef000989>
181. Sheridan, S.C. and C.C. Lee, 2018: Temporal trends in absolute and relative extreme temperature events across North America. *Journal of Geophysical Research: Atmospheres*, **123** (21), 11889–11898. <https://doi.org/10.1029/2018jd029150>
182. Cohen, J., L. Agel, M. Barlow, C.I. Garfinkel, and I. White, 2021: Linking Arctic variability and change with extreme winter weather in the United States. *Science*, **373** (6559), 1116–1121. <https://doi.org/10.1126/science.abi9167>
183. Barnes, E.A. and J.A. Screen, 2015: The impact of Arctic warming on the midlatitude jet-stream: Can it? Has it? Will it? *WIREs Climate Change*, **6** (3), 277–286. <https://doi.org/10.1002/wcc.337>
184. Blackport, R. and J.A. Screen, 2020: Insignificant effect of Arctic amplification on the amplitude of midlatitude atmospheric waves. *Science Advances*, **6** (8), 2880. <https://doi.org/10.1126/sciadv.aay2880>
185. Chamberlain, C.J., B.I. Cook, I. Morales-Castilla, and E.M. Wolkovich, 2021: Climate change reshapes the drivers of false spring risk across European trees. *New Phytologist*, **229** (1), 323–334. <https://doi.org/10.1111/nph.16851>
186. Richardson, A.D., K. Hufkens, T. Milliman, D.M. Aubrecht, M.E. Furze, B. Seyednasrollah, M.B. Krassovski, J.M. Latimer, W.R. Nettles, R.R. Heiderman, J.M. Warren, and P.J. Hanson, 2018: Ecosystem warming extends vegetation activity but heightens vulnerability to cold temperatures. *Nature*, **560** (7718), 368–371. <https://doi.org/10.1038/s41586-018-0399-1>
187. Kirchmeier-Young, M.C. and X. Zhang, 2020: Human influence has intensified extreme precipitation in North America. *Proceedings of the National Academy of Sciences of the United States of America*, **117** (24), 13308–13313. <https://doi.org/10.1073/pnas.1921628117>
188. Kluver, D. and D. Leathers, 2015: Regionalization of snowfall frequency and trends over the contiguous United States. *International Journal of Climatology*, **35** (14), 4348–4358. <https://doi.org/10.1002/joc.4292>
189. Zarzycki, C.M., 2018: Projecting changes in societally impactful northeastern U.S. snowstorms. *Geophysical Research Letters*, **45** (21), 12067–12075. <https://doi.org/10.1029/2018gl079820>
190. Payne, A.E., M.-E. Demory, L.R. Leung, A.M. Ramos, C.A. Shields, J.J. Rutz, N. Siler, G. Villarini, A. Hall, and F.M. Ralph, 2020: Responses and impacts of atmospheric rivers to climate change. *Nature Reviews Earth & Environment*, **1** (3), 143–157. <https://doi.org/10.1038/s43017-020-0030-5>
191. Guzman, O. and H. Jiang, 2021: Global increase in tropical cyclone rain rate. *Nature Communications*, **12** (1), 5344. <https://doi.org/10.1038/s41467-021-25685-2>
192. Patricola, C.M. and M.F. Wehner, 2018: Anthropogenic influences on major tropical cyclone events. *Nature*, **563** (7731), 339–346. <https://doi.org/10.1038/s41586-018-0673-2>
193. Wilhite, D.A. and M.H. Glantz, 1985: Understanding: The drought phenomenon: The role of definitions. *Water International*, **10** (3), 111–120. <https://doi.org/10.1080/02508068508686328>
194. Cook, B.I., J.S. Mankin, and K.J. Anchukaitis, 2018: Climate change and drought: From past to future. *Current Climate Change Reports*, **4** (2), 164–179. <https://doi.org/10.1007/s40641-018-0093-2>
195. Swann, A.L.S., 2018: Plants and drought in a changing climate. *Current Climate Change Reports*, **4** (2), 192–201. <https://doi.org/10.1007/s40641-018-0097-y>
196. Wehner, M.F., J.R. Arnold, T. Knutson, K.E. Kunkel, and A.N. LeGrande, 2017: Ch. 8. Droughts, floods, and wildfires. In: *Climate Science Special Report: Fourth National Climate Assessment, Volume I*. Wuebbles, D.J., D.W. Fahey, K.A. Hibbard, D.J. Dokken, B.C. Stewart, and T.K. Maycock, Eds. U.S. Global Change Research Program, Washington, DC, USA, 231–256. <https://doi.org/10.7930/j0cj8bnn>

197. Fye, F.K., D.W. Stahle, and E.R. Cook, 2003: Paleoclimatic analogs to twentieth-century moisture regimes across the United States. *Bulletin of the American Meteorological Society*, **84** (7), 901–910. <https://doi.org/10.1175/bams-84-7-901>
198. Cook, B.I., E.R. Cook, J.E. Smerdon, R. Seager, A.P. Williams, S. Coats, D.W. Stahle, and J.V. Díaz, 2016: North American megadroughts in the Common Era: Reconstructions and simulations. *Wiley Interdisciplinary Reviews: Climate Change*, **7** (3), 411–432. <https://doi.org/10.1002/wcc.394>
199. Williams, A.P., B.I. Cook, and J.E. Smerdon, 2022: Rapid intensification of the emerging southwestern North American megadrought in 2020–2021. *Nature Climate Change*, **12** (3), 232–234. <https://doi.org/10.1038/s41558-022-01290-z>
200. Williams, A.P., E.R. Cook, J.E. Smerdon, B.I. Cook, J.T. Abatzoglou, K. Bolles, S.H. Baek, A.M. Badger, and B. Livneh, 2020: Large contribution from anthropogenic warming to an emerging North American megadrought. *Science*, **368** (6488), 314–318. <https://doi.org/10.1126/science.aaz9600>
201. Douville, H., K. Raghavan, J. Renwick, R.P. Allan, P.A. Arias, M. Barlow, R. Cerezo-Mota, A. Cherchi, T.Y. Gan, J. Gergis, D. Jiang, A. Khan, W. Pokam Mba, D. Rosenfeld, J. Tierney, and O. Zolina, 2021: Ch. 8. Water cycle changes. In: *Climate Change 2021: The Physical Science Basis. Contribution of Working Group I to the Sixth Assessment Report of the Intergovernmental Panel on Climate Change*. Masson-Delmotte, V., P. Zhai, A. Pirani, S.L. Connors, C. Péan, S. Berger, N. Caud, Y. Chen, L. Goldfarb, M.I. Gomis, M. Huang, K. Leitzell, E. Lonnoy, J.B.R. Matthews, T.K. Maycock, T. Waterfield, O. Yelekçi, R. Yu, and B. Zhou, Eds. Cambridge University Press, Cambridge, UK and New York, NY, USA, 1055–1210. <https://doi.org/10.1017/9781009157896.010>
202. Marvel, K., B.I. Cook, C. Bonfils, J.E. Smerdon, A.P. Williams, and H. Liu, 2021: Projected changes to hydroclimate seasonality in the continental United States. *Earth's Future*, **9** (9), e2021EF002019. <https://doi.org/10.1029/2021ef002019>
203. Stevenson, S., S. Coats, D. Touma, J. Cole, F. Lehner, J. Fasullo, and B. Otto-Bliesner, 2022: Twenty-first century hydroclimate: A continually changing baseline, with more frequent extremes. *Proceedings of the National Academy of Sciences of the United States of America*, **119** (12), e2108124119. <https://doi.org/10.1073/pnas.2108124119>
204. Su, L., Q. Cao, M. Xiao, D.M. Mocko, M. Barlage, D. Li, C.D. Peters-Lidard, and D.P. Lettenmaier, 2021: Drought variability over the conterminous United States for the past century. *Journal of Hydrometeorology*, **22** (5), 1153–1168. <https://doi.org/10.1175/jhm-d-20-0158.1>
205. Hoell, A., M. Hoerling, X.-W. Quan, and R. Robinson, 2023: Recent high Missouri River Basin runoff was unlikely due to climate change. *Journal of Applied Meteorology and Climatology*, **62** (6), 657–675. <https://doi.org/10.1175/jamc-d-22-0158.1>
206. Cook, B.I., T.R. Ault, and J.E. Smerdon, 2015: Unprecedented 21st century drought risk in the American Southwest and Central Plains. *Science Advances*, **1** (1), e1400082. <https://doi.org/10.1126/sciadv.1400082>
207. Cook, B.I., J.S. Mankin, K. Marvel, A.P. Williams, J.E. Smerdon, and K.J. Anchukaitis, 2020: Twenty-first century drought projections in the CMIP6 forcing scenarios. *Earth's Future*, **8** (6), e2019EF001461. <https://doi.org/10.1029/2019ef001461>
208. Cook, B.I., J.S. Mankin, A.P. Williams, K.D. Marvel, J.E. Smerdon, and H. Liu, 2021: Uncertainties, limits, and benefits of climate change mitigation for soil moisture drought in southwestern North America. *Earth's Future*, **9** (9), e2021EF002014. <https://doi.org/10.1029/2021ef002014>
209. Berg, N. and A. Hall, 2017: Anthropogenic warming impacts on California snowpack during drought. *Geophysical Research Letters*, **44** (5), 2511–2518. <https://doi.org/10.1002/2016gl072104>
210. Griffin, D. and K.J. Anchukaitis, 2014: How unusual is the 2012–2014 California drought? *Geophysical Research Letters*, **41** (24), 9017–9023. <https://doi.org/10.1002/2014gl062433>
211. Williams, A.P., R. Seager, J.T. Abatzoglou, B.I. Cook, J.E. Smerdon, and E.R. Cook, 2015: Contribution of anthropogenic warming to California drought during 2012–2014. *Geophysical Research Letters*, **42** (16), 6819–6828. <https://doi.org/10.1002/2015gl064924>
212. Marlier, M.E., M. Xiao, R. Engel, B. Livneh, J.T. Abatzoglou, and D.P. Lettenmaier, 2017: The 2015 drought in Washington State: A harbinger of things to come? *Environmental Research Letters*, **12** (11), 114008. <https://doi.org/10.1088/1748-9326/aa8fde>

213. Mote, P.W., D.E. Rupp, S. Li, D.J. Sharp, F. Otto, P.F. Uhe, M. Xiao, D.P. Lettenmaier, H. Cullen, and M.R. Allen, 2016: Perspectives on the causes of exceptionally low 2015 snowpack in the western United States. *Geophysical Research Letters*, **43**, 10980–10988. <https://doi.org/10.1002/2016gl069965>
214. Xiao, M., B. Udall, and D.P. Lettenmaier, 2018: On the causes of declining Colorado River streamflows. *Water Resources Research*, **54** (9), 6739–6756. <https://doi.org/10.1029/2018wr023153>
215. Mankin, J.S., R. Seager, J.E. Smerdon, B.I. Cook, and A.P. Williams, 2019: Mid-latitude freshwater availability reduced by projected vegetation responses to climate change. *Nature Geoscience*, **12** (12), 983–988. <https://doi.org/10.1038/s41561-019-0480-x>
216. Abatzoglou, J.T., C.S. Juang, A.P. Williams, C.A. Kolden, and A.L. Westerling, 2021: Increasing synchronous fire danger in forests of the western United States. *Geophysical Research Letters*, **48** (2), e2020GL091377. <https://doi.org/10.1029/2020gl091377>
217. Abatzoglou, J.T. and A.P. Williams, 2016: Impact of anthropogenic climate change on wildfire across western US forests. *Proceedings of the National Academy of Sciences of the United States of America*, **113** (42), 11770–11775. <https://doi.org/10.1073/pnas.1607171113>
218. Burke, M., A. Driscoll, S. Heft-Neal, J. Xue, J. Burney, and M. Wara, 2021: The changing risk and burden of wildfire in the United States. *Proceedings of the National Academy of Sciences of the United States of America*, **118** (2), e2011048118. <https://doi.org/10.1073/pnas.2011048118>
219. Williams, A.P., J.T. Abatzoglou, A. Gershunov, J. Guzman-Morales, D.A. Bishop, J.K. Balch, and D.P. Lettenmaier, 2019: Observed impacts of anthropogenic climate change on wildfire in California. *Earth's Future*, **7** (8), 892–910. <https://doi.org/10.1029/2019ef001210>
220. Abatzoglou, J.T., D.S. Battisti, A.P. Williams, W.D. Hansen, B.J. Harvey, and C.A. Kolden, 2021: Projected increases in western US forest fire despite growing fuel constraints. *Communications Earth & Environment*, **2** (1), 227. <https://doi.org/10.1038/s43247-021-00299-0>
221. Seneviratne, S.I., X. Zhang, M. Adnan, W. Badi, C. Dereczynski, A.D. Luca, S. Ghosh, I. Iskandar, J. Kossin, S. Lewis, F. Otto, I. Pinto, M. Satoh, S.M. Vicente-Serrano, M. Wehner, and B. Zhou, 2021: Ch. 11. Weather and climate extreme events in a changing climate. In: *Climate Change 2021: The Physical Science Basis. Contribution of Working Group I to the Sixth Assessment Report of the Intergovernmental Panel on Climate Change*. Masson-Delmotte, V., P. Zhai, A. Pirani, S.L. Connors, C. Péan, S. Berger, N. Caud, Y. Chen, L. Goldfarb, M.I. Gomis, M. Huang, K. Leitzell, E. Lonnoy, J.B.R. Matthews, T.K. Maycock, T. Waterfield, O. Yelekçi, R. Yu, and B. Zhou, Eds. Cambridge University Press, Cambridge, UK and New York, NY, USA, 1513–1766. <https://doi.org/10.1017/9781009157896.013>
222. Zhang, W., M. Luo, S. Gao, W. Chen, V. Hari, and A. Khouakhi, 2021: Compound hydrometeorological extremes: Drivers, mechanisms and methods. *Frontiers in Earth Science*, **9**, 673495. <https://doi.org/10.3389/feart.2021.673495>
223. Zscheischler, J., O. Martius, S. Westra, E. Bevacqua, C. Raymond, R.M. Horton, B. van den Hurk, A. AghaKouchak, A. Jézéquel, M.D. Mahecha, D. Maraun, A.M. Ramos, N.N. Ridder, W. Thiery, and E. Vignotto, 2020: A typology of compound weather and climate events. *Nature Reviews Earth & Environment*, **1** (7), 333–347. <https://doi.org/10.1038/s43017-020-0060-z>
224. Boers, N., B. Goswami, A. Rheinwalt, B. Bookhagen, B. Hoskins, and J. Kurths, 2019: Complex networks reveal global pattern of extreme-rainfall teleconnections. *Nature*, **566** (7744), 373–377. <https://doi.org/10.1038/s41586-018-0872-x>
225. Cooley, D., E. Thibaud, F. Castillo, and M.F. Wehner, 2019: A nonparametric method for producing isolines of bivariate exceedance probabilities. *Extremes*, **22** (3), 373–390. <https://doi.org/10.1007/s10687-019-00348-0>
226. Donges, J.F., C.F. Schleussner, J.F. Siegmund, and R.V. Donner, 2016: Event coincidence analysis for quantifying statistical interrelationships between event time series. *The European Physical Journal Special Topics*, **225** (3), 471–487. <https://doi.org/10.1140/epjst/e2015-50233-y>
227. Sadegh, M., E. Ragno, and A. AghaKouchak, 2017: Multivariate Copula Analysis Toolbox (MvCAT): Describing dependence and underlying uncertainty using a Bayesian framework. *Water Resources Research*, **53** (6), 5166–5183. <https://doi.org/10.1002/2016wr020242>

228. Bevacqua, E., C. De Michele, C. Manning, A. Couasnon, A.F.S. Ribeiro, A.M. Ramos, E. Vignotto, A. Bastos, S. Blesić, F. Durante, J. Hillier, S.C. Oliveira, J.G. Pinto, E. Ragno, P. Rivoire, K. Saunders, K. van der Wiel, W. Wu, T. Zhang, and J. Zscheischler, 2021: Guidelines for studying diverse types of compound weather and climate events. *Earth's Future*, **9** (11), e2021EF002340. <https://doi.org/10.1029/2021ef002340>
229. Raymond, C., R.M. Horton, J. Zscheischler, O. Martius, A. AghaKouchak, J. Balch, S.G. Bowen, S.J. Camargo, J. Hess, K. Kornhuber, M. Oppenheimer, A.C. Ruane, T. Wahl, and K. White, 2020: Understanding and managing connected extreme events. *Nature Climate Change*, **10** (7), 611–621. <https://doi.org/10.1038/s41558-020-0790-4>
230. AghaKouchak, A., F. Chiang, L.S. Huning, C.A. Love, I. Mallakpour, O. Mazdidasni, H. Moftakhari, S.M. Papalexioiu, E. Ragno, and M. Sadegh, 2020: Climate extremes and compound hazards in a warming world. *Annual Review of Earth and Planetary Sciences*, **48** (1), 519–548. <https://doi.org/10.1146/annurev-earth-071719-055228>
231. Arrhenius, S., 1896: On the influence of carbonic acid in the air upon the temperature of the ground. *Philosophical Magazine and Journal of Science*, **41**, 237–276. [https://www.rsc.org/images/arrhenius1896\\_tcm18-173546.pdf](https://www.rsc.org/images/arrhenius1896_tcm18-173546.pdf)
232. Foote, E., 1856: Circumstances affecting the heat of the sun's rays. *The American Journal of Science and Arts*, **22** (66), 383–384. <https://www.davidmorrow.net/eunice-foote>
233. Tyndall, J., 1861: The Bakerian Lecture: On the absorption and radiation of heat by gases and vapours, and on the physical connexion of radiation, absorption, and conduction. *Philosophical Transactions of the Royal Society of London*, **151**, 1–36. <https://doi.org/10.1098/rstl.1861.0001>
234. Ramaswamy, V., W. Collins, J. Haywood, J. Lean, N. Mahowald, G. Myhre, V. Naik, K.P. Shine, B. Soden, G. Stenchikov, and T. Storelvmo, 2019: Radiative forcing of climate: The historical evolution of the radiative forcing concept, the forcing agents and their quantification, and applications. *Meteorological Monographs*, **59** (1). <https://doi.org/10.1175/amsmonographs-d-19-0001.1>
235. Eyring, V., N.P. Gillett, K.M.A. Rao, R. Barimalala, M.B. Parrillo, N. Bellouin, C. Cassou, P.J. Durack, Y. Kosaka, S. McGregor, S. Min, O. Morgenstern, and Y. Sun, 2021: Ch. 3. Human influence on the climate system. In: *Climate Change 2021: The Physical Science Basis. Contribution of Working Group I to the Sixth Assessment Report of the Intergovernmental Panel on Climate Change*. Masson-Delmotte, V., P. Zhai, A. Pirani, S.L. Connors, C. Péan, S. Berger, N. Caud, Y. Chen, L. Goldfarb, M.I. Gomis, M. Huang, K. Leitzell, E. Lonnoy, J.B.R. Matthews, T.K. Maycock, T. Waterfield, O. Yelekçi, R. Yu, and B. Zhou, Eds. Cambridge University Press, Cambridge, UK and New York, NY, USA, 423–552. <https://doi.org/10.1017/9781009157896.005>
236. Saunio, M., A.R. Stavert, B. Poulter, P. Bousquet, J.G. Canadell, R.B. Jackson, P.A. Raymond, E.J. Dlugokencky, S. Houweling, P.K. Patra, P. Ciais, V.K. Arora, D. Bastviken, P. Bergamaschi, D.R. Blake, G. Brailsford, L. Bruhwiler, K.M. Carlson, M. Carrol, S. Castaldi, N. Chandra, C. Crevoisier, P.M. Crill, K. Covey, C.L. Curry, G. Etiope, C. Frankenberg, N. Gedney, M.I. Hegglin, L. Höglund-Isaksson, G. Hugelius, M. Ishizawa, A. Ito, G. Janssens-Maenhout, K.M. Jensen, F. Joos, T. Kleinen, P.B. Krummel, R.L. Langenfelds, G.G. Laruelle, L. Liu, T. Machida, S. Maksyutov, K.C. McDonald, J. McNorton, P.A. Miller, J.R. Melton, I. Morino, J. Müller, F. Murguía-Flores, V. Naik, Y. Niwa, S. Noce, S. O'Doherty, R.J. Parker, C. Peng, S. Peng, G.P. Peters, C. Prigent, R. Prinn, M. Ramonet, P. Regnier, W.J. Riley, J.A. Rosentretter, A. Segers, I.J. Simpson, H. Shi, S.J. Smith, L.P. Steele, B.F. Thornton, H. Tian, Y. Tohjima, F.N. Tubiello, A. Tsuruta, N. Viovy, A. Voulgarakis, T.S. Weber, M. van Weele, G.R. van der Werf, R.F. Weiss, D. Worthy, D. Wunch, Y. Yin, Y. Yoshida, W. Zhang, Z. Zhang, Y. Zhao, B. Zheng, Q. Zhu, Q. Zhu, and Q. Zhuang, 2020: The global methane budget 2000–2017. *Earth System Science Data*, **12** (3), 1561–1623. <https://doi.org/10.5194/essd-12-1561-2020>
237. Tans, P., 2009: An accounting of the observed increase in oceanic and atmospheric CO<sub>2</sub> and an outlook for the future. *Oceanography*, **22** (4), 26–35. <https://doi.org/10.5670/oceanog.2009.94>
238. Basu, S., X. Lan, E. Dlugokencky, S. Michel, S. Schwietzke, J.B. Miller, L. Bruhwiler, Y. Oh, P.P. Tans, F. Apadula, L.V. Gatti, A. Jordan, J. Necki, M. Sasakawa, S. Morimoto, T. Di Iorio, H. Lee, J. Arduini, and G. Manca, 2022: Estimating emissions of methane consistent with atmospheric measurements of methane and  $\delta^{13}\text{C}$  of methane. *Atmospheric Chemistry and Physics*, **22** (23), 15351–15377. <https://doi.org/10.5194/acp-22-15351-2022>
239. Schwietzke, S., O.A. Sherwood, L.M.P. Bruhwiler, J.B. Miller, G. Etiope, E.J. Dlugokencky, S.E. Michel, V.A. Arling, B.H. Vaughn, J.W.C. White, and P.P. Tans, 2016: Upward revision of global fossil fuel methane emissions based on isotope database. *Nature*, **538** (7623), 88–91. <https://doi.org/10.1038/nature19797>
240. Ceppi, P. and P. Nowack, 2021: Observational evidence that cloud feedback amplifies global warming. *Proceedings of the National Academy of Sciences of the United States of America*, **118** (30), e2026290118. <https://doi.org/10.1073/pnas.2026290118>



241. Dessler, A.E., 2013: Observations of climate feedbacks over 2000–10 and comparisons to climate models. *Journal of Climate*, **26** (1), 333–342. <https://doi.org/10.1175/jcli-d-11-00640.1>
242. Klein, S.A., A. Hall, J.R. Norris, and R. Pincus, 2017: Low-cloud feedbacks from cloud-controlling factors: A review. *Surveys in Geophysics*, **38** (6), 1307–1329. <https://doi.org/10.1007/s10712-017-9433-3>
243. McCoy, D.T., P. Field, A. Bodas-Salcedo, G.S. Elsaesser, and M.D. Zelinka, 2020: A regime-oriented approach to observationally constraining extratropical shortwave cloud feedbacks. *Journal of Climate*, **33** (23), 9967–9983. <https://doi.org/10.1175/jcli-d-19-0987.1>
244. Vaillant de Guélis, T., H. Chepfer, R. Guzman, M. Bonazzola, D.M. Winker, and V. Noel, 2018: Space lidar observations constrain longwave cloud feedback. *Scientific Reports*, **8** (1), 16570. <https://doi.org/10.1038/s41598-018-34943-1>
245. Williams, I.N. and R.T. Pierrehumbert, 2017: Observational evidence against strongly stabilizing tropical cloud feedbacks. *Geophysical Research Letters*, **44** (3), 1503–1510. <https://doi.org/10.1002/2016gl072202>
246. Klein, S.A. and A. Hall, 2015: Emergent constraints for cloud feedbacks. *Current Climate Change Reports*, **1** (4), 276–287. <https://doi.org/10.1007/s40641-015-0027-1>
247. Thackeray, C.W., A. Hall, M.D. Zelinka, and C.G. Fletcher, 2021: Assessing prior emergent constraints on surface albedo feedback in CMIP6. *Journal of Climate*, **34** (10), 3889–3905. <https://doi.org/10.1175/jcli-d-20-0703.1>
248. Lenssen, N.J.L., G.A. Schmidt, J.E. Hansen, M.J. Menne, A. Persin, R. Ruedy, and D. Zyss, 2019: Improvements in the GISTEMP uncertainty model. *Journal of Geophysical Research: Atmospheres*, **124** (12), 6307–6326. <https://doi.org/10.1029/2018jd029522>
249. Morice, C.P., J.J. Kennedy, N.A. Rayner, J.P. Winn, E. Hogan, R.E. Killick, R.J.H. Dunn, T.J. Osborn, P.D. Jones, and I.R. Simpson, 2021: An updated assessment of near-surface temperature change from 1850: The HadCRUT5 data set. *Journal of Geophysical Research: Atmospheres*, **126** (3), e2019JD032361. <https://doi.org/10.1029/2019jd032361>
250. Andrews, T., J.M. Gregory, and M.J. Webb, 2015: The dependence of radiative forcing and feedback on evolving patterns of surface temperature change in climate models. *Journal of Climate*, **28** (4), 1630–1648. <https://doi.org/10.1175/jcli-d-14-00545.1>
251. Kageyama, M., S. Albani, P. Braconnot, S.P. Harrison, P.O. Hopcroft, R.F. Ivanovic, F. Lambert, O. Marti, W.R. Peltier, J.Y. Peterschmitt, D.M. Roche, L. Tarasov, X. Zhang, E.C. Brady, A.M. Haywood, A.N. LeGrande, D.J. Lunt, N.M. Mahowald, U. Mikolajewicz, K.H. Nisancioglu, B.L. Otto-Bliesner, H. Renssen, R.A. Tomas, Q. Zhang, A. Abe-Ouchi, P.J. Bartlein, J. Cao, Q. Li, G. Lohmann, R. Ohgaito, X. Shi, E. Volodin, K. Yoshida, X. Zhang, and W. Zheng, 2017: The PMIP4 contribution to CMIP6—Part 4: Scientific objectives and experimental design of the PMIP4-CMIP6 Last Glacial Maximum experiments and PMIP4 sensitivity experiments. *Geoscientific Model Development*, **10** (11), 4035–4055. <https://doi.org/10.5194/gmd-10-4035-2017>
252. Haywood, A.M., H.J. Dowsett, and A.M. Dolan, 2016: Integrating geological archives and climate models for the mid-Pliocene warm period. *Nature Communications*, **7** (1), 10646. <https://doi.org/10.1038/ncomms10646>
253. Lunt, D.J., M. Huber, E. Anagnostou, M.L.J. Baatsen, R. Caballero, R. DeConto, H.A. Dijkstra, Y. Donnadieu, D. Evans, R. Feng, G.L. Foster, E. Gasson, A.S. von der Heydt, C.J. Hollis, G.N. Inglis, S.M. Jones, J. Kiehl, S. Kirtland Turner, R.L. Korty, R. Kozdon, S. Krishnan, J.B. Ladant, P. Langebroek, C.H. Lear, A.N. LeGrande, K. Littler, P. Markwick, B. Otto-Bliesner, P. Pearson, C.J. Poulsen, U. Salzmann, C. Shields, K. Snell, M. Stärz, J. Super, C. Tabor, J.E. Tierney, G.J.L. Tourte, A. Tripathi, G.R. Upchurch, B.S. Wade, S.L. Wing, A.M.E. Winguth, N.M. Wright, J.C. Zachos, and R.E. Zeebe, 2017: The DeepMIP contribution to PMIP4: Experimental design for model simulations of the EECO, PETM, and pre-PETM (version 1.0). *Geoscientific Model Development*, **10** (2), 889–901. <https://doi.org/10.5194/gmd-10-889-2017>
254. Köhler, P., R. Bintanja, H. Fischer, F. Joos, R. Knutti, G. Lohmann, and V. Masson-Delmotte, 2010: What caused Earth's temperature variations during the last 800,000 years? Data-based evidence on radiative forcing and constraints on climate sensitivity. *Quaternary Science Reviews*, **29** (1), 129–145. <https://doi.org/10.1016/j.quascirev.2009.09.026>
255. von der Heydt, A.S. and P. Ashwin, 2017: State dependence of climate sensitivity: Attractor constraints and palaeoclimate regimes. *Dynamics and Statistics of the Climate System*, **1** (1). <https://doi.org/10.1093/climsys/dzx001>
256. Sherwood, S.C., S. Bony, O. Boucher, C. Bretherton, P.M. Forster, J.M. Gregory, and B. Stevens, 2015: Adjustments in the forcing-feedback framework for understanding climate change. *Bulletin of the American Meteorological Society*, **96** (2), 217–228. <https://doi.org/10.1175/bams-d-13-00167.1>



257. Harris, D.C., 2010: Charles David Keeling and the story of atmospheric CO<sub>2</sub> measurements. *Analytical Chemistry*, **82** (19), 7865–7870. <https://doi.org/10.1021/ac1001492>
258. Kansakar, P. and F. Hossain, 2016: A review of applications of satellite earth observation data for global societal benefit and stewardship of planet earth. *Space Policy*, **36**, 46–54. <https://doi.org/10.1016/j.spacepol.2016.05.005>
259. Novick, K.A., J.A. Biederman, A.R. Desai, M.E. Litvak, D.J.P. Moore, R.L. Scott, and M.S. Torn, 2018: The AmeriFlux network: A coalition of the willing. *Agricultural and Forest Meteorology*, **249**, 444–456. <https://doi.org/10.1016/j.agrformet.2017.10.009>
260. Chabbi, A. and H.W. Loescher, Eds., 2016: *Terrestrial Ecosystem Research Infrastructures: Challenges and Opportunities*. 1st ed., CRC Press, 558 pp. <https://doi.org/10.1201/9781315368252>
261. USGS, 2019: Surface Runoff and the Water Cycle. U.S. Geological Survey. <https://www.usgs.gov/special-topics/water-science-school/science/surface-runoff-and-water-cycle#overview>
262. Wild, M., 2017: Towards global estimates of the surface energy budget. *Current Climate Change Reports*, **3** (1), 87–97. <https://doi.org/10.1007/s40641-017-0058-x>
263. Montzka, S.A., 2022: NOAA's Annual Greenhouse Gas Index. National Oceanic and Atmospheric Administration, Global Monitoring Laboratory, accessed June 10, 2022. <https://gml.noaa.gov/aggi/>
264. Lumpkin, R., T. Özgökmen, and L. Centurioni, 2017: Advances in the application of surface drifters. *Annual Review of Marine Science*, **9** (1), 59–81. <https://doi.org/10.1146/annurev-marine-010816-060641>
265. Williams, N.L., L.W. Juranek, R.A. Feely, K.S. Johnson, J.L. Sarmiento, L.D. Talley, A.G. Dickson, A.R. Gray, R. Wanninkhof, J.L. Russell, S.C. Riser, and Y. Takeshita, 2017: Calculating surface ocean pCO<sub>2</sub> from biogeochemical Argo floats equipped with pH: An uncertainty analysis. *Global Biogeochemical Cycles*, **31** (3), 591–604. <https://doi.org/10.1002/2016gb005541>
266. Loeb, N.G., G.C. Johnson, T.J. Thorsen, J.M. Lyman, F.G. Rose, and S. Kato, 2021: Satellite and ocean data reveal marked increase in Earth's heating rate. *Geophysical Research Letters*, **48** (13), e2021GL093047. <https://doi.org/10.1029/2021gl093047>
267. Susskind, J., G.A. Schmidt, J.N. Lee, and L. Iredell, 2019: Recent global warming as confirmed by AIRS. *Environmental Research Letters*, **14** (4), 044030. <https://doi.org/10.1088/1748-9326/aafd4e>
268. Li, Z., J. Guo, B. Ji, X. Wan, and S. Zhang, 2022: A review of marine gravity field recovery from satellite altimetry. *Remote Sensing*, **14** (19). <https://doi.org/10.3390/rs14194790>
269. Fisher, J.B., B. Lee, A.J. Purdy, G.H. Halverson, M.B. Dohlen, K. Cawse-Nicholson, A. Wang, R.G. Anderson, B. Aragon, M.A. Arain, D.D. Baldocchi, J.M. Baker, H. Barral, C.J. Bernacchi, C. Bernhofer, S.C. Biraud, G. Bohrer, N. Brunzell, B. Cappelaere, S. Castro-Contreras, J. Chun, B.J. Conrad, E. Cremonese, J. Demarty, A.R. Desai, A. De Ligne, L. Foltýnová, M.L. Goulden, T.J. Griffis, T. Grünwald, M.S. Johnson, M. Kang, D. Kelbe, N. Kowalska, J.-H. Lim, I. Mainassara, M.F. McCabe, J.E.C. Missik, B.P. Mohanty, C.E. Moore, L. Morillas, R. Morrison, J.W. Munger, G. Posse, A.D. Richardson, E.S. Russell, Y. Ryu, A. Sanchez-Azofeifa, M. Schmidt, E. Schwartz, I. Sharp, L. Šigut, Y. Tang, G. Hulley, M. Anderson, C. Hain, A. French, E. Wood, and S. Hook, 2020: ECOSTRESS: NASA's next generation mission to measure evapotranspiration from the International Space Station. *Water Resources Research*, **56** (4), e2019WR026058. <https://doi.org/10.1029/2019wr026058>
270. Dubayah, R., J.B. Blair, S. Goetz, L. Fatoyinbo, M. Hansen, S. Healey, M. Hofton, G. Hurtt, J. Kellner, S. Luthcke, J. Armston, H. Tang, L. Duncanson, S. Hancock, P. Jantz, S. Marselis, P.L. Patterson, W. Qi, and C. Silva, 2020: The Global Ecosystem Dynamics Investigation: High-resolution laser ranging of the Earth's forests and topography. *Science of Remote Sensing*, **1**, 100002. <https://doi.org/10.1016/j.srs.2020.100002>
271. Green, R.O., N. Mahowald, C. Ung, D.R. Thompson, L. Bator, M. Bennet, M. Bernas, N. Blackway, C. Bradley, J. Cha, P. Clark, R. Clark, D. Cloud, E. Diaz, E.B. Dor, R. Duren, M. Eastwood, B.L. Ehlmann, L. Fuentes, P. Ginoux, J. Gross, Y. He, O. Kalashnikova, W. Kert, D. Keymeulen, M. Klimesh, D. Ku, H. Kwong-Fu, E. Liggett, L. Li, S. Lundeen, M.D. Makowski, A. Mazer, R. Miller, P. Mouroulis, B. Oaida, G.S. Okin, A. Ortega, A. Oyake, H. Nguyen, T. Pace, T.H. Painter, J. Pompejian, C.P. Garcia-Pando, T. Pham, B. Phillips, R. Pollock, R. Purcell, V. Realmuto, J. Schoolcraft, A. Sen, S. Shin, L. Shaw, M. Soriano, G. Swayze, E. Thingvold, A. Vaid, and J. Zan, 2020: The Earth surface mineral dust source investigation: An earth science imaging spectroscopy mission. In: *2020 IEEE Aerospace Conference*. 7–14 March 2020, 1–15. <https://doi.org/10.1109/aero47225.2020.9172731>

272. Zavodsky, B., J. Dunion, W. Blackwell, S. Braun, C. Velden, M. Brennan, and R. Adler, 2017: First Time-Resolved Observations of Precipitation structure and storm Intensity with a Constellation of SmallSats (TROPICS) mission applications workshop summary report. 8–10 May 2017. National Aeronautics and Space Administration, Earth Science Division Applied Science Program. <https://ntrs.nasa.gov/api/citations/20170010652/downloads/20170010652.pdf>
273. Goldberg, M. and L. Zhou, 2017: The joint polar satellite system—Overview, instruments, proving ground and risk reduction activities. In: *2017 IEEE International Geoscience and Remote Sensing Symposium (IGARSS)*. 23–28 July 2017, 2776–2778. <https://doi.org/10.1109/igarss.2017.8127573>
274. Morrow, R., L.-L. Fu, F. Ardhuin, M. Benkiran, B. Chapron, E. Cosme, F. d'Ovidio, J.T. Farrar, S.T. Gille, G. Lapeyre, P.-Y. Le Traon, A. Pascual, A. Ponte, B. Qiu, N. Rasche, C. Ubelmann, J. Wang, and E.D. Zaron, 2019: Global observations of fine-scale ocean surface topography with the Surface Water and Ocean Topography (SWOT) mission. *Frontiers in Marine Science*, **6**, 232. <https://doi.org/10.3389/fmars.2019.00232>
275. Painter, T.H., D.F. Berisford, J.W. Boardman, K.J. Bormann, J.S. Deems, F. Gehrke, A. Hedrick, M. Joyce, R. Laidlaw, D. Marks, C. Mattmann, B. McGurk, P. Ramirez, M. Richardson, S.M. Skiles, F.C. Seidel, and A. Winstral, 2016: The Airborne Snow Observatory: Fusion of scanning lidar, imaging spectrometer, and physically-based modeling for mapping snow water equivalent and snow albedo. *Remote Sensing of Environment*, **184**, 139–152. <https://doi.org/10.1016/j.rse.2016.06.018>
276. Eberts, S.M., C.R. Wagner, and M.D. Woodside, 2019: Water priorities for the Nation—The U.S. Geological Survey Next Generation Water Observing System. USGS Fact Sheet 2019–3046. U.S. Geological Survey, 2 pp. <https://doi.org/10.3133/fs20193046>
277. Moss, R.H., J.A. Edmonds, K.A. Hibbard, M.R. Manning, S.K. Rose, D.P. van Vuuren, T.R. Carter, S. Emori, M. Kainuma, T. Kram, G.A. Meehl, J.F.B. Mitchell, N. Nakicenovic, K. Riahi, S.J. Smith, R.J. Stouffer, A.M. Thomson, J.P. Weyant, and T.J. Wilbanks, 2010: The next generation of scenarios for climate change research and assessment. *Nature*, **463**, 747–756. <https://doi.org/10.1038/nature08823>
278. IPCC, 2013: *Climate Change 2013: The Physical Science Basis. Contribution of Working Group I to the Fifth Assessment Report of the Intergovernmental Panel on Climate Change*. Stocker, T.F., D. Qin, G.-K. Plattner, M. Tignor, S.K. Allen, J. Boschung, A. Nauels, Y. Xia, V. Bex, and P.M. Midgley, Eds. Cambridge University Press, Cambridge, UK and New York, NY, USA, 1535 pp. <https://www.ipcc.ch/report/ar5/wg1/>
279. Ebi, K.L., S. Hallegatte, T. Kram, N.W. Arnell, T.R. Carter, J. Edmonds, E. Kriegler, R. Mathur, B.C. O'Neill, K. Riahi, H. Winkler, D.P. Van Vuuren, and T. Zwickel, 2014: A new scenario framework for climate change research: Background, process, and future directions. *Climatic Change*, **122** (3), 363–372. <https://doi.org/10.1007/s10584-013-0912-3>
280. Tebaldi, C., K. Debeire, V. Eyring, E. Fischer, J. Fyfe, P. Friedlingstein, R. Knutti, J. Lowe, B. O'Neill, B. Sanderson, D. van Vuuren, K. Riahi, M. Meinshausen, Z. Nicholls, K.B. Tokarska, G. Hurtt, E. Kriegler, J.F. Lamarque, G. Meehl, R. Moss, S.E. Bauer, O. Boucher, V. Brovkin, Y.H. Byun, M. Dix, S. Gualdi, H. Guo, J.G. John, S. Kharin, Y. Kim, T. Koshiro, L. Ma, D. Olivié, S. Panickal, F. Qiao, X. Rong, N. Rosenbloom, M. Schupfner, R. Séférian, A. Sellar, T. Semmler, X. Shi, Z. Song, C. Steger, R. Stouffer, N. Swart, K. Tachiiri, Q. Tang, H. Tatebe, A. Voldoire, E. Volodin, K. Wyser, X. Xin, S. Yang, Y. Yu, and T. Ziehn, 2021: Climate model projections from the Scenario Model Intercomparison Project (ScenarioMIP) of CMIP6. *Earth System Dynamics*, **12** (1), 253–293. <https://doi.org/10.5194/esd-12-253-2021>
281. Deser, C., R. Knutti, S. Solomon, and A.S. Phillips, 2012: Communication of the role of natural variability in future North American climate. *Nature Climate Change*, **2** (11), 775–779. <https://doi.org/10.1038/nclimate1562>
282. Deser, C., A. Phillips, V. Bourdette, and H. Teng, 2012: Uncertainty in climate change projections: The role of internal variability. *Climate Dynamics*, **38** (3–4), 527–546. <https://doi.org/10.1007/s00382-010-0977-x>
283. Rodgers, K.B., J. Lin, and T.L. Frölicher, 2015: Emergence of multiple ocean ecosystem drivers in a large ensemble suite with an Earth system model. *Biogeosciences*, **12** (11), 3301–3320. <https://doi.org/10.5194/bg-12-3301-2015>
284. Maher, N., S. Milinski, L. Suarez-Gutierrez, M. Botzet, M. Dobrynin, L. Kornbluh, J. Kröger, Y. Takano, R. Ghosh, C. Hedemann, C. Li, H. Li, E. Manzini, D. Notz, D. Putrasahan, L. Boysen, M. Claussen, T. Ilyina, D. Olonscheck, T. Raddatz, B. Stevens, and J. Marotzke, 2019: The Max Planck Institute Grand ensemble: Enabling the exploration of climate system variability. *Journal of Advances in Modeling Earth Systems*, **11** (7), 2050–2069. <https://doi.org/10.1029/2019ms001639>
285. Pendergrass, A.G., D.B. Coleman, C. Deser, F. Lehner, N. Rosenbloom, and I.R. Simpson, 2019: Nonlinear response of extreme precipitation to warming in CESM1. *Geophysical Research Letters*, **46** (17–18), 10551–10560. <https://doi.org/10.1029/2019gl084826>

286. Cai, W., A. Santoso, M. Collins, B. Dewitte, C. Karamperidou, J.-S. Kug, M. Lengaigne, M.J. McPhaden, M.F. Stuecker, A.S. Taschetto, A. Timmermann, L. Wu, S.-W. Yeh, G. Wang, B. Ng, F. Jia, Y. Yang, J. Ying, X.-T. Zheng, T. Bayr, J.R. Brown, A. Capotondi, K.M. Cobb, B. Gan, T. Geng, Y.-G. Ham, F.-F. Jin, H.-S. Jo, X. Li, X. Lin, S. McGregor, J.-H. Park, K. Stein, K. Yang, L. Zhang, and W. Zhong, 2021: Changing El Niño–Southern Oscillation in a warming climate. *Nature Reviews Earth & Environment*, **2** (9), 628–644. <https://doi.org/10.1038/s43017-021-00199-z>
287. Haszpra, T., M. Herein, and T. Bódai, 2020: Investigating ENSO and its teleconnections under climate change in an ensemble view—A new perspective. *Earth System Dynamics*, **11** (1), 267–280. <https://doi.org/10.5194/esd-11-267-2020>
288. Maher, N., D. Matei, S. Milinski, and J. Marotzke, 2018: ENSO change in climate projections: Forced response or internal variability? *Geophysical Research Letters*, **45** (20), 11390–11398. <https://doi.org/10.1029/2018gl079764>
289. O'Brien, J.P. and C. Deser, 2022: Quantifying and understanding forced changes to unforced modes of atmospheric circulation variability over the North Pacific in a coupled model large ensemble. *Journal of Climate*, **36** (1), 19–37. <https://doi.org/10.1175/jcli-d-22-0101.1>
290. Milinski, S., N. Maher, and D. Olonscheck, 2020: How large does a large ensemble need to be? *Earth System Dynamics*, **11** (4), 885–901. <https://doi.org/10.5194/esd-11-885-2020>
291. Mankin, J.S., F. Lehner, S. Coats, and K.A. McKinnon, 2020: The value of initial condition large ensembles to robust adaptation decision-making. *Earth's Future*, **8** (10), e2012EF001610. <https://doi.org/10.1029/2020ef001610>
292. McKinnon, K.A. and C. Deser, 2021: The inherent uncertainty of precipitation variability, trends, and extremes due to internal variability, with implications for western U.S. water resources. *Journal of Climate*, **34** (24), 9605–9622. <https://doi.org/10.1175/jcli-d-21-0251.1>
293. Garcia-Menendez, F., E. Monier, and N.E. Selin, 2017: The role of natural variability in projections of climate change impacts on U.S. ozone pollution. *Geophysical Research Letters*, **44** (6), 2911–2921. <https://doi.org/10.1002/2016gl071565>
294. Saari, R.K., Y. Mei, E. Monier, and F. Garcia-Menendez, 2019: Effect of health-related uncertainty and natural variability on health impacts and cobenefits of climate policy. *Environmental Science & Technology*, **53** (3), 1098–1108. <https://doi.org/10.1021/acs.est.8b05094>
295. Frölicher, T.L., K.B. Rodgers, C.A. Stock, and W.W.L. Cheung, 2016: Sources of uncertainties in 21st century projections of potential ocean ecosystem stressors. *Global Biogeochemical Cycles*, **30** (8), 1224–1243. <https://doi.org/10.1002/2015gb005338>
296. Williamson, M.S., C.W. Thackeray, P.M. Cox, A. Hall, C. Huntingford, and F.J.M.M. Nijse, 2021: Emergent constraints on climate sensitivities. *Reviews of Modern Physics*, **93** (2), 025004. <https://doi.org/10.1103/revmodphys.93.025004>
297. Herring, S.C., N. Christidis, A. Hoell, M.P. Hoerling, and P.A. Stott, 2020: Explaining extreme events of 2018 from a climate perspective. *Bulletin of the American Meteorological Society*, **101** (1), S1–S140. <https://doi.org/10.1175/bams-explainingextremeevents2018.1>
298. Herring, S.C., N. Christidis, A. Hoell, M.P. Hoerling, and P.A. Stott, 2021: Explaining extreme events of 2019 from a climate perspective. *Bulletin of the American Meteorological Society*, **102** (1), S1–S115. <https://doi.org/10.1175/bams-explainingextremeevents2019.1>
299. Herring, S.C., A. Hoell, M.P. Hoerling, J.P. Kossin, C.J. Schreck III, and P.A. Stott, 2016: Explaining extreme events of 2015 from a climate perspective. *Bulletin of the American Meteorological Society*, **97** (12), S1–S145. <https://doi.org/10.1175/bams-explainingextremeevents2015.1>
300. Herring, S.C., M.P. Hoerling, J.P. Kossin, T.C. Peterson, and P.A. Stott, 2015: Introduction to explaining extreme events of 2014 from a climate perspective. *Bulletin of the American Meteorological Society*, **96** (12), S1–S4. <https://doi.org/10.1175/bams-d-15-00157.1>
301. Herring, S.C., M.P. Hoerling, T.C. Peterson, and P.A. Stott, 2014: Explaining extreme events of 2013 from a climate perspective. *Bulletin of the American Meteorological Society*, **95** (9), S1–S104. <https://doi.org/10.1175/1520-0477-95.9.s1.1>
302. Peterson, T.C., M.P. Hoerling, P.A. Stott, and S.C. Herring, 2013: Explaining extreme events of 2012 from a climate perspective. *Bulletin of the American Meteorological Society*, **94** (9), S1–S74. <https://doi.org/10.1175/bams-d-13-00085.1>

303. Peterson, T.C., P.A. Stott, and S. Herring, 2012: Explaining extreme events of 2011 from a climate perspective. *Bulletin of the American Meteorological Society*, **93** (7), 1041–1067. <https://doi.org/10.1175/bams-d-12-00021.1>
304. Reed, K.A., M.F. Wehner, A.M. Stansfield, and C.M. Zarzycki, 2021: Anthropogenic influence on Hurricane Dorian's extreme rainfall. *Bulletin of the American Meteorological Society*, **102** (1), S9–S15. <https://doi.org/10.1175/bams-d-20-0160.1>
305. Menne, M.J., I. Durre, R.S. Vose, B.E. Gleason, and T.G. Houston, 2012: An overview of the Global Historical Climatology Network-Daily database. *Journal of Atmospheric and Oceanic Technology*, **29** (7), 897–910. <https://doi.org/10.1175/jtech-d-11-00103.1>
306. Pearl, J., 2009: Causal inference in statistics: An overview. *Statistics Surveys*, **3**, 96–146. <https://doi.org/10.1214/09-ss057>
307. Easterling, D.R., K.E. Kunkel, M.F. Wehner, and L. Sun, 2016: Detection and attribution of climate extremes in the observed record. *Weather and Climate Extremes*, **11**, 17–27. <https://doi.org/10.1016/j.wace.2016.01.001>
308. Stott, P.A., N. Christidis, F.E.L. Otto, Y. Sun, J.-P. Vanderlinden, G.J. van Oldenborgh, R. Vautard, H. von Storch, P. Walton, P. Yiou, and F.W. Zwiers, 2016: Attribution of extreme weather and climate-related events. *WIREs Climate Change*, **7** (1), 23–41. <https://doi.org/10.1002/wcc.380>
309. Granger, C.W.J., 1969: Investigating causal relations by econometric models and cross-spectral methods. *Econometrica*, **37** (3), 424–438. <https://doi.org/10.2307/1912791>
310. Richey, A.S., B.F. Thomas, M.-H. Lo, J.T. Reager, J.S. Famiglietti, K. Voss, S. Swenson, and M. Rodell, 2015: Quantifying renewable groundwater stress with GRACE. *Water Resources Research*, **51** (7), 5217–5238. <https://doi.org/10.1002/2015wr017349>
311. Cheng, L., K.E. Trenberth, J. Fasullo, T. Boyer, J. Abraham, and J. Zhu, 2017: Improved estimates of ocean heat content from 1960 to 2015. *Science Advances*, **3** (3), e1601545. <https://doi.org/10.1126/sciadv.1601545>
312. Guo, Y., E.K.M. Chang, and S.S. Leroy, 2009: How strong are the Southern Hemisphere storm tracks? *Geophysical Research Letters*, **36** (22). <https://doi.org/10.1029/2009gl040733>
313. Hock, R., G. Rasul, C. Adler, B. Cáceres, S. Gruber, Y. Hirabayashi, M. Jackson, A. Käab, S. Kang, S. Kutuzov, A. Milner, U. Molau, S. Morin, B. Orlove, and H. Steltzer, 2019: Ch. 2. High mountain areas. In: *The Ocean and Cryosphere in a Changing Climate*. Pörtner, H.O., D.C. Roberts, V. Masson-Delmotte, P. Zhai, M. Tignor, E. Poloczanska, K. Mintenbeck, A. Alegría, M. Nicolai, A. Okem, J. Petzold, B. Rama, and N.M. Weyer, Eds. Cambridge University Press, Cambridge, UK, 131–202. <https://doi.org/10.1017/9781009157964.004>
314. Thornton, J.M., R. Therrien, G. Mariéthoz, N. Linde, and P. Brunner, 2022: Simulating fully-integrated hydrological dynamics in complex alpine headwaters: Potential and challenges. *Water Resources Research*, **58** (4), e2020WR029390. <https://doi.org/10.1029/2020wr029390>
315. Scaife, A.A. and D. Smith, 2018: A signal-to-noise paradox in climate science. *npj Climate and Atmospheric Science*, **1** (1), 28. <https://doi.org/10.1038/s41612-018-0038-4>
316. Hallam, S., G.D. McCarthy, X. Feng, S.A. Josey, E. Harris, A. Düsterhus, S. Ogungbenro, and J.J.M. Hirschi, 2023: The relationship between sea surface temperature anomalies, wind and translation speed and North Atlantic tropical cyclone rainfall over ocean and land. *Environmental Research Communications*, **5** (2), 025007. <https://doi.org/10.1088/2515-7620/acb31c>
317. Deser, C., 2020: Certain uncertainty: The role of internal climate variability in projections of regional climate change and risk management. *Earth's Future*, **8** (12), e2020EF001854. <https://doi.org/10.1029/2020ef001854>
318. Lee, J.-Y., J. Marotzke, G. Bala, L. Cao, S. Corti, J.P. Dunne, F. Engelbrecht, E. Fischer, J.C. Fyfe, C. Jones, A. Maycock, J. Mutemi, O. Ndiaye, S. Panickal, and T. Zhou, 2021: Ch. 4. Future global climate: Scenario-based projections and nearterm information. In: *Climate Change 2021: The Physical Science Basis. Contribution of Working Group I to the Sixth Assessment Report of the Intergovernmental Panel on Climate Change*. Masson-Delmotte, V., P. Zhai, A. Pirani, S.L. Connors, C. Péan, S. Berger, N. Caud, Y. Chen, L. Goldfarb, M.I. Gomis, M. Huang, K. Leitzell, E. Lonnoy, J.B.R. Matthews, T.K. Maycock, T. Waterfield, O. Yelekçi, R. Yu, and B. Zhou, Eds. Cambridge University Press, Cambridge, UK and New York, NY, USA, 553–672. <https://doi.org/10.1017/9781009157896.006>
319. Shaw, T.A. and A. Voigt, 2015: Tug of war on summertime circulation between radiative forcing and sea surface warming. *Nature Geoscience*, **8** (7), 560–566. <https://doi.org/10.1038/ngeo2449>



320. Chang, E.K.M., Y. Guo, and X. Xia, 2012: CMIP5 multimodel ensemble projection of storm track change under global warming. *Journal of Geophysical Research: Atmospheres*, **117** (D23). <https://doi.org/10.1029/2012jd018578>
321. Colle, B.A., J.F. Booth, and E.K.M. Chang, 2015: A review of historical and future changes of extratropical cyclones and associated impacts along the US East Coast. *Current Climate Change Reports*, **1** (3), 125–143. <https://doi.org/10.1007/s40641-015-0013-7>
322. Li, W., L. Li, M. Ting, and Y. Liu, 2012: Intensification of Northern Hemisphere subtropical highs in a warming climate. *Nature Geoscience*, **5** (11), 830–834. <https://doi.org/10.1038/ngeo1590>
323. Knutson, T.R. and J. Ploshay, 2021: Sea level pressure trends: Model-based assessment of detection, attribution, and consistency with CMIP5 historical simulations. *Journal of Climate*, **34** (1), 327–346. <https://doi.org/10.1175/jcli-d-19-0997.1>
324. Allan, R.P., M. Barlow, M.P. Byrne, A. Cherchi, H. Douville, H.J. Fowler, T.Y. Gan, A.G. Pendergrass, D. Rosenfeld, A.L.S. Swann, L.J. Wilcox, and O. Zolina, 2020: Advances in understanding large-scale responses of the water cycle to climate change. *Annals of the New York Academy of Sciences*, **1472** (1), 49–75. <https://doi.org/10.1111/nyas.14337>
325. Romps, D.M., 2014: An analytical model for tropical relative humidity. *Journal of Climate*, **27** (19), 7432–7449. <https://doi.org/10.1175/jcli-d-14-00255.1>
326. Byrne, M.P. and P.A. O’Gorman, 2015: The response of precipitation minus evapotranspiration to climate warming: Why the “wet-get-wetter, dry-get-drier” scaling does not hold over land. *Journal of Climate*, **28** (20), 8078–8092. <https://doi.org/10.1175/jcli-d-15-0369.1>
327. Friedlingstein, P., M. O’Sullivan, M.W. Jones, R.M. Andrew, J. Hauck, A. Olsen, G.P. Peters, W. Peters, J. Pongratz, S. Sitch, C. Le Quéré, J.G. Canadell, P. Ciais, R.B. Jackson, S. Alin, L.E.O.C. Aragão, A. Arneeth, V. Arora, N.R. Bates, M. Becker, A. Benoit-Cattin, H.C. Bittig, L. Bopp, S. Bultan, N. Chandra, F. Chevallier, L.P. Chini, W. Evans, L. Florentie, P.M. Forster, T. Gasser, M. Gehlen, D. Gilfillan, T. Gkritzalis, L. Gregor, N. Gruber, I. Harris, K. Hartung, V. Haverd, R.A. Houghton, T. Ilyina, A.K. Jain, E. Joetzier, K. Kadono, E. Kato, V. Kitidis, J.I. Korsbakken, P. Landschützer, N. Lefèvre, A. Lenton, S. Lienert, Z. Liu, D. Lombardozzi, G. Marland, N. Metz, D.R. Munro, J.E.M.S. Nabel, S.I. Nakaoka, Y. Niwa, K. O’Brien, T. Ono, P.I. Palmer, D. Pierrot, B. Poulter, B. Resplandy, E. Robertson, C. Rödenbeck, J. Schwinger, R. Séférian, I. Skjelvan, A.J.P. Smith, A.J. Sutton, T. Tanhua, P.P. Tans, H. Tian, B. Tilbrook, G. van der Werf, N. Vuichard, A.P. Walker, R. Wanninkhof, A.J. Watson, D. Willis, A.J. Wiltshire, W. Yuan, X. Yue, and S. Zaehle, 2020: Global carbon budget 2020. *Earth System Science Data*, **12** (4), 3269–3340. <https://doi.org/10.5194/essd-12-3269-2020>
328. Rödenbeck, C., D.C.E. Bakker, N. Gruber, Y. Iida, A.R. Jacobson, S. Jones, P. Landschützer, N. Metz, S. Nakaoka, A. Olsen, G.H. Park, P. Peylin, K.B. Rodgers, T.P. Sasse, U. Schuster, J.D. Shutler, V. Valsala, R. Wanninkhof, and J. Zeng, 2015: Data-based estimates of the ocean carbon sink variability—First results of the Surface Ocean pCO<sub>2</sub> Mapping intercomparison (SOCOM). *Biogeosciences*, **12** (23), 7251–7278. <https://doi.org/10.5194/bg-12-7251-2015>
329. Takahashi, T., S.C. Sutherland, R. Wanninkhof, C. Sweeney, R.A. Feely, D.W. Chipman, B. Hales, G. Friederich, F. Chavez, C. Sabine, A. Watson, D.C.E. Bakker, U. Schuster, N. Metz, H. Yoshikawa-Inoue, M. Ishii, T. Midorikawa, Y. Nojiri, A. Körtzinger, T. Steinhoff, M. Hoppema, J. Olafsson, T.S. Arnarson, B. Tilbrook, T. Johannessen, A. Olsen, R. Bellerby, C.S. Wong, B. Delille, N.R. Bates, and H.J.W. de Baar, 2009: Climatological mean and decadal change in surface ocean pCO<sub>2</sub>, and net sea–air CO<sub>2</sub> flux over the global oceans. *Deep Sea Research Part II: Topical Studies in Oceanography*, **56** (8), 554–577. <https://doi.org/10.1016/j.dsr2.2008.12.009>
330. Baldocchi, D.D., T.A. Black, P.S. Curtis, E. Falge, J.D. Fuentes, A. Granier, L. Gu, A. Knohl, K. Pilegaard, H.P. Schmid, R. Valentini, K. Wilson, S. Wofsy, L. Xu, and S. Yamamoto, 2005: Predicting the onset of net carbon uptake by deciduous forests with soil temperature and climate data: A synthesis of FLUXNET data. *International Journal of Biometeorology*, **49** (6), 377–387. <https://doi.org/10.1007/s00484-005-0256-4>
331. Wouters, B. and R.S.W. van de Wal, 2018: Global sea-level budget 1993–present. *Earth System Science Data*, **10** (3), 1551–1590. <https://doi.org/10.5194/essd-10-1551-2018>
332. Frederikse, T., K. Simon, C.A. Katsman, and R. Riva, 2017: The sea-level budget along the Northwest Atlantic coast: GIA, mass changes, and large-scale ocean dynamics. *Journal of Geophysical Research: Oceans*, **122** (7), 5486–5501. <https://doi.org/10.1002/2017jc012699>
333. Harvey, T.C., B.D. Hamlington, T. Frederikse, R.S. Nerem, C.G. Piecuch, W.C. Hammond, G. Blewitt, P.R. Thompson, D.P.S. Bekaert, F.W. Landerer, J.T. Reager, R.E. Kopp, H. Chandanpurkar, I. Fenty, D. Trossman, J.S. Walker, and C. Boening, 2021: Ocean mass, steric dynamic effects, and vertical land motion largely explain US coast relative sea level rise. *Communications Earth & Environment*, **2** (1), 233. <https://doi.org/10.1038/s43247-021-00300-w>



334. Rietbroek, R., S.-E. Brunnabend, J. Kusche, J. Schröter, and C. Dahle, 2016: Revisiting the contemporary sea-level budget on global and regional scales. *Proceedings of the National Academy of Sciences of the United States of America*, **113** (6), 1504–1509. <https://doi.org/10.1073/pnas.1519132113>
335. IPCC, 1990: *Climate Change: The IPCC 1990 and 1992 Assessment*. Houghton, J.T., G.J. Jenkins, and J.J. Ephraums, Eds. Cambridge University Press, Cambridge, UK and New York, NY, USA, 178 pp. <https://www.ipcc.ch/report/climate-change-the-ipcc-1990-and-1992-assessments/>
336. National Research Council, 1979: *Carbon Dioxide and Climate: A Scientific Assessment*. The National Academies Press, Washington, DC, 34 pp. <https://doi.org/10.17226/12181>
337. Cohen, J., X. Zhang, J. Francis, T. Jung, R. Kwok, J. Overland, T.J. Ballinger, U.S. Bhatt, H.W. Chen, D. Coumou, S. Feldstein, H. Gu, D. Handorf, G. Henderson, M. Ionita, M. Kretschmer, F. Laliberte, S. Lee, H.W. Linderholm, W. Maslowski, Y. Peings, K. Pfeiffer, I. Rigor, T. Semmler, J. Stroeve, P.C. Taylor, S. Vavrus, T. Vihma, S. Wang, M. Wendisch, Y. Wu, and J. Yoon, 2020: Divergent consensus on Arctic amplification influence on midlatitude severe winter weather. *Nature Climate Change*, **10** (1), 20–29. <https://doi.org/10.1038/s41558-019-0662-y>
338. Doblas-Reyes, F.J., A.A. Sörensson, M. Almazroui, A. Dosio, W.J. Gutowski, R. Haarsma, R. Hamdi, B. Hewitson, W.-T. Kwon, B.L. Lamptey, D. Maraun, T.S. Stephenson, I. Takayabu, L. Terray, A. Turner, and Z. Zuo, 2021: Ch. 10. Linking global to regional climate change. In: *Climate Change 2021: The Physical Science Basis. Contribution of Working Group I to the Sixth Assessment Report of the Intergovernmental Panel on Climate Change*. Masson-Delmotte, V., P. Zhai, A. Pirani, S.L. Connors, C. Péan, S. Berger, N. Caud, Y. Chen, L. Goldfarb, M.I. Gomis, M. Huang, K. Leitzell, E. Lonnoy, J.B.R. Matthews, T.K. Maycock, T. Waterfield, O. Yelekçi, R. Yu, and B. Zhou, Eds. Cambridge University Press, Cambridge, UK and New York, NY, USA, 1363–1512. <https://doi.org/10.1017/9781009157896.012>
339. Neelin, J.D., C. Martinez-Villalobos, S.N. Stechmann, F. Ahmed, G. Chen, J.M. Norris, Y.-H. Kuo, and G. Lenderink, 2022: Precipitation extremes and water vapor. *Current Climate Change Reports*, **8** (1), 17–33. <https://doi.org/10.1007/s40641-021-00177-z>
340. Swann, A.L.S., F.M. Hoffman, C.D. Koven, and J.T. Randerson, 2016: Plant responses to increasing CO<sub>2</sub> reduce estimates of climate impacts on drought severity. *Proceedings of the National Academy of Sciences of the United States of America*, **113** (36), 10019–10024. <https://doi.org/10.1073/pnas.1604581113>
341. Ukkola, A.M., I.C. Prentice, T.F. Keenan, A.I.J.M. van Dijk, N.R. Viney, Ranga B. Myneni, and J. Bi, 2016: Reduced streamflow in water-stressed climates consistent with CO<sub>2</sub> effects on vegetation. *Nature Climate Change*, **6** (1), 75–78. <https://doi.org/10.1038/nclimate2831>
342. Wang, R., L. Li, P. Gentile, Y. Zhang, J. Chen, X. Chen, L. Chen, L. Ning, L. Yuan, and G. Lü, 2022: Recent increase in the observation-derived land evapotranspiration due to global warming. *Environmental Research Letters*, **17** (2), 024020. <https://doi.org/10.1088/1748-9326/ac4291>
343. Mankin, J.S., J.E. Smerdon, B.I. Cook, A.P. Williams, and R. Seager, 2017: The curious case of projected twenty-first-century drying but Greening in the American West. *Journal of Climate*, **30** (21), 8689–8710. <https://doi.org/10.1175/jcli-d-17-0213.1>
344. Jung, M., C. Schwalm, M. Migliavacca, S. Walther, G. Camps-Valls, S. Koirala, P. Anthoni, S. Besnard, P. Bodesheim, N. Carvalhais, F. Chevallier, F. Gans, D.S. Goll, V. Haverd, P. Köhler, K. Ichii, A.K. Jain, J. Liu, D. Lombardozzi, J.E.M.S. Nabel, J.A. Nelson, M. O'Sullivan, M. Pallandt, D. Papale, W. Peters, J. Pongratz, C. Rödenbeck, S. Sitoh, G. Tramontana, A. Walker, U. Weber, and M. Reichstein, 2020: Scaling carbon fluxes from eddy covariance sites to globe: Synthesis and evaluation of the FLUXCOM approach. *Biogeosciences*, **17** (5), 1343–1365. <https://doi.org/10.5194/bg-17-1343-2020>
345. Natali, S.M., J.P. Holdren, B.M. Rogers, R. Treharne, P.B. Duffy, R. Pomerance, and E. MacDonald, 2021: Permafrost carbon feedbacks threaten global climate goals. *Proceedings of the National Academy of Sciences of the United States of America*, **118** (21), e2100163118. <https://doi.org/10.1073/pnas.2100163118>
346. Shirzaei, M., J. Freymueller, T.E. Törnqvist, D.L. Galloway, T. Dura, and P.S.J. Minderhoud, 2021: Measuring, modelling and projecting coastal land subsidence. *Nature Reviews Earth & Environment*, **2** (1), 40–58. <https://doi.org/10.1038/s43017-020-00115-x>
347. Seneviratne, S.I., T. Corti, E.L. Davin, M. Hirschi, E.B. Jaeger, I. Lehner, B. Orlowsky, and A.J. Teuling, 2010: Investigating soil moisture–Climate interactions in a changing climate: A review. *Earth-Science Reviews*, **99** (3–4), 125–161. <https://doi.org/10.1016/j.earscirev.2010.02.004>

348. Miralles, D.G., P. Gentile, S.I. Seneviratne, and A.J. Teuling, 2019: Land–atmospheric feedbacks during droughts and heatwaves: State of the science and current challenges. *Annals of the New York Academy of Sciences*, **1436** (1), 19–35. <https://doi.org/10.1111/nyas.13912>
349. Zhou, D., J. Xiao, S. Frolking, L. Zhang, and G. Zhou, 2022: Urbanization contributes little to global warming but substantially intensifies local and regional land surface warming. *Earth's Future*, **10** (5), e2021EF002401. <https://doi.org/10.1029/2021ef002401>
350. Merz, B., G. Blöschl, S. Vorogushyn, F. Dottori, J.C.J.H. Aerts, P. Bates, M. Bertola, M. Kemter, H. Kreibich, U. Lall, and E. Macdonald, 2021: Causes, impacts and patterns of disastrous river floods. *Nature Reviews Earth & Environment*, **2** (9), 592–609. <https://doi.org/10.1038/s43017-021-00195-3>
351. Schröter, K., M. Kunz, F. Elmer, B. Mühr, and B. Merz, 2015: What made the June 2013 flood in Germany an exceptional event? A hydro–meteorological evaluation. *Hydrology and Earth System Sciences*, **19** (1), 309–327. <https://doi.org/10.5194/hess-19-309-2015>
352. Fisher, R.A. and C.D. Koven, 2020: Perspectives on the future of land surface models and the challenges of representing complex terrestrial systems. *Journal of Advances in Modeling Earth Systems*, **12** (4), e2018MS001453. <https://doi.org/10.1029/2018ms001453>
353. Coumou, D., G. Di Capua, S. Vavrus, L. Wang, and S. Wang, 2018: The influence of Arctic amplification on mid-latitude summer circulation. *Nature Communications*, **9** (1), 2959. <https://doi.org/10.1038/s41467-018-05256-8>
354. Osman, M.B., S. Coats, S.B. Das, J.R. McConnell, and N. Chellman, 2021: North Atlantic jet stream projections in the context of the past 1,250 years. *Proceedings of the National Academy of Sciences of the United States of America*, **118** (38), e2104105118. <https://doi.org/10.1073/pnas.2104105118>
355. Overland, J.E., 2021: Causes of the record-breaking Pacific Northwest heatwave, late June 2021. *Atmosphere*, **12** (11), 1434. <https://doi.org/10.3390/atmos12111434>
356. Perkins-Kirkpatrick, S.E. and S.C. Lewis, 2020: Increasing trends in regional heatwaves. *Nature Communications*, **11** (1), 3357. <https://doi.org/10.1038/s41467-020-16970-7>
357. Kunkel, K.E., T.R. Karl, H. Brooks, J. Kossin, J. Lawrimore, D. Arndt, L. Bosart, D. Changnon, S.L. Cutter, N. Doesken, K. Emanuel, P.Y. Groisman, R.W. Katz, T. Knutson, J. O'Brien, C.J. Paciorek, T.C. Peterson, K. Redmond, D. Robinson, J. Trapp, R. Vose, S. Weaver, M. Wehner, K. Wolter, and D. Wuebbles, 2013: Monitoring and understanding trends in extreme storms: State of knowledge. *Bulletin of the American Meteorological Society*, **94** (4), 499–514. <https://doi.org/10.1175/bams-d-11-00262.1>
358. Vousdoukas, M.I., L. Mentaschi, E. Voukouvalas, M. Verlaan, S. Jevrejeva, L.P. Jackson, and L. Feyen, 2018: Global probabilistic projections of extreme sea levels show intensification of coastal flood hazard. *Nature Communications*, **9** (1), 2360. <https://doi.org/10.1038/s41467-018-04692-w>
359. Gudmundsson, L. and S. Seneviratne, 2016: Anthropogenic climate change affects meteorological drought risk in Europe. *Environmental Research Letters*, **11**, 044005. <https://doi.org/10.1088/1748-9326/11/4/044005>
360. Kelley, C.P., S. Mohtadi, M.A. Cane, R. Seager, and Y. Kushnir, 2015: Climate change in the Fertile Crescent and implications of the recent Syrian drought. *Proceedings of the National Academy of Sciences of the United States of America*, **112** (11), 3241–3246. <https://doi.org/10.1073/pnas.1421533112>
361. Otto, F., P. Wolski, F. Lehner, C. Tebaldi, G.J. Van Oldenborgh, S. Hogesteeger, R. Singh, P. Holden, N. Fuckar, R. Odoulami, and M. New, 2018: Anthropogenic influence on the drivers of the Western Cape drought 2015–2017. *Environmental Research Letters*, **13**, 124010. <https://doi.org/10.1088/1748-9326/aae9f9>
362. Seager, R., T.J. Osborn, Y. Kushnir, I.R. Simpson, J. Nakamura, and H. Liu, 2019: Climate variability and change of Mediterranean-type climates. *Journal of Climate*, **32** (10), 2887–2915. <https://doi.org/10.1175/jcli-d-18-0472.1>
363. Abram, N.J., B.J. Henley, A. Sen Gupta, T.J.R. Lippmann, H. Clarke, A.J. Dowdy, J.J. Sharples, R.H. Nolan, T. Zhang, M.J. Wooster, J.B. Wurtzel, K.J. Meissner, A.J. Pitman, A.M. Ukkola, B.P. Murphy, N.J. Tapper, and M.M. Boer, 2021: Connections of climate change and variability to large and extreme forest fires in southeast Australia. *Communications Earth & Environment*, **2** (1), 8. <https://doi.org/10.1038/s43247-020-00065-8>
364. Andela, N., D.C. Morton, L. Giglio, Y. Chen, G.R. van der Werf, P.S. Kasibhatla, R.S. DeFries, G.J. Collatz, S. Hantson, S. Kloster, D. Bachelet, M. Forrest, G. Lasslop, F. Li, S. Mangeon, J.R. Melton, C. Yue, and J.T. Randerson, 2017: A human-driven decline in global burned area. *Science*, **356** (6345), 1356–1362. <https://doi.org/10.1126/science.aal4108>